Title
Using Yeast Functional Toxicogenomics to Decipher the Toxicity of Environmental Contaminants

Author
Gaytan, Brandon David

Publication Date
2013

Peer reviewed|Thesis/dissertation

Using Yeast Functional Toxicogenomics to Decipher the Toxicity of Environmental Contaminants

By

Brandon David Gaytán

A dissertation submitted in partial satisfaction of the

requirements for the degree of

Doctor of Philosophy

in

Molecular Toxicology

in the

Graduate Division

of the

University of California, Berkeley

Committee in charge:

Professor Christopher D. Vulpe, Chair
Professor Martyn T. Smith
Professor John E. Casida
Professor Rachel Brem

Fall 2013

Abstract

Using Yeast Functional Toxicogenomics to Decipher the Toxicity of Environmental Contaminants

by

Brandon David Gaytán

Doctor of Philosophy in Molecular Toxicology

University of California, Berkeley

Professor Christopher D. Vulpe, Chair

The increased presence of chemical contaminants in the environment is an undeniable concern to human health and ecosystems. Historically, by relying heavily upon costly and laborious animal-based toxicity assays, the field of toxicology has often neglected examinations of the cellular and molecular mechanisms of toxicity for the majority of compounds – information that, if available, would strengthen risk assessment analyses. With its unique genetic tools and a high degree of conservation with more complex organisms, the model eukaryote *Saccharomyces cerevisiae* is an appealing organism in which to conduct functional inquiries into the modes of chemical toxicity. In this series of studies, the yeast deletion mutant collection was screened to identify strains exhibiting altered growth in the presence of various environmental contaminants. This technique, known as functional profiling or functional genomics, yielded (1) novel insights into chemical toxicity; (2) pathways and mechanisms deserving of further study; and (3) candidate human toxicant susceptibility or resistance genes.

Functional profiling determined the toxic mechanism of the dieldrin organochlorinated pesticide in yeast. Exposure to dieldrin has been linked to Parkinson's and Alzheimer's diseases, endocrine disruption, and cancer, but the cellular and molecular mechanisms of toxicity behind these effects remain largely unknown. A functional genomics approach in the model eukaryote *Saccharomyces cerevisiae* demonstrated that dieldrin altered leucine availability. This model was supported by multiple lines of congruent evidence: (1) mutants defective in amino acid signaling or transport were sensitive to dieldrin, which was reversed by the addition of exogenous leucine; (2) dieldrin sensitivity of wild-type or mutant strains was dependent upon leucine concentration in the media; (3) overexpression of proteins that increased intracellular leucine conferred resistance to dieldrin; (4) leucine uptake was inhibited in the presence of dieldrin; and (5) dieldrin induced the amino acid starvation response. Additionally, it was shown that appropriate negative regulation of the Ras/protein kinase A (PKA) pathway, along with an intact pyruvate dehydrogenase complex, was required for dieldrin tolerance. A model connecting leucine uptake, Ras/PKA signaling, and pyruvate dehydrogenase was hypothesized. Many yeast dieldrin tolerance genes described have orthologs that may modulate dieldrin toxicity in humans.

Yeast functional profiling was also conducted with toxaphene, an environmentally persistent mixture of chlorinated terpenes previously utilized as an insecticide. Toxaphene exposure has been previously associated with various cancers and diseases such as amyotrophic lateral sclerosis, but the cellular and molecular mechanisms responsible for these toxic effects have not been well established. In this section, a functional approach in the model eukaryote *Saccharomyces cerevisiae* demonstrated that toxaphene affected yeast mutants defective in (1) processes associated with transcription elongation and (2) nutrient utilization. Synergistic growth defects were observed upon exposure to both toxaphene and the known transcription elongation inhibitor mycophenolic acid (MPA). However, unlike MPA, toxaphene did not deplete nucleotides and additionally had no detectable effect on transcription elongation. It was concluded that toxaphene likely affects a process closely associated with transcription elongation, such as mRNA processing, mRNA nuclear export, or transcription-coupled nucleotide excision repair. Future studies are required to pinpoint the exact mechanism, and again, many of the yeast genes identified in this chapter have human homologs, warranting further investigations into the potentially conserved mechanisms of toxaphene toxicity.

A functional screen was devised to identify yeast cellular processes and pathways affected by dimethyl sulfoxide (DMSO), a solvent frequently utilized in toxicological and pharmaceutical investigations. As such, it is important to establish the cellular and molecular targets of DMSO in order to differentiate its intrinsic effects from those elicited by a compound of interest. A genome-wide functional screen in *Saccharomyces cerevisiae* identified deletion mutants exhibiting sensitivity to 1% DMSO, a concentration standard to yeast chemical profiling studies. Mutants defective in Golgi/ER transport were found to be sensitive to DMSO, including those lacking components of the conserved oligomeric Golgi (COG) complex. Moreover, strains deleted for members of the SWR1 histone exchange complex were hypersensitive to DMSO, with additional chromatin remodeling mutants displaying a range of growth defects. DNA repair genes were also identified as important for DMSO tolerance. Finally, it was demonstrated that overexpression of histone H2A.Z, which replaces chromatin-associated histone H2A in a SWR1-catalyzed reaction, conferred resistance to DMSO. Once again, many yeast DMSO tolerance genes described have homologs in more complex organisms, and the data provided is applicable to future investigations into the cellular and molecular mechanisms of DMSO toxicity.

Finally, a framework for semi-automated functional yeast screening of toxicants is described. Pool growths, chemical exposures, and DNA extraction of barcodes described above were conducted manually, which limited throughput. Additionally, identification of mutants with altered growth in a toxicant required hybridizations to costly microarrays. To transition to a more high-throughput environment, a liquid handler was utilized in conjunction with purpose-built software to perform five and fifteen generations screens of the homozygous diploid yeast deletion collection with various emerging environmental contaminants. Genomic DNA was extracted from the pools with robotics, and the barcodes uniquely identifying each deletion strain were amplified by PCR using primers indexed for sequencing on Illumina machinery. Future studies are needed to analyze the sequencing results and identify strains significantly sensitive or resistant to each of the compounds.

Table of Contents

Dedication

This dissertation is dedicated to those I love most: Mum and Dad, Alexa, Celina, Marisol, and Candice.

List of Figures and Tables

List of Abbreviations

2-CdA – 2-chloro-2'-deoxyadenosine
4-NQO – 4-nitroquinoline-N-oxide
6-AU – 6-azauracil
ANOVA – analysis of variance
ATSDR – Agency for Toxic Substances and Disease Registry
AUC – area under the curve
BDE-47 – brominated diphenyl ether congener 47
BDE-99 – brominated diphenyl ether congener 99
bp – base pair
CAS – Chemical Abstract Services
CGC – *Caenorhabditis* Genetics Center
CoA – coenzyme A
COG – conserved oligomeric Golgi
COX – chlorpyrifos oxon
CSM – complete synthetic media
CVT – cytoplasm to vacuole targeting
dAMP – decreased abundance by mRNA perturbation
DDT – dichlorodiphenyltrichloroethane
DE71 – brominated diphenyl ether technical mixture
DMEM – Dulbecco's modified Eagle's medium
DMSO – dimethyl sulfoxide
DNA – deoxyribonucleic acid
DSSA – differential strain sensitivity analysis
ENDO – endosulfan
ENR – enoyl-acyl carrier-protein reductase
EPA – Environmental Protection Agency
ER – endoplasmic reticulum
ERK – extracellular signal-regulated kinases
FBS – fetal bovine serum
FKBP12 – FK506 binding protein 12
FunSpec – Functional Specification resource
GABA – gamma-aminobutyric acid
GARP – Golgi-Associated Retrograde Protein
GEO – Gene Expression Omnibus
GET – Guided Entry of Tailanchored
GFP – green fluorescent protein
GLAM – Gene Length Accumulation of mRNA
GDP – guanosine diphosphate
GMP – guanosine monophosphate
GTP – guanosine triphosphate
GO – Gene Ontology
H2A – histone 2A

H2A.Z – histone 2A variant
H2B – histone 2B
H4 – histone 4
HFR – halogenated flame retardant
HIP – haploinsufficiency profiling
HIR – histone regulation complex
HOP – homozygous profiling
IARC – International Agency for Research on Cancer
IC20 – concentration at which growth is inhibited by 20%
IMPDH – inosine monophosphate dehydrogenase
MAPK – mitogen activated protein kinase
mCi – millicurie
MEK – mitogen-activated protein kinase kinase
MIPS – Munich Information Center for Protein Sequences
ml – milliliter
mM – millimolar
mm – millimeter
mmol – millimole
MORF – movable open reading frame
MPA – mycophenolic acid
MPTP – 1-methyl-4-phenyl-1,2,3,6-tetrahydropyridine
mRNA – messenger RNA
MRX – meiotic recombination complex
NA – not applicable
ND – not determined
NHANES – National Health and Nutrition Examination Surveys
ng – nanogram
nM – nanomolar
NPL – National Priorities List
NRC – National Research Council
NS – not significant
NTP – National Toxicology Program
OCP – organochlorinated pesticide
ORF – open reading frame
PCR – polymerase chain reaction
PDH – pyruvate dehydrogenase
PKA – protein kinase A
ppb – parts per billion
RNA – ribonucleic acid
RNAi – RNA interference
RPM – revolutions per minute
rRNA – ribosomal RNA
SC-Leu – synthetic complete media lacking leucine
SC-Ura – synthetic complete media lacking uracil

SD-N – starvation media
SE – standard error
shRNA – short hairpin RNA
TALENs – transcription activator-like effector nuclease chimeras
TBBPA – 3,3′,5,5′-tetrabromobisphenol A
TCEP – tris(2-chloroethyl) phosphate
TCPP – tris(1-chloro-2-propyl) phosphate
TCPy – 3,5,6-trichloro-2-pyridinol
TCS – triclosan
TDCPP – tris(1,3-dichloro-2-propyl) phosphate
T/NT – treated versus untreated
Tor – target of rapamycin
TSCA – Toxic Substances Control Act
µg – microgram
µl – microliter
µM – micromolar
vs. – versus
v-SNARE – vacuolar SNARE
WT – wild-type
YPD – yeast extract-peptone-dextrose yeast culture media
YPGal – yeast extract-peptone-galactose yeast culture media
YPGal+Raf – yeast extract-peptone-galactose-raffinose yeast culture media

Acknowledgements

I thank my major professor Chris Vulpe for the opportunity to be a part of his laboratory. I was able to work on many exciting projects, and was encouraged to disseminate my research within the scientific community through various meetings, collaborations, and travels. I appreciate the independence given to me, and I am especially grateful to have been treated as a colleague. I am glad for the mutual understanding that one can be a successful scientist while still maintaining an acceptable work-life balance.

Thank you to the faculty who provided guidance and advice by serving as committee members throughout my graduate career, including: Len Bjeldanes, Rachel Brem, John Casida, Terry Machen, Wally Wang, and Martyn Smith.

Many past and present Vulpe laboratory members must to be recognized for their helpfulness, advice, and support, including: Matthew North, Brie Fuqua, William Jo, Zouhair Attieh, and Stela Masle. Special thanks go to Vanessa De La Rosa, Abderrahmane (Mani) Tagmount, and Leona Scanlan – I would have been lost and unhappy without you around. The undergraduate students contributing to sections of this work were José Albarracín, Jan-Michael Lerot, Adriana Martinez, and Christina Monroy.

Funding was provided by the University of California, Berkeley Graduate Division and the National Science Foundation Graduate Research Fellowship Program (GRFP). The National Institute of Environmental Health Sciences (NIEHS) provided research funding for some of the studies addressed within.

Finally, I am thankful to the following people for making this ordeal a bit less of an ordeal. Family: I wish I could see you more often. Thank you for your support, love, visits, phone calls, and texts over the past few years. Candice: thank you for your undying faith in me – you have willed me to succeed. I'll forever do the same for you. Vanessa: I could not have asked for a better best in and out of lab friend. You made school more bearable. Steve: you kept me sane, yet also encouraged crazy. Don't leave. Tami and Joel: thank you for introducing me to expensive outdoor excursions and hobbies. Nora, Chuck, Diana, and Holly: thank you for being the premier all-knowing experienced graduate students and GGSNT founders. The UC Berkeley SACNAS chapter – Adrienne, Akemi, Astrid, Bubba, Dani, Galo, Joey, Lissette, Patty, Stefanie, and Vanessa – I learned a lot about community, family, leadership, and BBQing from you. I am proud of what we have accomplished as a chapter.

CHAPTER 1

INTRODUCTION

Chemical production and its implications

Current estimates project that global chemical production – currently growing 3% per year – will double every 25 years (Wilson *et al.*, 2006). In the United States alone, excluding fuels, pesticides, pharmaceuticals, or food products, about 42 billion pounds of chemicals are produced or imported daily (US EPA, 2005). Many chemicals are managed through the Toxic Substances Control Act (TSCA), but several independent analyses have concluded that these regulations seriously hinder (1) toxicity testing and hazard assessment; (2) control of chemicals of concern; and (3) investment in safer alternatives, such as those generated by the tenets of green chemistry (Wilson and Schwarzman, 2009). Combined with the widespread use and distribution of industrial chemicals, the data and safety gaps precipitated by TSCA elicit a situation in which chemical exposures to humans and ecosystems are oftentimes of unknown hazard and risk.

The present state of chemical toxicity testing

The field of toxicology currently employs extensive animal-based assays to evaluate chemical toxicity, a burdensome and prohibitively expensive approach that typically assesses a limited number of endpoints. Considering tens of thousands of in use chemicals lack adequate toxicity data (Judson *et al.*, 2009), it is unreasonable to rely upon these methods to fill data gaps. The National Research Council (NRC), realizing that more innovative approaches to testing were needed, envisioned that toxicology should commit to mechanistically-based high-throughput cellular *in vitro* assays (Andersen and Krewski, 2010; NRC, 2007). In this way, a more complete comprehension of chemical toxicity can be achieved, while expediting testing, decreasing costs, and reducing animal usage. Although high-throughput *in vitro* methods certainly signal progress in toxicity testing, they are limited to existing assays with known endpoints, such as analyses of stress response pathways induced by oxidative species, heat shock, DNA damage, hypoxia, and unfolded proteins (Simmons *et al.*, 2009). Another approach utilizes "omics" technologies such as gene expression profiling, proteomics lipidomics, and metabolomics to conduct targeted and untargeted investigations into chemical mechanisms of toxicity (reviewed by Hamadeh *et al.*, 2002; Gatzidou *et al*., 2007; Jayapal *et al*., 2010). However, by associating toxicant exposure with changes in mRNA, protein, lipid, or metabolite levels, these assays are correlative and do not provide direct links between genes and their requirements in the cellular toxicant response.

The advantages of functional toxicology

The concept of functional toxicology is based in the high-throughput use of cells/organisms harboring gene deletions or depleted proteins to systematically examine genetic requirements for toxicity tolerance. Any phenotype imaginable can be measured in response to a toxicant, but viability or fitness are the most conventional endpoints. Functional techniques can provide information distinct from the aforementioned correlative methodologies; for example, Giaever *et al.* (2002) found that expression of a gene is generally unrelated to its requirement for growth under a selective condition. Functional analyses, which have been conducted in budding and fission yeast, bacteria, nematodes, fruit flies, zebrafish, and human cell lines, can (1) contribute

novel insight into chemical mechanisms of action; (2) define more specific toxicological endpoints; and (3) inform further mechanistic-based assays.

Functional toxicology in yeasts

For many reasons, the eukaryotic budding (*Saccharomyces cerevisiae*) and fission (*Schizosaccharomyces pombe*) yeasts are ideal models in which to conduct functional toxicological studies. Numerous metabolic and signaling pathways, along with basic cellular processes, are conserved to more complex organisms such as humans. Human homologs have been identified for a large number of yeast genes, with several hundred of the conserved genes linked to disease in humans (Steinmetz *et al.*, 2002; Wood *et al.*, 2002). A long history of genetic manipulation in yeasts confers the ability to selectively target and examine conserved genes and pathways throughout their genomes, facilitating functional analyses. The ease of culture and availability of software resources, molecular protocols, and genetic and physical interaction data collectively bolster the value of yeasts in toxicology.

Barcoded mutant collections have been generated in budding (Giaever *et al*., 1999; Giaever *et al.*, 2002) and fission yeast (Chen *et al.*, 2012; Kennedy *et al*., 2008; Kim *et al*., 2010), allowing assessment of individual strain fitness in pooled cultures under selective conditions (reviewed by dos Santos *et al*., 2012; North and Vulpe, 2010). This technique, known as functional profiling, functional genomics, chemical genomics, or chemical-genetic profiling, can parenthetically identify the genetic requirements for tolerance to any substance that causes measurable growth inhibition in yeast. Figure 1.1 demonstrates the screening process, while Table 1.1 provides a summary of recent functional studies. Homozygous profiling (HOP) utilizes strains deleted for nonessential genes to establish the genetic requirements for chemical tolerance, while haploinsufficiency profiling (HIP) detects strains sensitized to a chemical targeting the product of their corresponding heterozygous locus (for a review, see Smith *et al*., 2010a). In brief, DNA sequences ("barcodes") uniquely identifying each deletion strain enable parallel growth analyses with thousands of pooled mutants in a chemical of interest. A PCR amplification of the barcodes and their subsequent counting via microarray hybridization or sequencing allows for discovery of strains with altered growth in the particular substance. The decreased abundance by mRNA perturbation (dAMP) collection complements heterozygote profiling by destabilizing a gene's mRNA (and thus depleting the encoded protein) via disruption of 3′-untranslated regions (Yan *et al.*, 2008). An additional tool that may benefit functional toxicology is the barcoded yeast overexpression library (Douglas *et al.*, 2012; Ho *et al.*, 2009). Similar to HOP and HIP, this technique enables highly parallel and systematic investigations of overexpression phenotypes in pooled cultures. Finally, a novel "functional variomics" approach utilizes high-complexity random mutagenesis to identify genes conferring drug resistance due to mutations or overexpression (Huang *et al.*, 2013a). The advent of multiplexed high-throughput barcode sequencing of pooled cultures (Han *et al.*, 2010; Smith *et al.* 2010b) promises a future of expedited and cost efficient functional genomic analyses.

The functional tools available in yeast provide unmatched resources for inquiries into potential cellular and molecular mechanisms of toxicity. Such analyses have informed functional experimentation in more complex organisms such as zebrafish or human cell lines. For example,

Ishizaki *et al.* (2010) utilized a yeast chemical-genetic screen to reveal that intracellular trafficking defects conferred sensitivity to copper limitation, and further reported that knockdown of zebrafish homologs to these yeast genes sensitized fish to copper-dependent hypopigmentation, a hallmark of copper deficiency in humans. Following identification of the Sas2p histone acetyltransferase as a modulator of arsenite tolerance in yeast, knockdown of its homolog MYST1 in human bladder epithelial cells was found to similarly induce arsenite sensitivity (Jo *et al.*, 2009). Another group demonstrated that the investigational cancer drug elesclomol affected electron transport mutants in yeast and extended their analysis by determining that elesclomol interacted with the electron transport chain in human cells (Blackman *et al.*, 2012). Likewise, a functional screen in yeast identified mitochondrial translation inhibition as the lethality mechanism of the antimicrobial and antileukemic compound tigecycline, and confirmed this activity in leukemic cells (Škrtić *et al.*, 2011).

Potential for functional toxicology in other fungi and bacteria

The recent development of the TagModule collection (Oh *et al.*, 2010a), building upon the work of Xu *et al.* (2007), takes advantage of barcoded transposons to extend the yeast DNA barcoding methodology to a variety of microorganisms. In essence, *in vitro* transposon mutagenesis is utilized to mutagenize a genomic DNA library, and subsequent transformation of barcoded genomic fragments into a compatible unicellular organism allows for genome-wide unbiased screening of chemical-genetic interactions. Akin to the yeast functional process, the barcodes can be amplified from pooled cultures and counted by microarray hybridization or high-throughput sequencing. Oh *et al.* (2010a) demonstrated the versatility of the TagModule collection by generating tagged mutants in the bacterium *Shewanella oneidensis* MR-1 and the fungal pathogen *Candida albicans*. As a proof of principle, the authors identified *S. oneidensis* mutants with growth deficiencies in minimal media and *C. albicans* mutants sensitive to the antifungal drug clotrimazole (Oh *et al.*, 2010a). The same group reports on additional haploinsufficiency screens in *C. albicans* (Oh *et al.*, 2010b) and *S. oneidensis* (Deutschbauer *et al.*, 2011) encompassing a wide variety of growth conditions and diverse chemical compounds. Furthermore, the method was applied to identify genes important for plant hydrolysate tolerance in *Zymomonas mobilis*, a bacterium with potential for commercial-scale cellulosic ethanol production (Skerker *et al.*, 2013). By facilitating barcoding of mutant or overexpression collections for pooled functional analyses in a range of organisms, the TagModule system can be a valuable tool for toxicity testing.

Alternative approaches utilizing deletion/overexpression strains, or high-throughput sequencing of tagged transposon mutants may have applications relevant to functional toxicology. A signature-tagged mutagenesis strategy permitted parallel analysis of *Cryptococcus neoformans* fungal mutants in experimental infections (Liu *et al.*, 2008), while high-throughput sequencing examined the relative quantities of human gut bacterium *Bacteroides thetaiotaomicron* transposon mutants in wild-type and immunodeficient gnotobiotic mice (Goodman *et al.*, 2009). Relative strain abundance has been quantified in a collection of homozygous *C. albicans* deletion mutants, albeit in a lower-throughput investigation (Noble *et al.*, 2010) than allowed by the TagModule system (Oh *et al.*, 2010a). Overexpression studies can be conducted in *C. albicans*, however the available ORFeome is confined to a few hundred genes (Chauvel *et al.*, 2012).

Genome-wide deletion libraries have been constructed in *Escherichia coli* (Baba *et al.*, 2006), *Bacillus subtilis* (Kobayashi *et al.*, 2003), and *Pseudomonas aeruginosa* (Jacobs *et al.*, 2003), with a limited set available in *Salmonella enterica* (Santiviago *et al.*, 2009). Thousands of specific genetic modifications were simultaneously evaluated to quantify population dynamics in various media and growth inhibitors in *E. coli* (Warner *et al.*, 2010). It is conceivable that functional toxicological or even pharmaceutical inquiries can be performed using any of these tools and/or organisms.

Functional toxicology in eukaryotes of increased complexity

Although large-scale targeted deletion collections have been generated in various unicellular organisms, comparable libraries do not exist for animal models, mainly due to their genetic intractability. Studies reported in the literature are not typically genome-wide, and have been somewhat confined to specific subsets of genes or cellular processes hypothesized to be affected by the chemical of interest.

The nematode *Caenorhabditis elegans*, owing to its simplicity and relative genetic flexibility, has been exploited in forward genetic and RNA interference (RNAi) screens (reviewed by Leung *et al.*, 2008). Following a round of mutagenesis and selection in a toxicant, next generation sequencing can identify individual *C. elegans* mutants (Doitsidou *et al.*, 2010). Various groups have utilized limited RNAi screens in nematodes to discover genes that, when silenced, confer chemical resistance or susceptibility. Examples include investigations with the herbicide paraquat (Kim and Sun, 2007), whereas gene expression analyses informed RNAi studies with cadmium (Cui *et al.*, 2007) and PCB-52 (Menzel *et al.*, 2007). Additionally, although many *C. elegans* homozygous deletion mutants are available through the Caenorhabditis Genetics Center, methods to assess these strains in a high-throughput parallel manner do not currently exist. The mutants may prove useful in follow-up analyses of conserved genes and pathways identified by chemical-genetic screens in yeasts or bacteria.

Forward chemical genetic screens in *Drosophila* cells and zebrafish identified small molecules inhibiting the cell cycle (Eggert *et al.*, 2004; Murphey *et al.*, 2006). While RNAi screens are possible in both of these organisms (Aleström *et al.*, 2006; Eggert *et al.*, 2004; Zhang *et al.*, 2010), they are underutilized for the purposes of toxicity testing, likely due to the experimental complexity of such assays. It is also important to recognize that RNAi screens are not without their limitations, with complications arising due to incomplete knockdown of target genes and off-target effects. The DT40 chicken cell lines are advantageous in the functional and mechanistic screening of genotoxicants, as they harbor various individual deletions in DNA repair genes (Lee *et al.*, 2013; Ridpath *et al.*, 2007; Yamamoto *et al.*, 2011), however, other cellular components and processes are not represented in the set of mutants.

At the present, more reasonable is the use of individual animal knockouts or knockdowns to confirm results acquired in less complex systems such as yeast. The generation of knockout animals such as mice remains a time-consuming and costly process that requires simplification to meet the needs of functional toxicologists. A system facilitating deletions in animals is the use of site-specific endonuclease TALE-nuclease chimeras (TALENs) to selectively target genes for

editing or mutagenesis (Miller *et al.*, 2011). For example, TALEN-mediated mutagenesis in mouse zygotes produced animals with genetic knockouts of the progesterone immunomodulatory binding factor 1 and selenoprotein W, muscle 1 (Sung *et al.*, 2013). It is imaginable that knockouts created by this methodology could expedite analyses of conserved toxicant mechanisms in a variety of animal models.

Functional toxicology in mammalian cells

The majority of functional genomic applications in human cells rely upon RNAi loss-of-function screens (reviewed by Mullenders and Bernards, 2009; North and Vulpe, 2010). Barcoded short hairpin RNA (shRNA) libraries enable identification of shRNAs that elicit a specific phenotype under toxicant selection. The relative abundance of barcodes in control and treated populations can be measured by hybridization to microarrays (Mullenders and Bernards, 2009) or sequencing (Kimura *et al.*, 2008; Sims *et al.*, 2011). This method is efficient at detecting shRNAs that increase fitness but cannot always discover shRNAs that decrease viability, and furthermore, the process is lengthy and requires significant optimization (Sims *et al.*, 2011). Nevertheless, RNAi-based screens have uncovered human genes whose suppression confers resistance to a wide range of drugs (reviewed by Berns and Bernards, 2012). Finally, a two-stage shRNA screen identified mammalian genetic interactions underlying ricin susceptibility (Bassik *et al.*, 2013).

An exciting development for the field of functional toxicology is the discovery of haploid mouse (Leeb and Wutz, 2011) and near haploid human (Carette *et al.*, 2009) cell lines. Transposon mutagenesis in mouse haploid embryonic stem cells has identifying genes required for resistance to 2-amino-6-mercaptopurine (Leeb and Wutz, 2011), the chemotherapeutic 6-thioguanine and the PARP 1/2 inhibitor olaparib (Pettitt *et al.*, 2013), and the bioweapon ricin (Elling *et al.*, 2011). Similarly, the human cells are a derivative of a chronic myeloid leukemia cell line haploid for all chromosomes except chromosome 8. Insertional mutagenesis generated null alleles that have been screened for resistance to host factors used by pathogens (Carette *et al.*, 2009; Carette *et al.*, 2011a; Jae *et al.*, 2013), the cancer drug candidate 3-bromopyruvate (Birsoy *et al.*, 2013), and the ER stressor tunicamycin (Reiling *et al.*, 2011). Especially encouraging is the use of deep sequencing to examine millions of mutant alleles via selection and sequencing of pools of cells (Carette *et al.*, 2011b), an improvement over the laborious analyses of individual clones. Finally, the TALE nuclease architecture has been utilized to regulate mammalian genes and engineer deletions within the endogenous human *NTF3* and *CCR5* genes (Miller *et al.*, 2011). The simplification and expedition of screening and deletion processes in mammalian cell lines will undoubtedly have considerable ramifications for functional toxicology.

The future of functional toxicology

Functional toxicological screening methods, i.e., those that identify genetic requirements for chemical tolerance, are powerful, unbiased tools deserving of expanded use in the field of toxicology. High-throughput screens of chemicals of concern or unknown toxicity will allow toxicologists to formulate hypotheses related to their corresponding mechanisms and pathways of toxicity. Automation and forays into deep parallel sequencing technologies will unquestionably increase the the throughput of functional techniques, but extensive computational resources and knowledge will be required to implement systems and analyze the resulting data.

Integration of functional assays across a variety of organisms can identify conserved modes of toxicity and direct studies most relevant to human health. The field of functional toxicology is primed to assist toxicologists meet the need for enhanced chemical toxicity testing.

Scope of this work

Functional toxicogenomic methodologies were utilized to understand the effects of various environmental contaminants on the budding yeast *Saccharomyces cerevisiae*. Pools of the homozygous diploid deletion mutant collection were exposed to toxicants to identify strains exhibiting altered growth. Subsequent computational and molecular analyses of the genetic requirements for tolerance elucidated or allowed for the formation of hypotheses concerning toxic mechanisms of action. This dissertation is divided into the four following sections: Chapter 2 discusses yeast functional profiling of the organochlorinated pesticide dieldrin, while Chapter 3 focuses on yeast functional studies with the organochlorinated pesticide mixture toxaphene. Yeast functional genomics of the common solvent dimethylsulfoxide (DMSO) is reported in Chapter 4, with Chapter 5 describing a transition to semi-automated chemical genetic screens of the yeast deletion library.

FIGURES

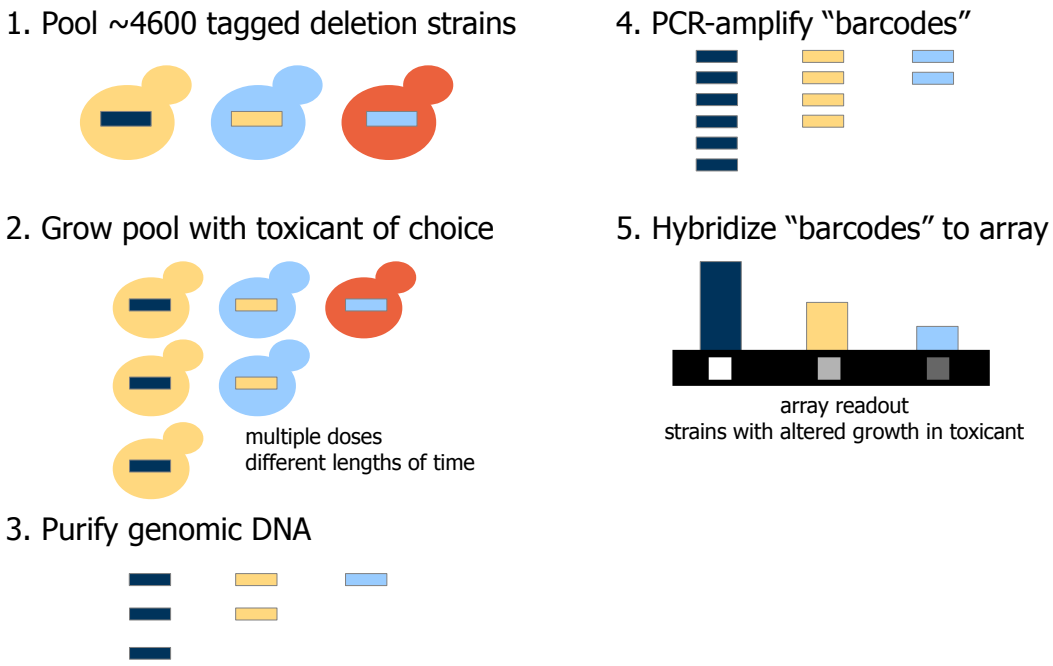

Figure 1.1. Overview of functional profiling in yeast. About 4600 deletion strains uniquely identified by DNA sequences (barcodes) are pooled and exposed to a toxicant at multiple doses and generation times (5 or 15). Barcodes are amplified from purified genomic DNA by PCR and counted by hybridization to a microarray or high-throughput sequencing methods. Subsequent analyses of individual strains can confirm susceptibility or resistance to the toxicant.

TABLES

Table 1.1. Summary of substances recently functionally profiled in yeasts. A literature search identified *S. cerevisiae* screens published from July 1, 2012 to July 24, 2013 and *S. pombe* screens published from 2008 to July 24, 2013.

Chemical class	Description	Organism	Reference
solvents	butanol	*S. cerevisiae*	González-Ramos *et al.* (2013)
	dimethylsulfoxide	*S. cerevisiae*	Zhang *et al.* (2013)
	dimethylsulfoxide	*S. cerevisiae*	Gaytán *et al.* (2013a)
metals	gold nanoparticles	*S. cerevisiae*	Smith *et al.* (2013)
	selenium	*S. cerevisiae*	Mániková *et al.* (2012)
	cobalt	*S. pombe*	Ryuko *et al.* (2012)
	cadmium	*S. pombe*	Kennedy *et al.* (2008)
persistent pollutants	dieldrin	*S. cerevisiae*	Gaytán *et al.* (2013b)
antimicrobials	thymol	*S. cerevisiae*	Darvishi *et al.* (2013)
	chitosan	*S. cerevisiae*	Galván Márquez *et al.* (2013)
	antimicrobial peptides	*S. cerevisiae*	Lis *et al.* (2013)
	TA-289	*S. cerevisiae*	Quek *et al.* (2013)
	2,4-diacetylphloroglucinol	*S. cerevisiae*	Troppens *et al.* (2013)
	DFD-VI-15	*S. cerevisiae*	Alex *et al.* (2012)
	micafungin	*S. pombe*	Zhou *et al.* (2013)
	various antifungals	*S. pombe*	Fang *et al.* (2012)
drugs	edelfosine	*S. cerevisiae*	Cuesta-Marbán *et al.* (2013)
	chloroquine	*S. cerevisiae*	Islahudin *et al.* (2013)
	FK506	*S. pombe*	Ma *et al.* (2011)
	caffeine	*S. pombe*	Calvo *et al.* (2009)
genotoxicants	methyl methanesulfonate	*S. cerevisiae*	Huang *et al.* (2013b)
	various	*S. cerevisiae*	Torres *et al.* (2013)
	various	*S. pombe*	Pan *et al.* (2013)
other	hydrolysate	*S. cerevisiae*	Skerker *et al.* (2013)
	NCI Diversity/Mechanistic sets	*S. cerevisiae/S. pombe*	Kapitsky *et al.* (2010)

REFERENCES

Aleström, P., Holter, J. L., Nourizadeh-Lillabadi, R. (2006). Zebrafish in functional genomics and aquatic biomedicine. *Trends in Biotechnology*. **24**, 15–21.

Alex, D., Gay-Andrieu, F., May, J., Thampi, L., Dou, D., Mooney, A., *et al.* (2012). Amino acid-derived 1,2-benzisothiazolinone derivatives as novel small-molecule antifungal inhibitors: identification of potential genetic targets. *Antimicrob. Agents Chemother.* **56**, 4630–4639.

Andersen, M. E., Krewski, D. (2010). The vision of toxicity testing in the 21st century: moving from discussion to action. *Toxicol. Sci.* **117**, 17–24.

Baba, T., Ara, T., Hasegawa, M., Takai, Y., Okumura, Y., Baba, M., *et al*. (2006). Construction of Escherichia coli K-12 in-frame, single-gene knockout mutants: the Keio collection. *Mol. Syst. Biol.* **2**, 2006.0008.

Bassik, M. C., Kampmann, M., Lebbink, R. J., Wang, S., Hein, M. Y., Poser, I., *et al.* (2013). A systematic mammalian genetic interaction map reveals pathways underlying ricin susceptibility. *Cell*. **152**, 909–922.

Berns, K., Bernards, R. (2012). Understanding resistance to targeted cancer drugs through loss of function genetic screens. *Drug Resist. Updates*. **15**, 268–275.

Birsoy, K., Wang, T., Possemato, R., Yilmaz, O. H., Koch, C. E., Chen, W. W., *et al*. (2013). MCT1-mediated transport of a toxic molecule is an effective strategy for targeting glycolytic tumors. *Nat Genet*. **45**, 104–108.

Blackman, R. K., Cheung-Ong, K., Gebbia, M., Proia, D. A., He, S., Kepros, J., *et al.* (2012). Mitochondrial electron transport is the cellular target of the oncology drug elesclomol. *PLoS ONE*. **7**, e29798.

Calvo, I. A., Gabrielli, N., Iglesias-Baena, I., García-Santamarina, S., Hoe, K.-L., Kim, D. U., *et al*. (2009). Genome-wide screen of genes required for caffeine tolerance in fission yeast. *PLoS ONE*. **4**, e6619.

Carette, J. E., Guimaraes, C. P., Varadarajan, M., Park, A. S., Wuethrich, I., Godarova, A., *et al.* (2009). Haploid genetic screens in human cells identify host factors used by pathogens. *Science*. **326**, 1231–1235.

Carette, J. E., Raaben, M., Wong, A. C., Herbert, A. S., Obernosterer, G., Mulherkar, N., *et al*. (2011a). Ebola virus entry requires the cholesterol transporter Niemann-Pick C1. *Nature*. **477**, 340–343.

Carette, J. E., Guimaraes, C. P., Wuethrich, I., Blomen, V. A., Varadarajan, M., Sun, C., *et al.* (2011b). Global gene disruption in human cells to assign genes to phenotypes by deep sequencing. *Nat Biotech*. **29**, 542–546.

Chauvel, M., Nesseir, A., Cabral, V., Znaidi, S., Goyard, S., Bachellier-Bassi, S., *et al.* (2012). A versatile overexpression strategy in the pathogenic yeast *Candida albicans*: identification of regulators of morphogenesis and fitness. *PLoS ONE*. **7**, e45912.

Chen, B.-R., Hale, D. C., Ciolek, P. J., Runge, K. W. (2012). Generation and analysis of a barcode-tagged insertion mutant library in the fission yeast *Schizosaccharomyces pombe*. *BMC Genomics*. **13**, 161.

Cuesta-Marbán, A., Botet, J., Czyz, O., Cacharro, L. M., Gajate, C., Hornillos, V., *et al.* (2013). Drug uptake, lipid rafts and vesicle trafficking modulate resistance to an anticancer lysophosphatidylcholine analogue in yeast. *J. Biol. Chem.* **288**, 8405–18.

Cui, Y., McBride, S. J., Boyd, W. A., Alper, S., Freedman, J. H. (2007). Toxicogenomic analysis of *Caenorhabditis elegans* reveals novel genes and pathways involved in the resistance to cadmium toxicity. *Genome Biol.* **8**, R122.

Darvishi, E., Omidi, M., Bushehri, A. A., Golshani, A., Smith, M. L. (2013). Thymol antifungal mode of action involves telomerase inhibition. *Med. Mycol.* [Epub ahead of print].

Deutschbauer, A., Price, M. N., Wetmore, K. M., Shao, W., Baumohl, J. K., Xu, Z., *et al.* (2011). Evidence-based annotation of gene function in *Shewanella oneidensis* MR-1 using genome-wide fitness profiling across 121 conditions. *PLoS Genet.* **7**, e1002385.

Doitsidou, M., Poole, R. J., Sarin, S., Bigelow, H., Hobert, O. (2010). *C. elegans* mutant identification with a one-step whole-genome-sequencing and SNP mapping strategy. *PLoS ONE*. **5**, e15435.

dos Santos, S. C., Teixeira, M. C., Cabrito, T. R., Sá-Correia, I. (2012). Yeast toxicogenomics: genome-wide responses to chemical stresses with impact in environmental health, pharmacology, and biotechnology. *Front Genet*. **3**, 63.

Douglas, A. C., Smith, A. M., Sharifpoor, S., Yan, Z., Durbic, T., Heisler, L. E., *et al*. (2012). Functional analysis with a barcoder yeast gene overexpression system. *G3 (Bethesda)*. **2**, 1279–1289.

Eggert, U. S., Kiger, A. A., Richter, C., Perlman, Z. E., Perrimon, N., Mitchison, T. J., *et al.* (2004). Parallel chemical genetic and genome-wide RNAi screens identify cytokinesis inhibitors and targets. *PLoS Biol*. **2**, e379.

Elling, U., Taubenschmid, J., Wirnsberger, G., O'Malley, R., Demers, S.-P., Vanhaelen, Q., *et al.* (2011). Forward and reverse genetics through derivation of haploid mouse embryonic stem cells. *Cell Stem Cell*. **9**, 563–574.

Fang, Y., Hu, L., Zhou, X., Jaiseng, W., Zhang, B., Takami, T., *et al.* (2012). A genome-wide screen in *Schizosaccharomyces pombe* for genes affecting the sensitivity of antifungal drugs that target ergosterol biosynthesis. *Antimicrob. Agents Chemother.* **56**, 1949–1959.

Galván Márquez, I., Akuaku, J., Cruz, I., Cheetham, J., Golshani, A., Smith, M. L. (2013). Disruption of protein synthesis as antifungal mode of action by chitosan. *Int. J. Food Microbiol.* **164**, 108–112.

Gatzidou, E. T., Zira, A. N., Theocharis, S. E. (2007). Toxicogenomics: a pivotal piece in the puzzle of toxicological research. *J Appl. Toxicol*. **27**, 302–309.

Gaytán, B. D., Loguinov, A. V., De La Rosa, V. Y., Lerot, J.-M., Vulpe, C. D. (2013a). Functional genomics indicates yeast requires Golgi/ER transport, chromatin remodeling, and DNA repair for low dose DMSO tolerance. *Front. Genet.* **4,** 154.

Gaytán, B. D., Loguinov, A. V., Lantz, S. R., Lerot, J.-M., Denslow, N. D., Vulpe, C. D. (2013b). Functional profiling discovers the dieldrin organochlorinated pesticide affects leucine availability in yeast. *Toxicol. Sci.* **132**, 347–358.

Giaever, G., Chu, A. M., Ni, L., Connelly, C., Riles, L., Véronneau, S., *et al.* (2002). Functional profiling of the *Saccharomyces cerevisiae* genome. *Nature*. **418**, 387–391.

Giaever, G., Shoemaker, D. D., Jones, T. W., Liang, H., Winzeler, E. A., Astromoff, A., *et al.* (1999). Genomic profiling of drug sensitivities via induced haploinsufficiency. *Nat. Genet.* **21**, 278–283.

González-Ramos, D., van den Broek, M., van Maris, A. J., Pronk, J. T., Daran, J.-M. G. (2013). Genome-scale analyses of butanol tolerance in *Saccharomyces cerevisiae* reveal an essential role of protein degradation. *Biotechnol Biofuels*. **6**, 48.

Goodman, A. L., McNulty, N. P., Zhao, Y., Leip, D., Mitra, R. D., Lozupone, C. A., *et al*. (2009). Identifying genetic determinants needed to establish a human gut symbiont in its habitat. *Cell Host Microbe*. **6**, 279–289.

Hamadeh, H. K., Amin, R. P., Paules, R. S., Afshari, C. A. (2002). An overview of toxicogenomics. *Curr Issues Mol Biol*. **4**, 45–56.

Han, T. X., Xu, X.-Y., Zhang, M.-J., Peng, X., Du, L.-L. (2010). Global fitness profiling of fission yeast deletion strains by barcode sequencing. *Genome Biology*. **11**, R60.

Ho, C. H., Magtanong, L., Barker, S. L., Gresham, D., Nishimura, S., Natarajan, P., *et al.* (2009). A molecular barcoded yeast ORF library enables mode-of-action analysis of bioactive compounds. *Nat. Biotechnol.* **27**, 369–377.

Huang, Z., Chen, K., Zhang, J., Li, Y., Wang, H., Cui, D., *et al*. (2013a). A functional variomics tool for discovering drug-resistance genes and drug targets. *Cell Rep*. **3**, 577–585.

Huang, D., Piening, B. D., Paulovich, A. G. (2013b). The preference for error-free or error-prone postreplication repair in *Saccharomyces cerevisiae* exposed to low-dose methyl methanesulfonate is cell cycle dependent. *Mol. Cell. Biol.* **33**, 1515–1527.

Ishizaki, H., Spitzer, M., Wildenhain, J., Anastasaki, C., Zeng, Z., Dolma, S., *et al.* (2010). Combined zebrafish-yeast chemical-genetic screens reveal gene-copper-nutrition interactions that modulate melanocyte pigmentation. *Dis Model Mech*. **3**, 639–651.

Islahudin, F., Khozoie, C., Bates, S., Ting, K.-N., Pleass, R. J., Avery, S. V. (2013). Cell-wall perturbation sensitizes fungi to the antimalarial drug chloroquine. *Antimicrob. Agents Chemother.* [Epub ahead of print].

Jacobs, M. A., Alwood, A., Thaipisuttikul, I., Spencer, D., Haugen, E., Ernst, S., *et al.* (2003). Comprehensive transposon mutant library of *Pseudomonas aeruginosa*. *Proc. Natl. Acad. Sci. U.S.A.* **100**, 14339–14344.

Jae, L. T., Raaben, M., Riemersma, M., Beusekom, E. van, Blomen, V. A., Velds, A., *et al*. (2013). Deciphering the glycosylome of dystroglycanopathies using haploid screens for Lassa virus entry. *Science*. **340**, 479–483.

Jayapal, M., Bhattacharjee, R. N., Melendez, A. J., Hande, M. P. (2010). Environmental toxicogenomics: a post-genomic approach to analysing biological responses to environmental toxins. *Int. J. Biochem. Cell Biol.* **42**, 230–240.

Jo, W. J., Ren, X., Chu, F., Aleshin, M., Wintz, H., Burlingame, A., *et al*. (2009). Acetylated H4K16 by MYST1 protects UROtsa cells from arsenic toxicity and is decreased following chronic arsenic exposure. *Toxicol. Appl. Pharmacol.* **241**, 294–302.

Judson, R., Richard, A., Dix, D. J., Houck, K., Martin, M., Kavlock, R., *et al*. (2009). The toxicity data landscape for environmental chemicals. *Environ. Health Perspect.* **117**, 685–695.

Kapitzky, L., Beltrao, P., Berens, T. J., Gassner, N., Zhou, C., Wüster, A., *et al.* (2010). Cross-species chemogenomic profiling reveals evolutionarily conserved drug mode of action. *Mol. Syst. Biol.* **6**, 451.

Kennedy, P. J., Vashisht, A. A., Hoe, K.-L., Kim, D.-U., Park, H.-O., Hayles, J., *et al.* (2008). A genome-wide screen of genes involved in cadmium tolerance in *Schizosaccharomyces pombe*. *Toxicol. Sci.* **106**, 124–139.

Kim, D.-U., Hayles, J., Kim, D., Wood, V., Park, H.-O., Won, M., *et al*. (2010). Analysis of a genome-wide set of gene deletions in the fission yeast *Schizosaccharomyces pombe*. *Nat. Biotechnol.* **28**, 617–623.

Kim, Y., Sun, H. (2007). Functional genomic approach to identify novel genes involved in the regulation of oxidative stress resistance and animal lifespan. *Aging Cell*. **6**, 489–503.

Kimura, J., Nguyen, S. T., Liu, H., Taira, N., Miki, Y., Yoshida, K. (2008). A functional genome-wide RNAi screen identifies TAF1 as a regulator for apoptosis in response to genotoxic stress. *Nucleic Acids Res*. **36**, 5250–5259.

Kobayashi, K., Ehrlich, S. D., Albertini, A., Amati, G., Andersen, K. K., Arnaud, M., *et al.* (2003). Essential *Bacillus subtilis* genes. *Proc. Natl. Acad. Sci. U.S.A.* **100**, 4678–4683.

Lee, S., Liu, X., Takeda, S., Choi, K. (2013). Genotoxic potentials and related mechanisms of bisphenol A and other bisphenol compounds: A comparison study employing chicken DT40 cells. *Chemosphere*. doi: 10.1016/j.chemosphere.2013.05.029

Leeb, M., Wutz, A. (2011). Derivation of haploid embryonic stem cells from mouse embryos. *Nature*. **479**, 131–134.

Leung, M. C. K., Williams, P. L., Benedetto, A., Au, C., Helmcke, K. J., Aschner, M., *et al.* (2008). *Caenorhabditis elegans*: An emerging model in biomedical and environmental toxicology. *Toxicol. Sci.* **106**, 5–28.

Lis, M., Bhatt, S., Schoenly, N. E., Lee, A. Y., Nislow, C., Bobek, L. A. (2013). Chemical genomic screening of a *Saccharomyces cerevisiae* genomewide mutant collection reveals genes required for defense against four antimicrobial peptides derived from proteins found in human saliva. *Antimicrob. Agents Chemother.* **57**, 840–847.

Liu, O. W., Chun, C. D., Chow, E. D., Chen, C., Madhani, H. D., Noble, S. M. (2008). Systematic genetic analysis of virulence in the human fungal pathogen *Cryptococcus neoformans*. *Cell*. **135**, 174–188.

Ma, Y., Jiang, W., Liu, Q., Ryuko, S., Kuno, T. (2011). Genome-wide screening for genes associated with FK506 sensitivity in fission yeast. *PLoS ONE*. **6**, e23422.

Mániková, D., Vlasáková, D., Letavayová, L., Klobučniková, V., Griač, P., Chovanec, M. (2012). Selenium toxicity toward yeast as assessed by microarray analysis and deletion mutant library screen: a role for DNA repair. *Chem. Res. Toxicol.* **25**, 1598–1608.

Menzel, R., Yeo, H. L., Rienau, S., Li, S., Steinberg, C. E. W., Stürzenbaum, S. R. (2007). Cytochrome P450s and short-chain dehydrogenases mediate the toxicogenomic response of PCB52 in the nematode *Caenorhabditis elegans*. *J. Mol. Biol*. **370**, 1–13.

Miller, J. C., Tan, S., Qiao, G., Barlow, K. A., Wang, J., Xia, D. F., *et al.* (2011). A TALE nuclease architecture for efficient genome editing. *Nat. Biotechnol.* **29**, 143–148.

Mullenders, J., Bernards, R. (2009). Loss-of-function genetic screens as a tool to improve the diagnosis and treatment of cancer. *Oncogene*. **28**, 4409–4420.

Murphey, R. D., Stern, H. M., Straub, C. T., Zon, L. I. (2006). A chemical genetic screen for cell cycle inhibitors in zebrafish embryos. *Chem. Biol. Drug Design*. **68**, 213–219.

Noble, S. M., French, S., Kohn, L. A., Chen, V., Johnson, A. D. (2010). Systematic screens of a *Candida albicans* homozygous deletion library decouple morphogenetic switching and pathogenicity. *Nat. Genet.* **42**, 590–598.

North, M., Vulpe, C. D. (2010). Functional toxicogenomics: mechanism-centered toxicology. *Int J Mol Sci*. **11**, 4796–4813.

NRC (National Research Council) of the National Academies. 2007. Committee on Toxicity Testing and Assessment of Environmental Agents. Toxicity Testing in the 21st Century: A Vision and a Strategy; The National Academies Press: Washington, D.C., USA.

Oh, J., Fung, E., Price, M. N., Dehal, P. S., Davis, R. W., Giaever, G., *et al*. (2010a). A universal TagModule collection for parallel genetic analysis of microorganisms. *Nucleic Acids Res.* **38**, e146.

Oh, J., Fung, E., Schlecht, U., Davis, R. W., Giaever, G., St Onge, R. P., *et al.* (2010b). Gene annotation and drug target discovery in *Candida albicans* with a tagged transposon mutant collection. *PLoS Pathog.* **6**, e1001140.

Pan, X., Lei, B., Zhou, N., Feng, B., Yao, W., Zhao, X., *et al.* (2012). Identification of novel genes involved in DNA damage response by screening a genome-wide *Schizosaccharomyces pombe* deletion library. *BMC Genomics*. **13**, 662.

Pettitt, S. J., Rehman, F. L., Bajrami, I., Brough, R., Wallberg, F., Kozarewa, I., *et al.* (2013). A genetic screen using the PiggyBac transposon in haploid cells identifies Parp1 as a mediator of olaparib toxicity. *PLoS ONE*. **8**, e61520.

Pierce, S. E., Davis, R. W., Nislow, C., Giaever, G. (2007). Genome-wide analysis of barcoded *Saccharomyces cerevisiae* gene-deletion mutants in pooled cultures. *Nat. Protocols*. **2**, 2958–2974.

Quek, N. C. H., Matthews, J. H., Bloor, S. J., Jones, D. A., Bircham, P. W., Heathcott, R. W., *et al.* (2013). The novel equisetin-like compound, TA-289, causes aberrant mitochondrial morphology which is independent of the production of reactive oxygen species in *Saccharomyces cerevisiae*. *Mol Biosyst*. doi: 10.1039/c3mb70056a

Reiling, J. H., Clish, C. B., Carette, J. E., Varadarajan, M., Brummelkamp, T. R., Sabatini, D. M. (2011). A haploid genetic screen identifies the major facilitator domain containing 2A (MFSD2A) transporter as a key mediator in the response to tunicamycin. *Proc. Natl. Acad. Sci. U.S.A.* **108**, 11756–11765.

Ridpath, J. R., Nakamura, A., Tano, K., Luke, A. M., Sonoda, E., Arakawa, H., *et al.* (2007). Cells deficient in the FANC/BRCA pathway are hypersensitive to plasma levels of formaldehyde. *Cancer Res.* **67**, 11117–11122.

Ryuko, S., Ma, Y., Ma, N., Sakaue, M., Kuno, T. (2012). Genome-wide screen reveals novel mechanisms for regulating cobalt uptake and detoxification in fission yeast. *Mol. Genet. Genomics*. **287**, 651–662.

Santiviago, C. A., Reynolds, M. M., Porwollik, S., Choi, S.-H., Long, F., Andrews-Polymenis, H. L., *et al*. (2009). Analysis of pools of targeted *Salmonella* deletion mutants identifies novel genes affecting fitness during competitive infection in mice. *PLoS Pathog*. **5**, e1000477.

Simmons, S. O., Fan, C.-Y., Ramabhadran, R. (2009). Cellular stress response pathway system as a sentinel ensemble in toxicological screening. *Toxicol. Sci.* **111**, 202–225.

Sims, D., Mendes-Pereira, A. M., Frankum, J., Burgess, D., Cerone, M.-A., Lombardelli, C., *et al*. (2011). High-throughput RNA interference screening using pooled shRNA libraries and next generation sequencing. *Genome Biol*. **12**, R104.

Skerker, J. M., Leon, D., Price, M. N., Mar, J. S., Tarjan, D. R., Wetmore, K. M., *et al*. (2013). Dissecting a complex chemical stress: chemogenomic profiling of plant hydrolysates. *Mol. Syst. Biol.* **9**, 674.

Skrtić, M., Sriskanthadevan, S., Jhas, B., Gebbia, M., Wang, X., Wang, Z., *et al*. (2011). Inhibition of mitochondrial translation as a therapeutic strategy for human acute myeloid leukemia. *Cancer Cell*. **20**, 674–688.

Smith, A. M., Ammar, R., Nislow, C., Giaever, G. (2010a). A survey of yeast genomic assays for drug and target discovery. *Pharmacol Ther*. **127**, 156–164.

Smith, A. M., Heisler, L. E., St.Onge, R. P., Farias-Hesson, E., Wallace, I. M., Bodeau, J., *et al*. (2010b). Highly-multiplexed barcode sequencing: an efficient method for parallel analysis of pooled samples. *Nucleic Acids Res*. **38**, e142.

Smith, M. R., Boenzli, M. G., Hindagolla, V., Ding, J., Miller, J. M., Hutchison, J. E., *et al*. (2013). Identification of gold nanoparticle-resistant mutants of *Saccharomyces cerevisiae* suggests a role for respiratory metabolism in mediating toxicity. *Appl. Environ. Microbiol.* **79**, 728–733.

Steinmetz, L. M., Scharfe, C., Deutschbauer, A. M., Mokranjac, D., Herman, Z. S., Jones, T., *et al.* (2002). Systematic screen for human disease genes in yeast. *Nat. Genet.* **31**, 400–404.

Sung, Y. H., Baek, I.-J., Kim, D. H., Jeon, J., Lee, J., Lee, K., *et al.* (2013). Knockout mice created by TALEN-mediated gene targeting. *Nat Biotech.* **31**, 23–24.

Torres, N. P., Lee, A. Y., Giaever, G., Nislow, C., Brown, G. W. (2013). A high-throughput yeast assay identifies synergistic drug combinations. *Assay Drug Dev Technol*. **11**, 299–307.

Troppens, D. M., Dmitriev, R. I., Papkovsky, D. B., O'Gara, F., Morrissey, J. P. (2013). Genome-wide investigation of cellular targets and mode of action of the antifungal bacterial metabolite 2,4-diacetylphloroglucinol in *Saccharomyces cerevisiae*. *FEMS Yeast Res.* **13**, 322–334.

U.S. EPA. 2005. How Can EPA More Efficiently Identify Potential Risks and Facilitate Risk Reduction Decision for Non-HPV Existing Chemicals? Washington, DC: U.S. Environmental Protection Agency, National Pollution Prevention and Toxics Advisory Committee, Broader Issues Work Group. [accessed 1 July 2013]. Available: http://epa.gov/oppt/npptac/pubs/finaldraftnonhpvpaper051006.pdf.

Warner, J. R., Reeder, P. J., Karimpour-Fard, A., Woodruff, L. B. A., Gill, R. T. (2010). Rapid profiling of a microbial genome using mixtures of barcoded oligonucleotides. *Nat Biotech*. **28**, 856–862.

Wilson, M. P., Chia, D. A., Ehlers, B. C. (2006). Green chemistry in California: a framework for leadership in chemicals policy and innovation. *New Solut*. **16**, 365–372.

Wilson, M. P., Schwarzman, M. R. (2009). Toward a new U.S. chemicals policy: rebuilding the foundation to advance new science, green chemistry, and environmental health. *Environ. Health Perspect.* **117**, 1202–1209.

Wood, V., Gwilliam, R., Rajandream, M.-A., Lyne, M., Lyne, R., Stewart, A., *et al.* (2007). Genome-wide fitness test and mechanism-of-action studies of inhibitory compounds in *Candida albicans*. *PLoS Pathog.* **3**, e92.

Yamamoto, K. N., Hirota, K., Kono, K., Takeda, S., Sakamuru, S., Xia, M., *et al.* (2011). Characterization of environmental chemicals with potential for DNA damage using isogenic DNA repair-deficient chicken DT40 cell lines. *Environ. Mol. Mutagen.* **52**, 547–561.

Yan, Z., Costanzo, M., Heisler, L. E., Paw, J., Kaper, F., Andrews, B. J., *et al.* (2008). Yeast Barcoders: a chemogenomic application of a universal donor-strain collection carrying bar-code identifiers. *Nat. Methods*. **5**, 719–725.

Zhang, L., Liu, N., Ma, X., Jiang, L. (2013). The transcriptional control machinery as well as the cell wall integrity and its regulation are involved in the detoxification of the organic solvent dimethyl sulfoxide in *Saccharomyces cerevisiae*. *FEMS Yeast Research*. **13**, 200–218.

Zhang, S., Binari, R., Zhou, R., Perrimon, N. (2010). A genome-wide RNA interference screen for modifiers of aggregates formation by mutant Huntingtin in *Drosophila*. *Genetics*. **184**, 1165–1179.

Zhou, X., Ma, Y., Fang, Y., Gerile, W., Jaiseng, W., Yamada, Y., *et al*. (2013). A genome-wide screening of potential target genes to enhance the antifungal activity of micafungin in *Schizosaccharomyces pombe*. *PLoS ONE*. **8**, e65904.

CHAPTER 2

FUNCTIONAL PROFILING OF THE DIELDRIN ORGANOCHLORINATED PESTICIDE IN YEAST

INTRODUCTION

The persistent and bioaccumulative nature of organochlorinated pesticides (OCPs), combined with their widespread use during the mid to late 20th century, resulted in pervasive environmental contamination that exists to the present day. Dieldrin (Fig. 2.1A) and aldrin (which is converted to dieldrin in biological systems) were two of the most heavily applied cyclodiene OCPs in the United States, utilized to control insects on corn, cotton, and citrus and to prevent or treat termite infestations (ATSDR, 2002). Dieldrin has been detected in soil, water, air, wildlife, and human samples (reviewed in Jorgenson, 2001) and is found at 159 of the 1363 current or proposed Environmental Protection Agency National Priorities List (NPL) hazardous waste sites. It is currently ranked 18th on the Agency for Toxic Substances and Disease Registry (ATSDR) Priority List of Hazardous Substances, a list of compounds that possibly threaten human health on account of their toxicity and potential for exposure at NPL sites. Although the use of dieldrin has been banned or restricted in many countries, concern remains over its persistence in sediment and potential to bioaccumulate in wildlife and humans. Acute exposure to dieldrin results in antagonism of the GABA-A receptor, prompting excessive neurotransmission and convulsions (ATSDR, 2002). In both animals and humans, dieldrin has been linked to cancer (reviewed in ATSDR, 2002; Jorgenson, 2001), Alzheimer's and Parkinson's diseases (Richardson *et al.*, 2006; Singh *et al.*, 2013; Weisskopf *et al.*, 2010), and endocrine modulation (reviewed in Jorgenson, 2001), but the cellular and molecular mechanisms behind these effects remain largely unknown.

The conservation of basic metabolic pathways and fundamental cellular processes to humans, as well as unmatched genetic resources, makes the eukaryotic yeast *Saccharomyces cerevisiae* an ideal model system for identifying potential cellular and molecular mechanisms of toxicity. Sequence comparison has identified a close human homolog for much of the yeast genome, with several hundred of the conserved genes implicated in human disease (Steinmetz *et al.*, 2002). The development of a yeast deletion library (Giaever *et al.*, 2002) enables the use of functional toxicogenomics (also known as functional profiling) to determine the importance of individual yeast genes for toxicant susceptibility. Unlike typical gene expression experiments that correlate toxicant exposure to changes in mRNA levels, this approach identifies genes functionally involved in toxicant response. Functional profiling has been utilized to discover yeast genes required for tolerance to a broad array of toxicants, including arsenic, iron, benzene, and more (reviewed in dos Santos *et al.*, 2012). In addition, human homologs or functional orthologs of yeast genes uncovered by this approach have been associated with sensitivity to the same toxicant in human cells (Jo *et al.*, 2009a).

In this study, a genome-wide functional screen identified the genetic requirements for tolerance to the dieldrin OCP in yeast. To our knowledge, it is the first comprehensive report investigating the yeast genes necessary for growth in the presence of a persistent organic pollutant, with the results demonstrating that dieldrin toxicity can be primarily attributed to altered leucine availability. Additionally, both proper regulation of the Ras/protein kinase A (PKA) pathway and components of the pyruvate dehydrogenase (PDH) complex are required for dieldrin tolerance. Many yeast genes involved in dieldrin resistance have human homologs that may also play a role in dieldrin response.

MATERIALS AND METHODS

Yeast strains, culture, and plasmids. The diploid yeast deletion strains used for functional profiling and confirmation analyses were of the BY4743 background (*MATa/MATα his3Δ1/his3Δ1 leu2Δ0/leu2Δ0 lys2Δ0/LYS2 MET15/met15Δ0 ura3Δ0/ura3Δ0,* Invitrogen). The haploid yeast *LEU2* MORF overexpression strain was of the Y258 background (*MATa*, *pep4*-3, *his4*-580, *ura3*-53, *leu2*-3,112, Open Biosystems). The *BAP2* HIP FlexGene expression vector, the B180 plasmid (*GCN4-lacZ*), and linearized pRS305 plasmid containing the *LEU2* gene were transformed into the BY4743 background. For deletion pool growth, cells were grown in liquid rich media (1% yeast extract, 2% peptone, 2% dextrose, YPD), whereas confirmation assays were performed in YPD or liquid synthetic complete media lacking leucine (0.68% yeast nitrogen base without amino acids, 0.077% CSM-Leu dropout mixture, 2% dextrose, SC-Leu) at 30°C with shaking at 200 revolutions per minute (rpm). Starvation media (SD-N) was composed of 0.68% yeast nitrogen base without amino acids and 2% dextrose. Protein overexpression was induced as in North *et al.* (2011) using liquid rich media containing 2% galactose and 2% raffinose (YPGal+Raf).

Dose-finding and growth curve assays. Dose-finding and growth curve experiments were performed as in North *et al.* (2011). Briefly, cells were grown to mid-log phase, diluted to an optical density at 600nm (OD_{600}) of 0.0165, and dispensed into nontreated polystyrene plates. Dieldrin (a gift from N. Denslow) stock solutions were prepared in dimethyl sulfoxide (DMSO) and added to the desired final concentrations (1% or less by volume) with at least two technical replicates per dose. Based upon literature searches for dieldrin toxicity in human cells (Ledirac *et al.*, 2005), the dieldrin yeast dose-response curve was narrowed to 200–800μM, which was examined in three independent experiments. Plates were incubated in Tecan microplate readers set to 30°C with shaking and OD_{595} measurements were taken every 15min for 24h. The raw absorbance data were averaged, background corrected, and plotted as a function of time. The area under the curve was calculated with Apache OpenOffice Calc and expressed as a percentage of the untreated control.

Functional profiling of the yeast genome. Growth of the deletion pools, genomic DNA extraction, barcode amplification, Affymetrix TAG4 array hybridization, and differential strain sensitivity analysis (DSSA) were performed as described (Jo *et al.*, 2009b). Briefly, pools of homozygous diploid deletion mutants ($n = 4607$) were grown in YPD at various dieldrin concentrations for 15 generations and genomic DNA was extracted using the YDER kit (Pierce Biotechnology). The DNA sequences unique to each strain (barcodes) were amplified by PCR and hybridized to TAG4 arrays (Affymetrix), which were incubated overnight, stained, and then scanned at an emission wavelength of 560nm with a GeneChip Scanner (Affymetrix). Data files are available at the Gene Expression Omnibus database.

Overenrichment and network mapping analyses. Significantly overrepresented Gene Ontology (GO) and MIPS (Munich Information Center for Protein Sequences) categories within the DSSA data were identified by a hypergeometric distribution using the Functional Specification resource, FunSpec, with a p value cutoff of 0.001 and Bonferroni correction. For the network mapping, fitness scores for strains displaying sensitivity to at least two doses of dieldrin were

mapped onto the BioGrid *S. cerevisiae* functional interaction network using the Cytoscape software. The jActiveModules plugin then identified subnetworks of genes enriched with fitness data, and the BiNGO plugin assessed overrepresentation of GO categories within these subnetworks.

Analysis of relative strain growth by flow cytometry. Assays were performed as in North *et al*. (2012), with slight modifications. Briefly, green fluorescent protein (GFP)-tagged wild-type and untagged mutant strains were grown overnight in YPD, diluted to 0.5 OD_{600}, and mixed in approximately equal numbers. Cells were inoculated into YPD or SC-LEU at 0.00375 OD_{600} in microplate format, treated with dieldrin, and grown for 24h at 30°C with shaking at 200 rpm. Approximately 20,000 cells per culture were analyzed at T = 0 and T = 24 h using a FACSCalibur flow cytometer. GFP-expressing wild-type cells were distinguishable from untagged mutant cells. The percentages of wild-type GFP and untagged mutant cells present in the cultures were used to calculate a ratio of growth for untagged cells in treated versus untreated samples. Statistically significant differences between the means of three independent DMSO-treated and dieldrin-treated cultures were determined using Student's *t*-test. Raw *p* values were corrected for multiplicity of comparisons using Benjamini-Hochberg correction.

Leucine uptake assays. Leucine transport was measured as in Heitman *et al*. (1993), with slight modifications. Briefly, overnight cultures were diluted, incubated for 4h at 30°C to mid-logarithmic phase, and washed with wash buffer (10mM sodium citrate, pH 4.5). Cells were resuspended in 10mM sodium citrate (pH 4.5)-20mM $(NH_4)_2SO_2$-2% glucose and the OD_{600} was measured. Import reactions contained resuspended cells, DMSO or dieldrin at a final concentration of 460µM, and 15.9µl of L-[^{14}C]leucine (53 mCi/mmol, 5µM final concentration) in a total of 3ml. Aliquots (0.5 ml) of the import reaction were taken at 0, 2, 5, 10, 30, and 60min and vacuum filtered through 25 mm Whatman GF/C glass microfiber filters presoaked in wash buffer. Filters were washed four times with 0.5ml wash buffer containing 2mM unlabeled L-leucine and bound radioactivity was quantified in Safety-Solve counting cocktail using a Beckman LS-6000IC liquid scintillation counter.

Amino acid starvation analyses. Cells harboring the B180 plasmid (containing a *GCN4-lacZ* reporter) were cultured overnight in SC-ura 2% dextrose, diluted to 0.25 OD_{600}, and spun down at 3500rpm following a 5-h period of growth. A wash and resuspension occurred in either SC-ura 2% dextrose or starvation media (SD-N), upon which cells were aliquoted to a microplate and treated with DMSO or the dieldrin IC20 (460µM) for 3 h. β-Galactosidase activity was assayed with the yeast β-galactosidase assay kit (ThermoScientific) and Miller units were calculated with the equation (1000 x A_{420})/(minutes of incubation x volume in milliliters x OD_{660}).

RESULTS

A genome-wide screen identifies mutants with altered growth in the presence of dieldrin

Growth curve assays were performed to determine the toxicity of dieldrin to yeast (Fig. 2.1B), based upon knowledge that (1) dieldrin causes physiological effects in human cell culture systems at 25-50µM (Ledirac *et al.*, 2005) and (2) the cell wall and abundant multidrug transporters often lend yeast resistance to chemical insult. From the growth curves, the IC_{20}, a

concentration determined as appropriate for use in the functional screen (Jo *et al.*, 2009b), was calculated as 460μM (Fig. 2.1C). To discover genes important for growth in dieldrin, pools of yeast homozygous diploid deletion mutants (n = 4607) were grown for 15 generations at the IC20 (460μM), 50% IC20 (230μM), and 25% IC20 (115μM). A differential strain sensitivity analysis (DSSA) identified 427 mutants as sensitive and 320 mutants as resistant to at least one dose of dieldrin (Appendix 1), with the top twenty-five sensitive strains at the IC20 shown in Table 2.1. Strains sensitive to dieldrin were the focus of this study.

Enrichment analyses and network mapping identify attributes necessary for dieldrin tolerance
A list of mutant strains displaying sensitivity to at least two of the dieldrin treatments (n = 219) was analyzed for significantly overrepresented biological attributes using FunSpec. Both GO and MIPS categories were enriched for various classifications at a corrected p value of 0.001, including nitrogen utilization, protein phosphorylation, the PDH complex, negative regulation of Ras signaling, and sensitivity to amino acid analogs (Table 2.2). For additional insight into the attributes required for dieldrin tolerance, network mapping was performed with the Cytoscape visualization tool and plugins identifying enriched categories. Similar to the FunSpec evaluation, nitrogen processes and phosphorylation were overrepresented within the network data (Fig. 2.2). These enrichment analyses guided the selection of candidate cellular processes and components for further experimentation.

Mutants defective in amino acid uptake and nitrogen signaling are sensitive to dieldrin
Overrepresentation analyses with FunSpec and Cytoscape implicated nitrogen processes as important for dieldrin tolerance. Therefore, we used flow cytometry to assay relative growth of a wild-type strain to mutants deficient in amino acid signaling and uptake, as well as nitrogen utilization. Both DSSA and flow cytometry identified *bap2*Δ, which lacks a gene encoding for a high-affinity leucine permease, as one of the strains most sensitive to dieldrin (Fig. 2.3A). Additional amino acid signaling genes were confirmed to be required for dieldrin tolerance, including *NPR1* (a kinase that prevents degradation of several amino acid transporters), *STP1* (a component of the Ssy1p-Ptr3p-Ssy5p SPS system that transduces extracellular amino acid status), and *LEU3* (a transcription factor regulating branched-chain amino acid biosynthesis and amino acid permeases) (Fig. 2.3A). The *NPR2*, *NPR3*, and *URE2* genes involved in the cellular response to nitrogen were also identified as necessary for growth in dieldrin (Fig. 2.3A).

Leucine availability is linked to dieldrin toxicity
With the determination that *bap2*Δ (which lacks a high-affinity leucine permease) was sensitive to dieldrin, we hypothesized that supplementation of YPD-dieldrin medium with excess leucine might mitigate the toxicity of dieldrin. Indeed, addition of 5mM leucine reversed the sensitivity not only of *bap2*Δ but also *leu3*Δ, *npr1*Δ, and *stp1*Δ to dieldrin (Fig. 2.3A). Although leucine moderately rescued the dieldrin sensitivity of the *ure2*Δ mutant, it did not rescue *npr2*Δ or *npr3*Δ (Fig. 2.3A). Bap2p can also transport isoleucine, valine, and tryptophan (Regenberg *et al.*, 1999), but supplementing YPD medium with these amino acids did not reverse the sensitivity of *bap2*Δ to dieldrin (Fig. 2.3B). Deletion of additional amino acid transporter genes (*AGP1*, *BAP3*, *GAP1*, and *GNP1*) known to facilitate uptake of leucine (Regenberg *et al.*, 1999) or other amino acids did not result in sensitivity to dieldrin (Fig. 2.3C). To further demonstrate that dieldrin toxicity in

yeast was linked to leucine availability, wild-type BY4743 and *bap2*Δ strains were grown in media containing defined concentrations of leucine. Dieldrin sensitivity was exacerbated at low concentrations of leucine and remediated by increased leucine levels in the media (Figs. 2.4A and 2.4B). The deletion strains utilized in this study were leucine auxotrophs, of the BY4743 background that lacks *LEU2*, the β-isopropylmalate deyhydrogenase responsible for catalyzing the penultimate step in leucine biosynthesis. Restoration of leucine prototrophy through knock-in of the *LEU2* gene resulted in resistance to dieldrin at decreased concentrations of leucine (Fig. 2.5A). Finally, overexpression of Bap2p (the high-affinity leucine permease) or Leu2p (an enzyme involved in leucine biosynthesis) conferred resistance to dieldrin (Figs. 2.5B and 2.5C). Collectively, these data suggest that leucine availability plays a key role in the response to dieldrin.

Dieldrin inhibits leucine uptake and causes amino acid starvation

BY4743 strains are leucine auxotrophs dependent on leucine import from the external environment. It was therefore hypothesized that dieldrin did not affect leucine availability by interfering with leucine biosynthesis but instead altered the uptake of leucine from the media. To test this, mid-log phase wild-type cells were incubated with radiolabelled leucine in the presence or absence of the dieldrin IC20 (460μM). Results show that dieldrin significantly inhibited leucine import at various time points as compared with untreated controls (Fig. 2.6A). With leucine uptake inhibited, it was anticipated that dieldrin would starve the cell for leucine and induce the general control response, a signaling cascade in which increased *GCN4* mRNA levels promote transcription of amino acid biosynthetic machinery and permeases (Hinnebusch, 1990). To examine amino acid starvation, a plasmid harboring a *GCN4-lacZ* fusion gene was transformed into yeast cells and assayed for β-galactosidase activity following dieldrin exposure. As shown in Figure 6B, dieldrin induces β-galactosidase expression from the *GCN4-lacZ* fusion in both wild-type and *bap2*Δ cells, demonstrating that amino acid starvation occurs in the presence of dieldrin. Interestingly, although autophagy mutants (which are involved in the starvation response) were identified as sensitive by DSSA at the highest dose of dieldrin, we were unable to confirm growth defects in YPD (after 24 or 48 h) or leucine deficient media (Table 2.4 and data not shown).

Ras/PKA signaling, but not the target of rapamycin pathway, is implicated in dieldrin toxicity

In *S. cerevisiae*, the two main nutrient signal transduction pathways are Ras/PKA and target of rapamycin (Tor); signaling through either may be affected during starvation for amino acids such as leucine. Rapamycin inhibits the yeast Tor pathway and induces a nitrogen starvation-like phenotype via formation of a toxic complex with Fpr1p (FKBP12) (Lorenz and Heitman, 1995). We hypothesized that dieldrin was acting similarly to rapamycin, as rapamycin also affects amino acid availability (Beck *et al.*, 1999) and various amino acid signaling mutants sensitive to dieldrin (Fig. 2.3A) have been confirmed as sensitive to rapamycin (Xie *et al.*, 2005). However, multiple lines of evidence suggest otherwise. Deletion of *FPR1* or *TOR1* confers resistance or sensitivity, respectively, to rapamycin (Xie *et al.*, 2005) but neither of these mutants was affected by dieldrin (Fig. 2.7A). Moreover, removal of components downstream of Tor (*SIT4*, *SAP4*, *SAP155*, *TIP41*, *RRD1*, and *RRD2*) and peptidyl-prolyl cis-trans isomerases related to Fpr1p (*FPR2*, *FPR3*, and *FPR4*) did not affect growth in dieldrin (Table 2.4 and data not shown). In

contrast, mutants known to exhibit altered Ras/PKA signaling were sensitive to dieldrin, including those unable to negatively regulate Ras (*gpb1*Δ, *gpb2*Δ, and *ira2*Δ) or PKA (*bcy1*Δ, deleted for the PKA regulatory subunit), with most unable to be rescued by leucine addition (Fig. 2.7B). Other mutants (*pfk26*Δ, *fpb26*Δ, *rmd5*Δ, and *vid30*Δ) lacking genes involved in the regulation of glucose metabolism, a process under the control of PKA, were sensitive to dieldrin (Fig. 2.9A), with *rmd5*Δ displaying leucine-dependent sensitivity to dieldrin (Fig. 2.9B). Together, these data show that proper Ras/PKA regulation is required for dieldrin tolerance, but the Tor pathway is not.

The PDH complex is necessary for resistance to dieldrin

The mitochondrially localized PDH complex catalyzes the oxidative decarboxylation of pyruvate to acetyl-CoA, thus linking glycolysis to the citric acid cycle. Our DSSA and meta-analysis identified four out of the five subunits of PDH (Lpd1p, Lat1p, Pdx1p, and Pdb1, but not Pda1p) as sensitive to dieldrin, which was confirmed by the flow cytometry relative growth assay (Fig. 2.8A and Table 2.4). Surprisingly, exogenous leucine moderately reversed the sensitivity of these mutants to dieldrin. In addition, similar to BY4743 wild-type, *bap2*Δ , and *rmd5*Δ (Fig. 2.4 and 2.S2B), the *pdb1*Δ and *lat1*Δ PDH mutants were more sensitive to dieldrin when the leucine concentration in the media was decreased (Fig. 2.8B).

DISCUSSION

Dieldrin is a bioaccumulative and persistent pollutant with the potential to cause adverse effects on both the environment and human health (ATSDR, 2002). In this study, we performed a functional screen to identify nonessential yeast deletion mutants experiencing growth defects in dieldrin. Functional profiling of yeast mutants has not been reported for dieldrin or any other environmentally persistent halogenated contaminant. Confirmation of the yeast genes required for dieldrin tolerance, many of which are conserved in humans (Table 2.3), suggested a mechanism of toxicity – altered leucine availability – that was validated by further experimentation. In yeast, the toxic mechanism of dieldrin is different from that of the toxaphene OCP (Gaytán *et al.*, in submission). Overlapping GO categories were not identified between our study and gene expression profiles in dieldrin-exposed largemouth bass (Martyniuk *et al.*, 2010), but specific transcriptional responses do not always correlate with genes required for growth under a selective condition (Giaever *et al.*, 2002).

Yeast functional genomics, although an invaluable tool in the field of toxicology, is not without its limitations. First, achieving toxicity in yeast often requires high concentrations of xenobiotic; considering the presence of a cell wall and multidrug resistance machinery, this is not surprising. To increase toxicant sensitivity, a strain deleted for important drug resistance transporters could potentially serve as the deletion library background. Dieldrin concentrations used in this study (115-690μM) are higher than those reported as toxic to human cells (25-50μM) (Ledirac *et al.*, 2005). Since the ban of dieldrin, National Health and Nutrition Examination Surveys (NHANES) surveys describe a steady decrease in mean human blood serum concentrations (maximum 1.4 ppb in the 1976-1980 data); therefore, our results may be most relevant to (1) those with a history of dieldrin exposure; (2) populations living in termiticide-treated homes; and (3) communities consuming fish or other bioaccumulating aquatic species caught adjacent to

dieldrin-contaminated hazardous waste sites. Second, although endogenous P450 enzymes can mediate xenobiotic biotransformation in yeast (Käppeli, 1986), differences in metabolism complicates direct comparison with humans. To address these concerns, human S-9 liver microsomes may be added to catalyze toxicant activation. Third, one cannot identify target organs or adverse systemic effects, such as perturbations of the endocrine, immune, or circulatory systems. The discovery of non-obvious equivalent mutant phenotypes between different species (i.e., orthologous phenotypes) may prove useful in this arena. For example, McGary *et al.* (2010) identified five genes shared between studies examining yeast deletion strain sensitivity to the hypercholesterolemia drug lovastatin and abnormal angiogenesis in mutant mice, suggesting that despite the lack of blood vessels, yeast can model the genetics of mammalian vasculature formation. Similar analyses of yeast functional toxicogenomics data, although not performed within this study, may reveal potential mechanisms of action related to more complex biological processes not present in yeast.

Compounds other than dieldrin alter amino acid availability in yeast, including the immunosuppressant drugs rapamycin (Beck *et al.*, 1999), FK506 (Heitman *et al.*, 1993), and FTY720 (Welsch *et al.*, 2003), the anti-malarial drug quinine (Khozoie *et al.*, 2009), the anesthetic isoflurane (Palmer *et al.*, 2002), and the orphan drug phenylbutyrate (Grzanowski *et al.*, 2002). The chemical structure of dieldrin does not exhibit similarity to any of these compounds. Portions of our data suggested that the mechanism of action for dieldrin is similar to rapamycin, but removal of the rapamycin targets Fpr1p or Tor1p, which results in rapamycin resistance and sensitivity, respectively, does not affect growth in the presence of dieldrin (Fig. 2.7A). FK506 and FTY720 inhibit uptake of leucine and tryptophan (Heitman *et al.*, 1993; Welsch *et al.*, 2003); however, a mutant lacking *TAT2*, a high-affinity tryptophan and tyrosine permease, was not sensitive to dieldrin (Fig. 2.3C). Moreover, inhibition of amino acid uptake is dependent upon a 4-5h preincubation of yeast cells with FK506 or FTY720, indicating that time is needed for the drug's effects, possibly because transporter folding, assembly, or transport is altered. In contrast, dieldrin inhibited amino acid uptake without preincubation, a result similar to that for the antimalarial drug quinine, which competitively inhibits tryptophan uptake via the Tat2p permease (Khozoie *et al.*, 2009). Further studies are needed to determine if dieldrin inhibits amino acid transport by binding directly to a leucine permease.

Although our results do not indicate that dieldrin's toxic mechanism in yeast is conserved to humans, studies have demonstrated that dieldrin and other OCPs can alter availability of amino acids or their derivatives in mammalian systems. An oral dose of dieldrin to rhesus monkeys depressed leucine uptake in the intestine (Mahmood *et al.*, 1981), whereas a series of ip injections of lindane, a related OCP, decreased leucine transport in chicken enterocytes (Moreno *et al.*, 1994). Leucine uptake was decreased in rat intestine after a single oral dose of9 endosulfan, another OCP (Wali *et al.*, 1982). Of greater concern is the potential for dieldrin, a known neurotoxicant linked to Alzheimer's and Parkinson's diseases, to affect the levels of amino acids or their derivatives in the brain. Several neurotransmitters are amino acids (glutamate, aspartate, and glycine) or amino acid derivatives (tryptophan is the precursor for serotonin, tyrosine for dopamine, and glutamate for GABA). Leucine is neither a neurotransmitter nor a precursor, but it furnishes α-NH_2 groups for glutamate synthesis via the branched-chain amino

acid aminotransferase, thus playing a major role in regulating cellular pools of the glutamate neurotransmitter (Yudkoff *et al.*, 1994). Further experimentation is necessary to determine whether dieldrin inhibits leucine uptake in human cells or more complex organisms.

Genes encoding proteins that negatively regulate Ras (the *GPB1*/*GPB2* paralogs and *IRA2*) or PKA (*BCY1*) are required for dieldrin tolerance (Fig. 2.7B). Combined with evidence that *gpb1*Δ*gpb2*Δ , *ira2*Δ, and *bcy1*Δ strains are intolerant to nitrogen starvation (Harashima and Heitman, 2002; Tanaka *et al.*, 1990), these data are consistent with dieldrin's ability to decrease leucine (nitrogen) availability (Fig. 2.6A) and induce nitrogen starvation via Gcn4p (Fig. 2.6B). Double *GPB1*/*2* as well as single *IRA2* or *BCY1* deletion mutants also display phenotypes consistent with hyperactive Ras or PKA (Harashima and Heitman, 2002), phenomena linked to cancer in humans. A constitutively active Ras2Val19 protein reduces the response of leucine transport to a poor nitrogen source (Sáenz *et al.*, 1997), but experiments with a Ras2Val19 allele did not alter sensitivity to dieldrin (data not shown). Dieldrin has tumor-promoting properties in rodents (ATSDR, 2002), possibly via inhibition of intracellular gap junction channels (Matesic *et al.*, 2001). Chaetoglobosin K, a compound with Ras tumor suppressor activity, alleviates dieldrin inhibition of gap junction channels (Matesic *et al.*, 2001). Dieldrin also affects signaling downstream of Ras, increasing phosphorylated Raf, MEK1/2, and ERK1/2 in human keratinocytes (Ledirac *et al.*, 2005). Human homologs of the Ras/PKA signaling genes required for dieldrin resistance in yeast are posited tumor suppressors, including the *IRA2* homolog neurofibromin 1 and the *GPB1*/*2* functional ortholog *ETEA* (Phan *et al.*, 2010). If our data are validated in higher organisms, it may suggest that an individual with altered Ras/PKA signaling is more susceptible to dieldrin.

Components of the highly conserved mitochondrial PDH complex were also identified as necessary for dieldrin tolerance (Fig. 2.8 and Table 2.3). PDH links glycolysis to the citric acid cycle by catalyzing the oxidative decarboxylation of pyruvate to acetyl-CoA (reviewed in Pronk *et al.*, 1996). Leucine modestly reversed the sensitivity of PDH mutants to dieldrin, indicating that leucine is necessary for or a product of a PDH-mediated process needed for dieldrin tolerance. Except for *LAT1*, all PDH genes contain putative recognition sites for the master regulator of the amino acid starvation response, *GCN4* (Wenzel *et al.*, 1992), with *LPD1* under the control of Gcn4p during amino acid starvation (Zaman *et al.*, 1999). This suggests that PDH is involved in the starvation response, which we show is induced by dieldrin (Fig. 2.6B). In addition, the *pda1*Δ strain demonstrates a partial leucine requirement for growth (Wenzel *et al.*, 1992). Reduced PDH activity has been associated with various neurodegenerative diseases, including Alzheimer's and Huntington's diseases (Sorbi *et al.*, 1983), and mice deficient in dihydrolipoamide dehydrogenase (*DLD* - the *LPD1* homolog) show increased vulnerability to 1-methyl-4-phenyl-1,2,3,6-tetrahydropyridine (MPTP), a dopaminergic neurotoxicant used as a model for Parkinson's disease (Klivenyi *et al.*, 2004).

We hypothesize a simple model connecting leucine uptake, Ras/PKA signaling, and PDH. Our results suggest that dieldrin likely affects leucine uptake at the amino acid transporter level. Leucine auxotrophs, along with strains lacking leucine transporters or requisite amino acid signaling, cannot adequately cope with the resulting leucine starvation and therefore experience

growth defects in dieldrin. Leucine starvation caused by dieldrin would also be detrimental to strains unable to negatively regulate Ras/PKA, as activation of this signaling pathway promotes cell growth, a cellular process incompatible with the starvation response. Finally, the sensitivity of PDH mutants may be explained by their inability to activate starvation pathways essential for the response to dieldrin-induced leucine depletion. Our results underscore the value of functional profiling in yeast and provide data useful for further gene or pathway specific studies.

FIGURES

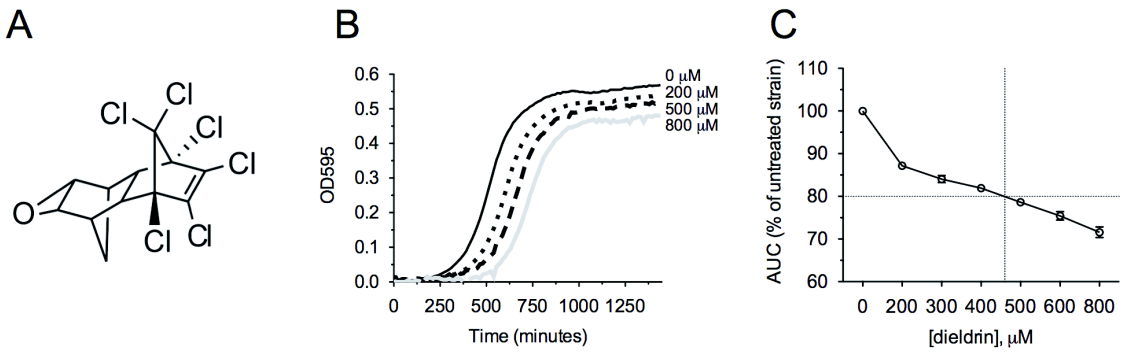

Figure 2.1. Dose determination of dieldrin IC20 for functional profiling. (A) The chemical structure of dieldrin. (B) Representative growth curves for the BY4743 wild-type strain treated with dieldrin in YPD media. Curves were performed for 200, 300, 400, 500, 600, and 800µM dieldrin, but for clarity, only the 200, 500, and 800µM doses are shown. (C) The area under the curve (AUC) at each dose was expressed as the mean and SEs of three independent experiments and plotted as a percentage of the untreated control. Dashed lines indicate the dose (460µM) at which growth was inhibited by 20% (IC20).

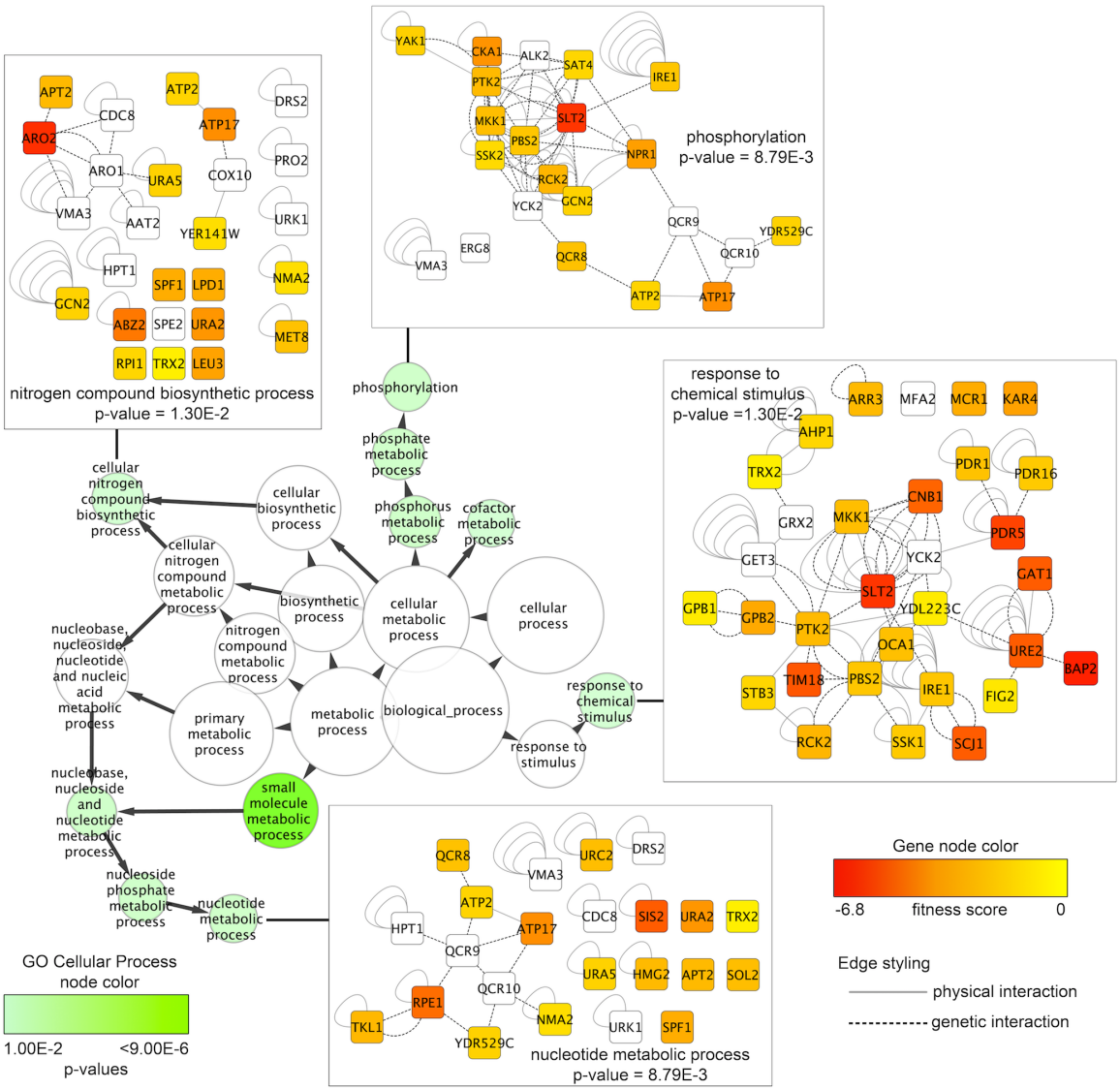

Figure 2.2. Cytoscape network mapping identifies biological attributes required for dieldrin tolerance. Fitness scores (the difference in the mean of the log2 hybridization signal between DMSO and dieldrin treatment) for strains displaying sensitivity to at least two dieldrin treatments were mapped onto the *S. cerevisiae* BioGRID interaction dataset using Cytoscape. A smaller subnetwork (235 genes) was created containing genetic and physical interactions between the sensitive, non-sensitive, and essential genes. Significantly overrepresented (*p* value cutoff of 0.03) GO categories were visualized as a network in which the green node color corresponds to significance, whereas node size indicates the number of genes present in the category. Edge arrows indicate hierarchy of GO terms. Gene networks corresponding to various GO categories are shown, where node color signifies the deletion strain fitness score (fitness not determined for white nodes) and edge styling defines the interaction between nodes.

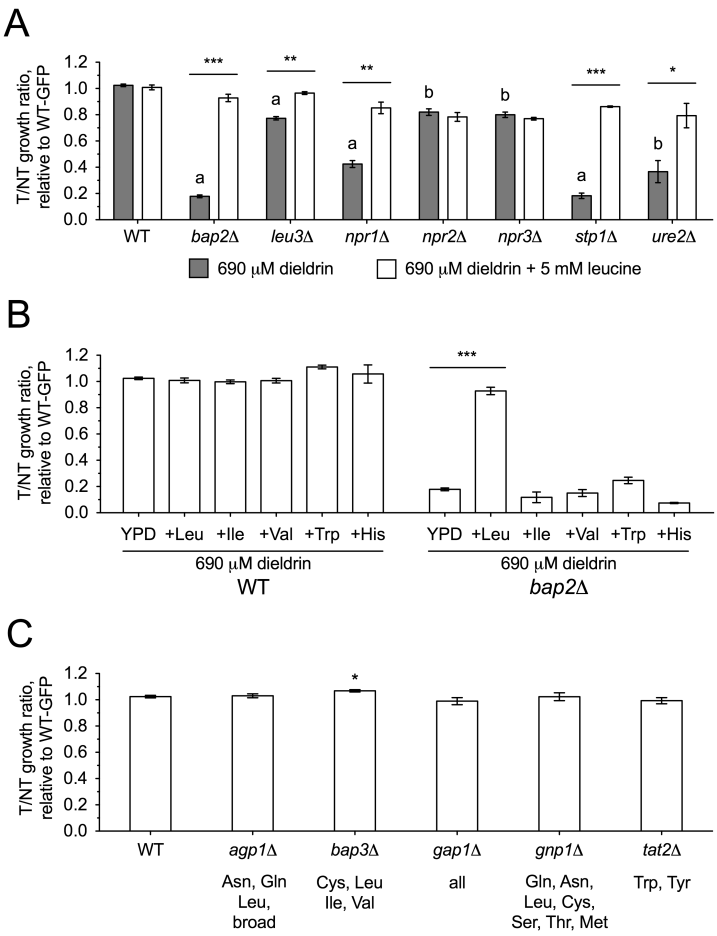

Figure 2.3. Dieldrin sensitivity of mutants involved in amino acid or nitrogen processes is reversed by leucine. Deletion mutants were tested for sensitivity to the dieldrin IC25 (690μM) by flow cytometry, in which relative growth of each mutant was compared with a wild-type GFP strain after 24 hours. Means of the growth ratios (treatment vs. control - T/NT) to wild-type GFP are shown with SEs for three independent cultures. Significance values were calculated by Student's *t*-test, where [a]=p<0.001 and [b]=p<0.01 for dieldrin-treated wild-type vs. mutant, whereas ***=*p*<0.001, **=*p*<0.01, and *=*p*<0.05 for dieldrin vs. dieldrin-leucine treatment. (A) Amino acid uptake and signaling mutants, as well as those involved in nitrogen utilization, are sensitive to dieldrin, with most mutants rescued by addition of 5mM leucine. (B) Amino acids related to leucine or transported by Bap2p cannot reverse dieldrin sensitivity in *bap2*Δ. Leucine, isoleucine, valine, and histidine were added to YPD media at a final concentration of 5mM, whereas tryptophan was present at 2.5mM. (C) Mutants lacking amino acid transporters other than Bap2p are not sensitive to dieldrin. Amino acids reported to be transported by the missing protein are indicated below the strain. Statistically significant differences between the dieldrin-treated wild-type and mutant strains were determined with Student's *t*-test, where *=*p*<0.05.

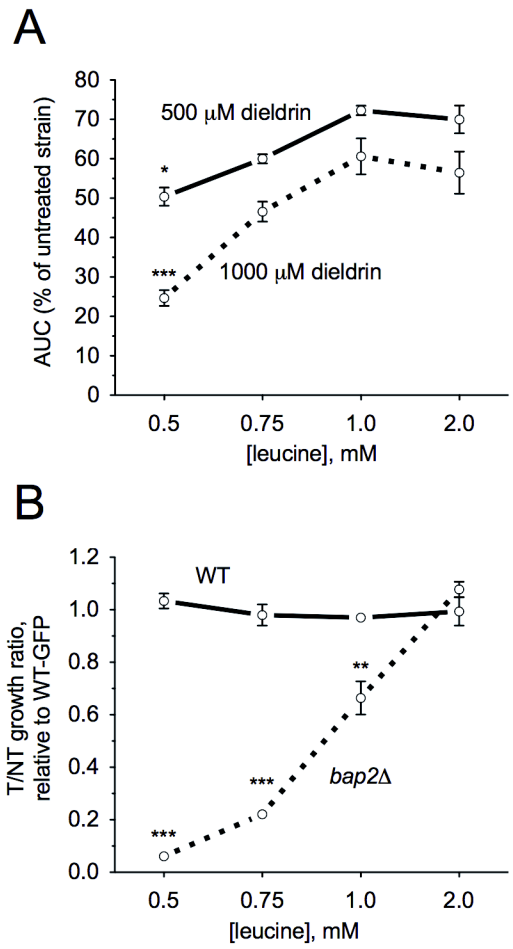

Figure 2.4. Limiting leucine exacerbates dieldrin sensitivity. Cells were cultured in media containing defined concentrations of leucine. (A) The BY4743 wild-type strain is dependent on leucine for dieldrin tolerance. Growth curves were performed for the indicated doses of dieldrin and the area under the curve (AUC) was calculated. Graphs express AUC as a percentage of untreated wild-type with SE for three independent cultures. Statistical significance between the 2mM leucine AUC and the 0.5, 0.75, and 1mM leucine AUCs was determined by Student's *t*-test, where ***=$p<0.001$ and *=$p<0.05$. (B) The *bap2*Δ strain exhibits increased sensitivity to the dieldrin IC25 (690μM) at decreased leucine concentrations. Flow cytometry confirmed altered growth ratios, with data displayed as the mean and SEs of three independent cultures. Statistical significance between the corresponding leucine doses in wild-type and *bap2*Δ was calculated by Student's *t*-test, where ***=$p<0.001$ and **=$p<0.01$.

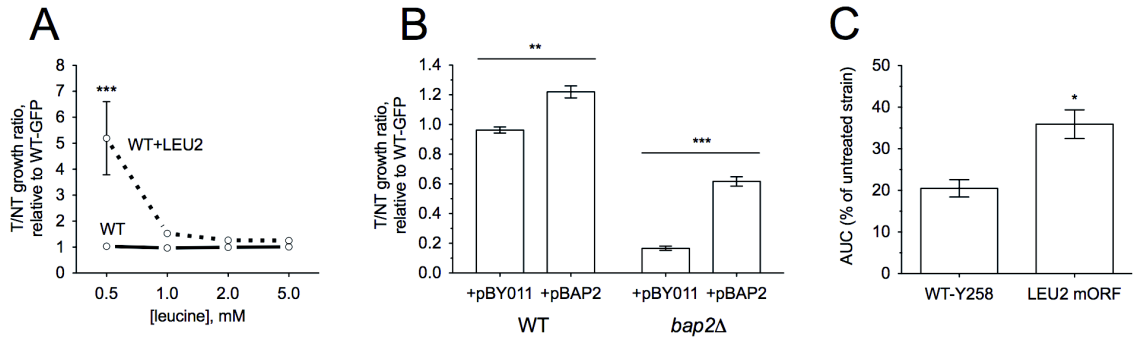

Figure 2.5. Increasing intracellular leucine results in dieldrin resistance. All data shown represent the mean and SEs for three independent cultures. (A) Knock-in of the *LEU2* gene into BY4743 wild-type increases dieldrin resistance. Cells were cultured in media (SC-LEU) containing defined concentrations of leucine along with the dieldrin IC25 (690 μM) and assayed for relative growth to the GFP-expressing BY4743 wild-type strain, which lacks *LEU2*. Resistance was not seen in YPD media (data not shown). Data were analyzed with two-way ANOVA with a Bonferroni post-test, where ***=p<0.001, compared with the corresponding leucine dose in wild-type. (B) Wild-type or *bap2*Δ strains overexpressing Bap2p exhibit increased resistance to dieldrin. Cells harboring empty vector or the HIP FlexGene *BAP2* ORF were cultured in SC-LEU media containing 1mM leucine and the dieldrin IC25 (690μM). Relative growth to a wild-type-GFP strain was assayed by flow cytometry and statistical significance was determined by Student's *t*-test, where ***=p<0.001 and **=p<0.01. (C) Overexpression of Leu2p imparts resistance to dieldrin in the Y258 haploid wild-type strain. Growth curve analyses were performed in YPD for dieldrin-treated (IC25: 690μM) Y258 cells overexpressing Leu2p. The area under the curve (AUC) is expressed as a percentage of the untreated strain. Statistical significance was calculated with Student's *t*-test, with *=p<0.05.

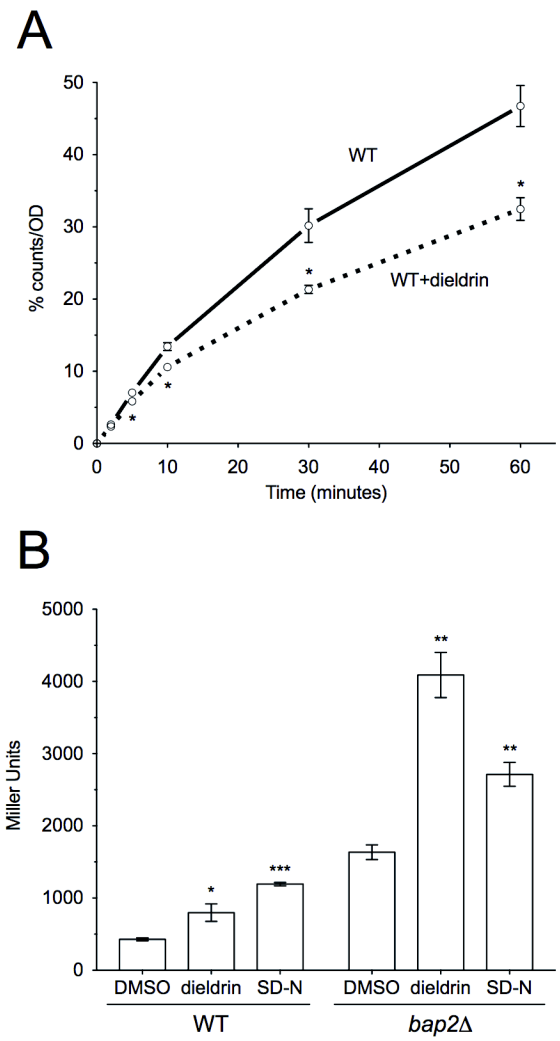

Figure 2.6. Dieldrin inhibits leucine uptake and induces the starvation response. (A) Leucine uptake is inhibited in the presence of dieldrin. Radiolabelled leucine was incubated with yeast cells with or without the dieldrin IC20 (460µM) and uptake was measured by counting radioactivity bound to the filter. Each time point was normalized for cell number and expressed as a percentage of combined total measured radioactivity over the time course for the control. The means and SEs for three independent experiments are shown. Statistical significance between corresponding time points was determined by Student's *t*-test, where *=p<0.05. (B) Dieldrin induces amino acid starvation. *GCN4-lacZ* expression was measured via β-galactosidase activity after treating wild-type or *bap2*Δ cells with the dieldrin IC20 (460µM) in SC-ura or SD-N media. Miller Units were calculated as described in Materials and Methods. The means and SEs for two to three independent cultures are shown. Data were analyzed with Student's *t*-test. ***=p<0.001, **=p<0.01, *=p<0.05.

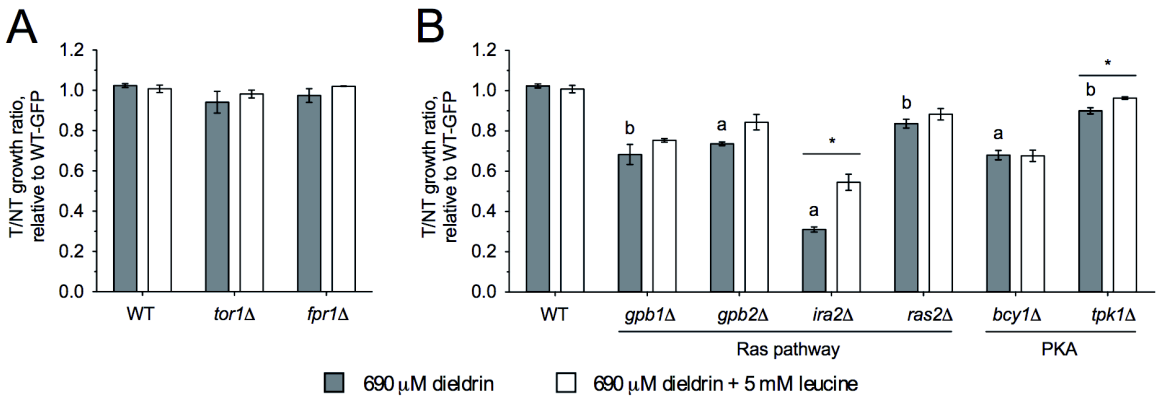

Figure 2.7. Altered Ras/PKA, but not Tor signaling, causes dieldrin sensitivity. Relative growth ratios (treatment vs. control) to the GFP-expressing wild-type strain were obtained. All data represent the mean and SE for three independent YPD cultures treated with the dieldrin IC25 (690μM). Statistical significance between dieldrin-treated wild-type and mutant strains were determined with Student's *t*-test, where $^{a}p<0.001$ and $^{b}p<0.01$. Statistical differences between a dieldrin-treated strain versus the same strain treated with dieldrin and leucine are shown as $*=p<0.05$. (A) Dieldrin does not affect strains lacking components involved in Tor signaling. (B) Strains unable to negatively regulate Ras or PKA are sensitive to dieldrin.

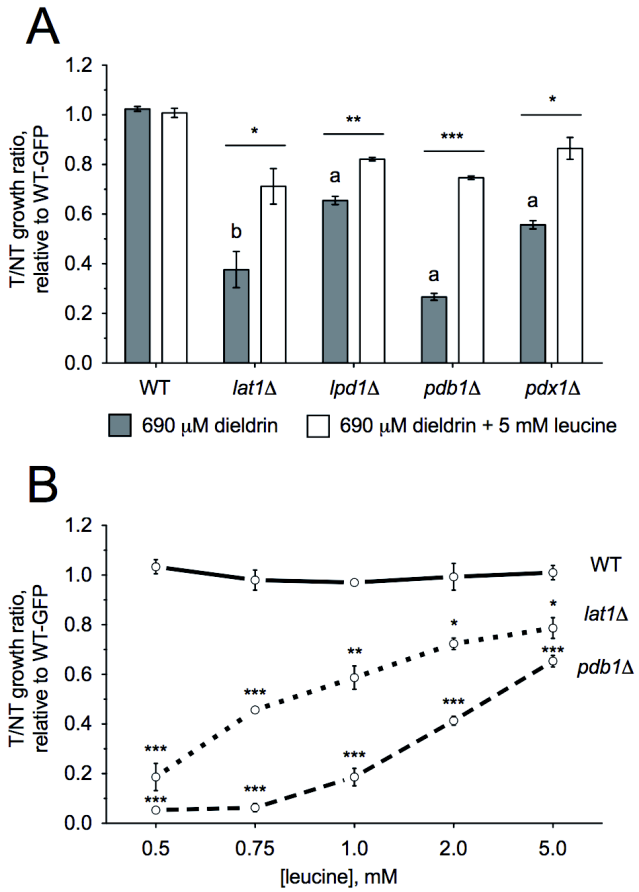

Figure 2.8. The PDH complex is required for dieldrin tolerance. Relative growth ratios (treatment vs. control) to the GFP-expressing wild-type strain were obtained for three independent YPD cultures, for which the means and SEs are shown. Dieldrin was added at a final concentration of 690μM (IC25). (A) Four PDH subunits are necessary for dieldrin resistance in YPD. (B) The *lat1*Δ and *pdb1*Δ strains exhibit dieldrin sensitivity that is dependent on leucine concentration. Strains were grown in media containing defined concentrations of leucine and assayed for relative growth to a wild-type GFP strain. Statistical significance between corresponding leucine doses in wild-type and mutant strains was determined by Student's *t*-test, where ***=$p<0.001$, **=$p<0.01$, and *=$p<0.05$.

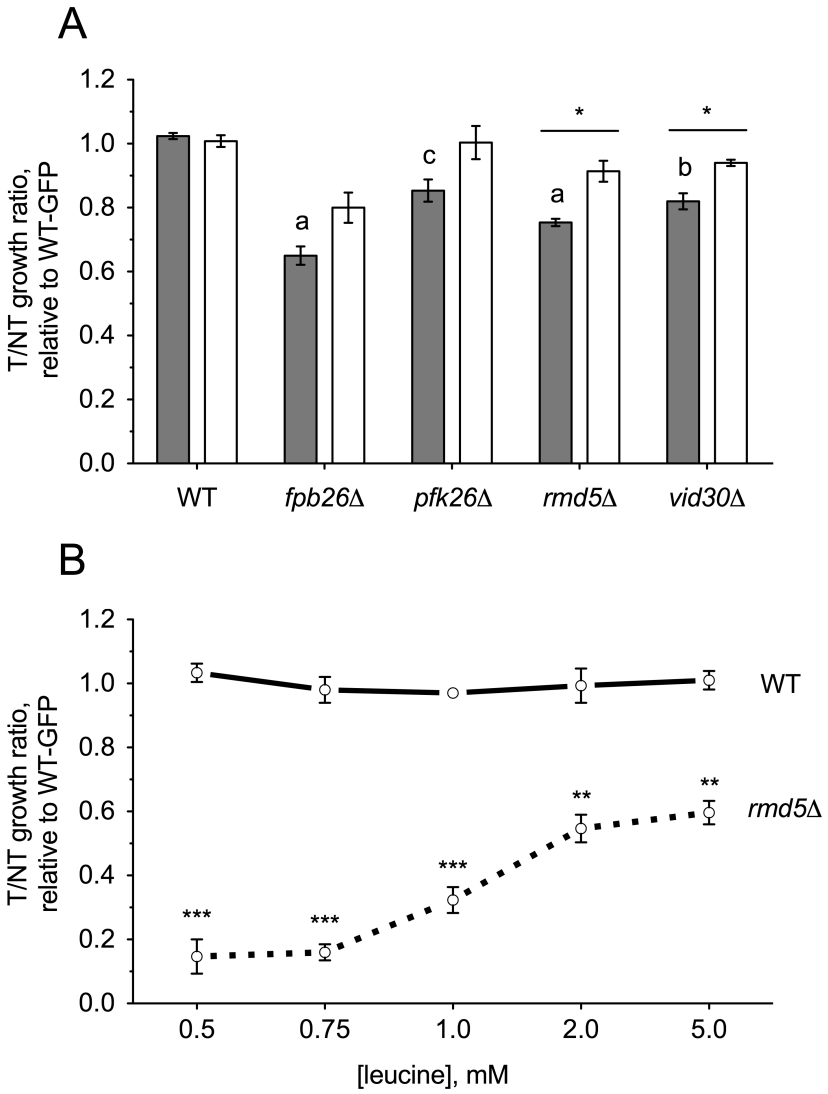

Figure 2.9. Proper regulation of glucose metabolism is required for dieldrin resistance. Relative growth ratios (treatment vs. control) to a GFP-expressing wild-type strain were obtained for three independent cultures exposed to the dieldrin IC25 (690μM), for which the means and standard errors are shown. (A) Genes involved in the regulation of glucose metabolism (a process partly under the control of PKA) are required for dieldrin tolerance. Strains were grown in YPD. Statistically significant differences between dieldrin-treated wild-type and mutant strains were determined with Student's *t*-test, where ^{a}=p<0.001, ^{b}=p<0.01, ^{c}=p<0.05, and *=p<0.05 for differences between a dieldrin-treated strain versus the same strain treated with dieldrin and leucine. (B) Limiting leucine exacerbates dieldrin sensitivity in the *rmd5*Δ strain. The mutant strain was cultured in SC-LEU media containing defined concentrations of leucine. Statistical significance between corresponding leucine doses in wild-type and *rmd5*Δ was determined by Student's *t*-test where ***=p<0.001 and **=p<0.01.

TABLES

Table 2.1. Fitness scores for the top 25 mutants identified as significantly sensitive to the dieldrin IC20 (460µM) after 15 generations of growth. Fitness scores quantify the requirement of a gene for growth and are defined as the normalized log2 ratio of the deletion strain's growth in the presence versus absence of dieldrin. A total of 427 genes were important for fitness (i.e., had negative fitness scores) in at least one dieldrin treatment. Appendix 1 contains a list of all genes identified as significant by DSSA.

log2 values				
25% IC20	**50% IC20**	**100% IC20**	**Deleted Gene**	**Description**
-3.90	-4.95	-6.80	***IRA2***	GTPase-activating protein; negatively regulates Ras
-4.00	-4.40	-6.10	***GYP1***	GTPase-activating protein; involved in vesicle docking
-5.60		-5.65	***BAP2***	High-affinity leucine permease
-3.75	-4.85	-5.60	***PDC1***	Major of three pyruvate decarboxylase isozymes
-3.10	-3.95	-5.25	***YJL120W***	Dubious ORF; partially overlaps the verified gene RPE1
-4.90	-4.50	-5.05	***PDR5***	Multidrug transporter
-4.70	-5.20	-5.00	***YCR007C***	Putative integral membrane protein
-3.10	-3.10	-4.90	***IRS4***	Regulates PtdIns(4,5)P2 levels and autophagy
-1.30	-1.60	-4.90	***SOK2***	Regulator of PKA signal transduction pathway
-1.65	-1.45	-4.85	***TCB3***	Lipid-binding protein
-3.80	-5.30	-4.80	***SLT2***	MAPK involved in cell wall integrity and cell cycle progression
-4.90	-4.90	-4.80	***YML079W***	Unknown function; structurally similar to plant storage proteins
-4.15	-4.45	-4.70	***TIM18***	Component of the mitochondrial TIM22 complex
-2.00	-2.40	-4.70	***OPI3***	Phospholipid methyltransferase
-3.20	-3.40	-4.60	***SIS2***	Negative regulatory subunit of protein phosphatase 1
-2.55	-2.35	-4.60	***SCJ1***	Homolog of bacterial chaperone DnaJ
-4.20	-3.50	-4.50	***SIW14***	Tyr phosphatase; involved in actin organization and endocytosis
-2.10	-2.55	-4.45	***CNB1***	Calcineurin B; the regulatory subunit of calcineurin
-2.30	-2.75	-4.35	***OSH3***	Oxysterol-binding protein; functions in sterol metabolism
-1.90	-2.85	-4.25	***UFD2***	Ubiquitin chain assembly factor (E4)
-3.05	-4.90	-4.10	***IMP2'***	Transcriptional activator; maintains ion homeostasis
-3.05	-2.75	-4.10	***BRE5***	Ubiquitin protease cofactor; forms complex with Ubp3p
-4.00	-4.30	-4.00	***SAP4***	Protein required for function of the Sit4p protein phosphatase
-2.90	-3.60	-4.00	***ECM30***	Non-essential protein of unknown function
-2.60	-2.40	-4.00	***BST1***	GPI inositol deacylase; negatively regulates vesicle formation

Table 2.2. Genes required for growth in the presence of dieldrin and their associated MIPS or GO categories. A list of strains exhibiting sensitivity to at least two out of the three doses of dieldrin was entered into the FunSpec tool and analyzed for overrepresented biological attributes (see Materials and Methods section). [a]Number of genes in category identified as sensitive to dieldrin. [b]Number of genes in GO or MIPS category.

GO Biological Process	***p* value**	**Genes identified**	**k[a]**	**f[b]**
protein folding in endoplasmic reticulum [GO:0034975]	3.23E-004	*EMC1 JEM1 EMC2 SCJ1*	4	11
regulation of nitrogen utilization [GO:0006808]	3.43E-004	*VID30 NPR1 URE2*	3	5
protein phosphorylation [GO:0006468]	4.34E-004	*SAT4 GCN2 SLT2 IRE1 CKA1 PBS2 YAK1 PTK2 RCK2 NPR1 SSK2 MKK1 DBF20*	13	133
negative regulation of Ras protein signal transduction [GO:0046580]	6.68E-004	*GPB2 IRA2 GPB1*	3	6
MIPS Functional Classification	***p* value**	**Genes identified**	**k[a]**	**f[b]**
regulation of nitrogen metabolism [01.02.07.01]	7.42E-005	*GAT1 VID30 NPR1 URE2*	4	8
modification by phosphorylation, dephosphorylation, autophosphorylation [14.07.03]	1.33E-004	*SAT4 GCN2 SAP4 SLT2 IRE1 CKA1 PBS2 YAK1 PTK2 CNB1 RCK2 SIW14 OCA1 NPR1 SSK2 MKK1 DBF20*	17	186
G1/S transition of mitotic cell cycle [10.03.01.01.03]	1.77E-004	*SAT4 BCK2 SAP4 CKA1 VHS2 PTK2 SIS2*	7	37
regulation of glycolysis and gluconeogenesis [02.01.03]	3.05E-004	*RMD5 UBC8 VID30 PFK26 FBP26*	5	19
pyruvate dehydrogenase complex [02.08]	3.43E-004	*PDB1 LPD1 PDX1*	3	5
degradation of glycine [01.01.09.01.02]	6.68E-004	*GCV3 LPD1 SHM2*	3	6
phosphate metabolism [01.04]	7.16E-004	*SAT4 RBK1 GCN2 PPN1 YND1 SAP1 SAP4 SLT2 INM1 IRE1 CKA1 PFK26 PBS2 YAK1 FBP26 PTK2 CNB1 RCK2 SIW14 OCA1 NPR1 PEX6 SSK2 LCB4 MKK1 DBF20*	26	401
MIPS Phenotypes	***p* value**	**Genes identified**	**k[a]**	**f[b]**
Sensitivity to other aminoacid analogs and other drugs [92.99]	3.72E-005	*RVS161 PDR1 LST7 PBS2 PTK2 HMG2 LEU3 TAT2 PDR5*	9	51
Starvation sensitivity [62.10]	1.64E-004	*RVS161 VID30 SLT2 IRA2 MKK1 ATG13*	6	26

Table 2.3. Selected yeast genes required for dieldrin tolerance and their human orthologs. Deletion of any of these genes caused sensitivity to dieldrin (listed in alphabetical order).

Yeast gene(s)	Human ortholog	Human protein
BAP2	*SLC7A1*	cationic amino acid transport permease
BCY1	*PRKAR2A*	cAMP-dependent protein kinase regulatory subunit
FBP26/PFK26	*PFKFB1*	6-phosphofructo-2-kinase/fructose-2,6-bisphosphatase
GCN2	*EIF2AK4*	eukaryotic translation initiation factor 2-alpha kinase
GPB1/2	*ETEA*	functional ortholog of *GPB1/2*; inhibits neurofibromin 1
IRA2	*NF1*	neurofibromin 1, tumor suppressor protein
LAT1	*DLAT*	dihydrolipoamide acetyltransferase component of PDH complex
LPD1	*DLD*	dihydrolipoamide dehydrogenase component of PDH complex
NPR2	*NPRL2*	nitrogen permease regulator-like 2, tumor suppressor candidate
PDB1	*PDHB*	PDH, E1 component
PDX1	*PDHX*	anchors DLD to the DLAT core in the PDH complex
RAS2	*KRAS*	v-Ki-ras2 Kirsten rat sarcoma viral oncogene homolog
RMD5	*RMND5A*	required for meiotic nuclear division 5 *S. cerevisiae* homolog
VID30	*RANBP10*	Ran-binding protein 10

Table 2.4. Confirming dieldrin sensitivity for various strains by flow cytometry. A list of strains not shown in the main text that were tested for sensitivity to dieldrin. Ratios are defined as relative growth to a wild-type GFP strain between treated and control cultures. Statistically significant differences between wild-type and mutant strains as well as non-leucine and leucine treated strains were determined by Student's *t*-test, where ***=$p<0.001$, **=$p<0.01$, and *=$p<0.05$. ND=not determined, NA=not applicable, NS=not significant.

Strain	Description of deleted gene	dieldrin IC25 (690 µM) Ratio	SEM	*p*-value to WT	dieldrin IC25 (690 µM) + 5mM leucine Ratio	SEM	*p*-value to no leucine	Human homolog of deleted gene
Kinases and phosphatases								
oca1Δ	Tyrosine phosphatase	**0.389**	0.043	***	**0.884**	0.042	**	
ssk2Δ	MAPKKK of the HOG1 mitogen-activated signaling pathway	**0.787**	0.007	***	**0.949**	0.016	***	MAP3K4
ssk1Δ	Cytoplasmic response regulator	**0.854**	0.014	***	**0.990**	0.037	*	
cka1Δ	Alpha catalytic subunit of casein kinase 2	**0.888**	0.004	***	ND	ND	NA	CSNK2A1
gcn2Δ	Protein kinase; initiates starvation response	**0.907**	0.054	NS	**1.203**	0.046	*	EIF2AK4
ptc6Δ	Mitochondrial type 2C protein phosphatase	**0.909**	0.021	**	ND	ND	NA	PPM1K
Downstream of Tor								
sap155Δ	Required for function of the Sit4p protein phosphatase	**0.927**	0.022	*	**0.915**	0.027	NS	PPP6R1
sit4Δ	Type 2A-related serine-threonine phosphatase	**0.957**	0.020	NS	**0.957**	0.022	NS	PPP6
sap4Δ	Required for function of the Sit4p protein phosphatase	**1.036**	0.017	NS	**1.007**	0.019	NS	
Transcription activators/repressors								
imp2Δ'	Transcriptional activator; maintains ion homeostasis	**0.373**	0.091	**	ND	ND	NA	
spt8Δ	Subunit of the SAGA transcriptional regulatory complex	**0.470**	0.016	***	**0.825**	0.017	***	
mot3Δ	Transcriptional repressor	**0.633**	0.015	***	ND	ND	NA	
gat1Δ	Transcriptional activator for nitrogen catabolite repression genes	**1.027**	0.013	NS	0.983	0.019	NS	
Autophagy (48H treatment)								
atg13Δ	Required for vesicle formation during autophagy	**0.933**	0.023	*	**0.947**	0.026	NS	ATG13
atg12Δ	Ubiquitin-like modifier involved in autophagy and Cvt pathway	**0.993**	0.015	NS	**1.023**	0.034	NS	APG12
atg5Δ	Involved in autophagy and the Cvt pathway	**1.010**	0.012	NS	**0.987**	0.023	NS	ATG5
Other								
pdr5Δ	Multidrug transporter	**0.314**	0.040	***	**0.486**	0.037	*	ABCG2
opi3Δ	Phospholipid methyltransferase	**0.711**	0.045	**	ND	ND	NA	PEMT
bre5Δ	Ubiquitin protease cofactor	**0.714**	0.030	***	ND	ND	NA	
ufd2Δ	Ubiquitin chain assembly factor (E4)	**0.746**	0.061	*	ND	ND	NA	UBE4B
yen1Δ	Holliday junction resolvase	**0.754**	0.027	***	ND	ND	NA	GEN1
sac3Δ	Nuclear pore-associated protein	**0.757**	0.035	**	ND	ND	NA	MCM3AP
tim18Δ	Component of the mitochondrial TIM22 complex	**0.775**	0.024	***	ND	ND	NA	
par32Δ	Unknown function; phosphorylated upon rapamycin treatment	**0.787**	0.062	*	ND	ND	NA	
cnb1Δ	Calcineurin B; the regulatory subunit of calcineurin	**0.913**	0.008	**	**0.908**	0.016	NS	PPP3R1
thi3Δ	Role in branched chain amino acid degradation	**0.941**	0.014	**	ND	ND	NA	HACL1
pda1Δ	E1 alpha subunit of the pyruvate dehydrogenase complex	**0.969**	0.028	NS	ND	ND	NA	PDHA1

REFERENCES

Agency for Toxic Substances and Disease Registry (ATSDR). (2002). *Toxicological Profile for Aldrin/Dieldrin.* US Dept of Health and Human Services, ATSDR, Atlanta, GA.

Beck, T., Schmidt, A., Hall, M. N. (1999). Starvation Induces Vacuolar Targeting and Degradation of the Tryptophan Permease in Yeast. *J Cell Biol*. **146**, 1227–1238.

dos Santos, S. C., Teixeira, M. C., Cabrito, T. R., Sá-Correia, I. (2012). Yeast toxicogenomics: genome-wide responses to chemical stresses with impact in environmental health, pharmacology, and biotechnology. *Front Genet*. **3**, 63.

Gaytán, B. D., Loguinov, A. V., Lantz, S. R., Lerot, J.-M., Denslow, N. D., Vulpe, C. D. (2013). Functional profiling discovers the dieldrin organochlorinated pesticide affects leucine availability in yeast. *Toxicol. Sci.* **132**, 347–358.

Giaever, G., Chu, A. M., Ni, L., Connelly, C., Riles, L., Véronneau, S., Dow, S., Lucau-Danila, A., Anderson, K., André, B., *et al*. (2002). Functional profiling of the *Saccharomyces cerevisiae* genome. *Nature*. **418**, 387–391.

Grzanowski, A., Needleman, R., Brusilow, W. S. A. (2002). Immunosuppressant-like effects of phenylbutyrate on growth inhibition of *Saccharomyces cerevisiae*. *Curr. Genet.* **41**, 142–149.

Harashima, T., Heitman, J. (2002). The Gα protein Gpa2 controls yeast differentiation by interacting with kelch repeat proteins that mimic Gβ subunits. *Mol. Cell*. **10**, 163–173.

Heitman, J., Koller, A., Kunz, J., Henriquez, R., Schmidt, A., Movva, N. R., Hall, M. N. (1993). The immunosuppressant FK506 inhibits amino acid import in *Saccharomyces cerevisiae*. *Mol. Cell Biol.* **13**, 5010–5019.

Hinnebusch, A. G. (1990). Involvement of an initiation factor and protein phosphorylation in translational control of *GCN4* mRNA. *Trends Biochem. Sci.* **15**, 148–152.

Jo, W. J., Ren, X., Chu, F., Aleshin, M., Wintz, H., Burlingame, A., Smith, M. T., Vulpe, C. D., Zhang, L. (2009a). Acetylated H4K16 by MYST1 protects UROtsa cells from arsenic toxicity and is decreased following chronic arsenic exposure. *Toxicol. Appl. Pharmacol.* **241**, 294–302.

Jo, W. J., Loguinov, A., Wintz, H., Chang, M., Smith, A. H., Kalman, D., Zhang, L., Smith, M. T., Vulpe, C. D. (2009b). Comparative functional genomic analysis identifies distinct and overlapping sets of genes required for resistance to monomethylarsonous acid (MMAIII) and arsenite (AsIII) in yeast. *Toxicol Sci*. **111**, 424–436.

Jorgenson, J. L. (2001). Aldrin and dieldrin: a review of research on their production, environmental deposition and fate, bioaccumulation, toxicology, and epidemiology in the United States. *Environ. Health Perspect*. **109**, 113–139.

Käppeli, O. (1986). Cytochromes P-450 of yeasts. *Microbiol Rev*. **50**, 244–258.

Khozoie, C., Pleass, R. J., Avery, S. V. (2009). The antimalarial drug quinine disrupts Tat2p-mediated tryptophan transport and causes tryptophan starvation. *J. Biol. Chem.* **284**, 17968–17974.

Klivenyi, P., Starkov, A. A., Calingasan, N. Y., Gardian, G., Browne, S. E., Yang, L., Bubber, P., Gibson, G. E., Patel, M. S., Beal, M. F. (2004). Mice deficient in dihydrolipoamide dehydrogenase show increased vulnerability to MPTP, malonate and 3-nitropropionic acid neurotoxicity. *J. Neurochem.* **88**, 1352–1360.

Ledirac, N., Antherieu, S., d'Uby, A. D., Caron, J. C., Rahmani R. (2005). Effects of organochlorine insecticides on MAP kinase pathways in human HaCaT keratinocytes: key role of reactive oxygen species. *Toxicol. Sci*. **86**, 444–452.

Lorenz, M. C., Heitman, J. (1995). TOR mutations confer rapamycin resistance by preventing interaction with FKBP12-rapamycin. *J. Biol. Chem.* **270**, 27531–27537.

Mahmood, A., Agarwal, N., Sanyal, S., Dudeja, P. K., Subrahmanyam, D. (1981). Acute dieldrin toxicity: effect on the uptake of glucose and leucine and on brush border enzymes in monkey intestine. *Chem. Biol. Interact.* **37**, 165–170.

Martyniuk, C. J., Kroll, K. J., Doperalski, N. J., Barber, D. S., Denslow, N. D. (2010). Genomic and proteomic responses to environmentally relevant exposures to dieldrin: indicators of neurodegeneration? *Toxicol. Sci.* **117**, 190–199.

Matesic, D. F., Blommel, M. L., Sunman, J. A., Cutler, S. J., Cutler, H. G. (2001). Prevention of organochlorine-induced inhibition of gap junctional communication by chaetoglobosin K in astrocytes. *Cell Biol. Toxicol.* **17**, 395–408.

McGary, K. L., Park, T. J., Woods, J. O., Cha, H. J., Wallingford, J. B., Marcotte, E. M. (2010). Systematic discovery of nonobvious human disease models through orthologous phenotypes. *Proc. Natl. Acad. Sci. U.S.A.* **107**, 6544–6549.

Moreno, M. J., Pellicer, S., Marti, A., Arenas, J. C., Fernández-Otero, M. P. (1994). Effect of lindane on galactose and leucine transport in chicken enterocytes. *Comp. Biochem. Physiol. C Pharmacol. Toxicol. Endocrinol.* **109**, 159–166.

North, M., Steffen, J., Loguinov, A. V., Zimmerman, G. R., Vulpe, C. D., Eide, D. J. (2012). Genome-wide functional profiling identifies genes and processes important for zinc-limited growth of *Saccharomyces cerevisiae*. *PLoS Genet.* **8**, e1002699.

North, M., Tandon, V. J., Thomas, R., Loguinov, A., Gerlovina, I., Hubbard, A. E., Zhang, L., Smith, M. T., Vulpe, C. D. (2011). Genome-wide functional profiling reveals genes required for tolerance to benzene metabolites in yeast. *PLoS ONE*. **6**, e24205.

Palmer, L. K., Wolfe, D., Keeley, J. L., Keil, R. L. (2002). Volatile anesthetics affect nutrient availability in yeast. *Genetics*. **161**, 563–574.

Phan, V. T., Ding, V. W., Li, F., Chalkley, R. J., Burlingame, A., McCormick, F. (2010). The RasGAP proteins Ira2 and neurofibromin are negatively regulated by Gpb1 in yeast and ETEA in humans. *Mol. Cell Biol.* **30**, 2264–2279.

Pronk, J. T., Yde Steensma, H., Van Dijken, J. P. (1996). Pyruvate metabolism in *Saccharomyces cerevisiae*. *Yeast*. **12**, 1607–1633.

Regenberg, B., Düring-Olsen, L., Kielland-Brandt, M. C., Holmberg, S. (1999). Substrate specificity and gene expression of the amino-acid permeases in *Saccharomyces cerevisiae*. *Curr. Genet.* **36**, 317–328.

Richardson, J. R., Caudle, W. M., Wang, M., Dean, E. D., Pennell, K. D., Miller, G. W. (2006). Developmental exposure to the pesticide dieldrin alters the dopamine system and increases neurotoxicity in an animal model of Parkinson's disease. *FASEB J*. **20**, 1695–1697.

Sáenz, D. A., Chianelli, M. S., Stella, C. A., Mattoon, J. R., Ramos, E. H. (1997). RAS2/PKA pathway activity is involved in the nitrogen regulation of L-leucine uptake in *Saccharomyces cerevisiae*. *Int. J. Biochem. Cell Biol.* **29**, 505–512.

Singh, N., Chhillar, N., Banerjee, B., Bala, K., Basu, M., Mustafa, M. (2013). Organochlorine pesticide levels and risk of Alzheimer's disease in north Indian population. *Hum Exp Toxicol*. **32**, 24-30.

Sorbi, S., Bird, E. D., Blass, J. P. (1983). Decreased pyruvate dehydrogenase complex activity in Huntington and Alzheimer brain. *Ann. Neurol.* **13**, 72–78.

Steinmetz, L. M., Scharfe, C., Deutschbauer, A. M., Mokranjac, D., Herman, Z. S., Jones, T., Chu, A. M., Giaever, G., Prokisch, H., Oefner, P. J., *et al.* (2002). Systematic screen for human disease genes in yeast. *Nat. Genet.* **31**, 400–404.

Tanaka, K., Nakafuku, M., Satoh, T., Marshall, M. S., Gibbs, J. B., Matsumoto, K., Kaziro, Y., Toh-e, A. (1990). *S. cerevisiae* genes IRA1 and IRA2 encode proteins that may be functionally equivalent to mammalian ras GTPase activating protein. *Cell*. **60**, 803–807.

Wali, R. K., Singh, R., Dudeja, P. K., Mahmood, A. (1982). Effect of a single oral dose of endosulfan on intestinal uptake of nutrients and on brush-border enzymes in rats. *Toxicol. Lett.* **12**, 7–12.

Weisskopf, M. G., Knekt, P., O'Reilly, E. J., Lyytinen, J., Reunanen, A., Laden, F., Altshul, L., Ascherio, A. (2010). Persistent organochlorine pesticides in serum and risk of Parkinson disease. *Neurology*. **74**, 1055–1061.

Welsch, C. A., Hagiwara, S., Goetschy, J. F., Movva, N. R. (2003). Ubiquitin pathway proteins influence the mechanism of action of the novel immunosuppressive drug FTY720 in *Saccharomyces cerevisiae*. *J. Biol. Chem.* **278**, 26976–26982.

Wenzel, T. J., van den Berg, M. A., Visser, W., van den Berg, J. A., Steensma, H. Y. (1992). Characterization of *Saccharomyces cerevisiae* mutants lacking the E1 alpha subunit of the pyruvate dehydrogenase complex. *Eur. J. Biochem.* **209**, 697–705.

Xie, M. W., Jin, F., Hwang, H., Hwang, S., Anand, V., Duncan, M. C., Huang, J. (2005). Insights into TOR function and rapamycin response: chemical genomic profiling by using a high-density cell array method. *Proc. Natl Acad. Sci. U.S.A.* **102**, 7215–7220.

Yudkoff, M., Daikhin, Y., Lin, Z.-P., Nissim, L., Stern, J., Pleasure, D., Nissim, I. (1994). Interrelationships of Leucine and Glutamate Metabolism in Cultured Astrocytes. *J. Neurochem*. **62**, 1192–1202.

Zaman, Z., Bowman, S. B., Kornfeld, G. D., Brown, A. J., Dawes, I. W. (1999). Transcription factor GCN4 for control of amino acid biosynthesis also regulates the expression of the gene for lipoamide dehydrogenase. *Biochem. J.* **340 (Pt 3)**, 855–862.

CHAPTER 3

FUNCTIONAL PROFILING OF THE TECHNICAL TOXAPHENE ORGANOCHLORINATED PESTICIDE MIXTURE IN YEAST

INTRODUCTION

Toxaphene is a complex mixture of polychlorinated camphenes and bornanes primarily used to control insects on cotton during the 1960-80s (Figure 3.1A; ATSDR, 2010). After the ban of DDT in 1972, toxaphene became the most heavily applied pesticide in the United States, but all registered uses were cancelled by the U.S. Environmental Protection Agency (EPA) in 1989 over concerns related to its toxicity and persistence (NTP, 2011). Today, toxaphene remains a problematic environmental contaminant, ranking 32nd on the Agency for Toxic Substances and Disease Registry (ATSDR) Priority List of Hazardous Substances, a list of compounds that possibly threaten human health via their toxicity and possibility for exposure at EPA National Priorities List hazardous waste sites. Toxaphene's most persistent congeners and degradation products have been detected in water, air, and sediment, and are known to bioaccumulate in wildlife and humans (ATSDR, 2010). Animal studies have deemed toxaphene a neuro-, nephro-, immuno-, and hepatotoxicant, an endocrine disruptor, and a carcinogen, with the International Agency for Research on Cancer (IARC) classifying toxaphene as Group 2B (possibly carcinogenic to humans) (ATSDR, 2010; de Geus *et al.*, 1999). Epidemiological analyses have linked toxaphene to leukemia (Mills *et al.,* 2005), non-Hodgkin's lymphoma (Schroeder *et al.*, 2001), melanoma (Purdue *et al.*, 2007), and more recently, amyotrophic lateral sclerosis (Kamel *et al.*, 2012). However, the cellular and molecular processes that toxaphene perturbs to result in these toxicities and disease states remain unclear.

The eukaryotic yeast *Saccharomyces cerevisiae* is a valuable model in which to conduct toxicological studies. First, basic cellular processes, along with metabolic and signaling pathways, are conserved to higher organisms. Second, a close human homolog has been identified for a significant portion of yeast genes, with several hundred of the conserved genes linked to disease in humans (Steinmetz *et al.*, 2002). Finally, the availability of deletion mutant collections, overexpression libraries, and genetic and physical interaction data provide unmatched resources for inquiries into potential cellular and molecular mechanisms of toxicity. With the deletion mutant collection (Giaever *et al.*, 2002), functional toxicogenomic analyses (also known as functional profiling) can be conducted by examining, in parallel, the sensitivity or resistance of each mutant strain to a compound of interest. Such investigations, through the identification of yeast genes required for chemical tolerance, have discovered molecular mechanisms for numerous drugs and toxicants (reviewed by dos Santos *et al.*, 2012), with several studies confirming results in human cells (Blackman *et al.*, 2012; Jo *et al.*, 2009a; Skrtić *et al.*, 2011).

Here we present the results of a functional screen devised to identify yeast genes necessary for growth in the presence of toxaphene. It is the first known genome-wide study in any organism to examine the genetic requirements for toxaphene tolerance. Our results demonstrate that similar to the known transcription elongation inhibitors mycophenolic acid (MPA) and 6-azauracil (6-AU), mutants defective in processes linked to transcription elongation are sensitive to toxaphene. While toxaphene does display synergism with MPA, it apparently exhibits a mechanism of action distinct from that of MPA/6-AU and additionally does not appear to directly affect transcription elongation. Many yeast genes required for toxaphene resistance have human homologs that may play a role in human toxicity.

MATERIALS AND METHODS

Yeast strains and culture. The diploid non-essential yeast deletion strains used for functional profiling and confirmation analyses were of the BY4743 background (*MATa/MATα his3Δ1/his3Δ1 leu2Δ0/leu2Δ0 lys2Δ0/LYS2 MET15/met15Δ0 ura3Δ0/ura3Δ0,* Life Technologies). Yeast growth was performed in liquid rich media (1% yeast extract, 2% peptone, 2% dextrose, YPD) at 30°C with shaking at 200 revolutions per minute (rpm). For the elongation assays, the *GAL1-YLR454* strain (Mason and Struhl, 2005) was grown in rich media containing galactose (1% yeast extract, 2% peptone, 2% galactose, YPGal).

Dose-finding and growth curve assays. Dose-finding and growth curves were performed as in Gaytán *et al.* (2013). Toxaphene and MPA (Sigma Aldrich) solutions were prepared in dimethylsulfoxide (DMSO) and added to the desired final concentrations (1% or less by volume) with at least three technical replicates per dose. The area means and standard error (SE) for the growth of each strain (as measured by the area under the curve) was derived from three independent cultures.

Functional profiling of the yeast genome. The functional screen and differential strain sensitivity analysis (DSSA) were performed as previously described (Jo *et al.*, 2009b). Briefly, pools of deletion mutants (n = 4607) were cultured for 15 generations in YPD at various toxaphene concentrations. Following extraction of genomic DNA with the YDER kit (Pierce Biotechnology), DNA sequences unique to each strain were amplified by PCR and subsequently hybridized to TAG4 arrays (Affymetrix). Arrays were incubated overnight, stained, and scanned at 560 nm with a GeneChip Scanner (Affymetrix). Data files are available at the Gene Expression Omnibus database (http://www.ncbi.nlm.nih.gov/geo/).

Over-enrichment and network mapping analyses. The Functional Specification (FunSpec) resource (Robinson *et al.*, 2002) identified significantly overrepresented Gene Ontology (GO) and MIPS (Munich Information Center for Protein Sequences) categories within the DSSA data using a p value cutoff of 0.002 and Bonferroni correction. Gene interaction networks were generated in Cytoscape (Shannon *et al.*, 2003) by mapping fitness scores for toxaphene-sensitive strains onto the BioGrid *Saccharomyces cerevisiae* functional interaction network. The jActiveModules Cytoscape plugin identified sub-networks enriched with fitness data, within which the BiNGO plugin discovered overrepresented GO categories.

Analysis of relative strain growth by flow cytometry. Analyses of relative strain growth were performed as in Gaytán *et al.* (2013). Briefly, green fluorescent protein (GFP)-tagged wild-type and untagged deletion strains were mixed in approximately equal numbers and cultured for 24 hours at 30°C in the presence of toxaphene. At least 20,000 cells were analyzed at T=0 and T=24 hours using a FACSCalibur flow cytometer. A ratio of growth was calculated for untagged cells in treated versus untreated samples using the percentages of wild-type GFP and untagged mutant cells present. Statistically significant differences between the means of three independent DMSO-treated and toxaphene-treated cultures were determined with Student's t-test.

Analyses of transcription elongation. Gene Length Accumulation of mRNA (GLAM) assays were performed as described (Morillo-Huesca *et al.*, 2006). Chromatin immunoprecipitation experiments were performed as described (Rodríguez-Gil *et al.*, 2010), except mouse monoclonal anti-Rpb3 (1Y26, Abcam) antibody was used. Immunoprecipitated DNA was measured by quantitative PCR in a LightCycler (Roche), using the primers listed below. Normalizations required for RNA polymerase II processivity comparisons were applied as described (Mason and Struhl, 2005).

Primer Name	Sequence
1_100.txt-3F	GATGTTTCCGATTAATGTTCTACTGTACAA
1_100-66R	GCTCCATAAGAAAGTCACTGCAAA
1900-2000-3F	AGACAGAAGGAAATTTTACCAAGCG
1900-2000-63R	AATCGAAAAAATCAGGTAGTTGCTG
3800-4100-191F	GATATGCTTCAATCCGACAGAGAG
3800-4100-258R	TCAACAGTTACCGATGGTATTAAAGG
5800-6100-2F	AGCCGGACAAACAGAACAGC
5800-6100-71R	CAGGGTCTTTTTGGTGTTTTTCA
7600_7700.txt-21F	GTTGGACAATCTTAAAGTCGGGA
7600_7700.txt-92R	GTTGGACAATCTTAAAGTCGGGA

RESULTS

Functional profiling in yeast identifies genes required for toxaphene tolerance

The IC20, the concentration at which growth is inhibited by 20%, is a dose frequently utilized in functional screens, as it elicits a response without being overly toxic (Jo *et al.*, 2009b). After performing growth curve analyses for wild-type yeast treated with increasing concentrations of toxaphene (Fig. 3.1B), the toxaphene IC20 was calculated as 640μM (Fig. 3.1C). Pools of yeast homozygous diploid deletion mutants (n = 4607) were grown for 15 generations at the toxaphene IC20 (640μM), 50% IC20 (320μM), and 25% IC20 (160μM) to identify genes important for growth in toxaphene. DSSA deemed 130 strains sensitive and 542 strains resistant to at least one dose of toxaphene (Appendix 2). Sensitive strains were the focus of this study, with the top 30 displaying growth defects shown in Table 3.1.

Overrepresentation analyses identify biological attributes needed for toxaphene resistance

All toxaphene-sensitive strains identified by DSSA (n = 122; Appendix 2) were analyzed with FunSpec for significantly overrepresented biological attributes at a corrected p value of 0.002 (Table 3.2). Transcription elongation and aerobic respiration were enriched in both GO and MIPS categories, indicating that mutants lacking genes associated with these processes are sensitive to toxaphene. Other overrepresented GO classifications included mitochondrial respiratory chain complex IV biogenesis and aromatic amino acid biosynthesis. To supplement the FunSpec evaluation, network mapping was performed with Cytoscape to identify additional attributes required for toxaphene tolerance. The BiNGO plugin revealed that transcription elongation, aerobic respiration, and aromatic amino acid biosynthesis were over-represented within the network data (Fig. 3.2). Other categories uncovered were cell death and metabolic salvage.

Mutants defective in transcription elongation associated processes are sensitive to toxaphene
FunSpec and Cytoscape analyses indicated enrichment of transcription elongation mutants within the functional profiling data. Accordingly, growth curves were obtained for the transcription elongation mutants identified in the screen and compared to the BY4743 wild-type strain, with five out of the six (*cdc73*Δ, *dst1*Δ , *mft1*Δ, *thp2*Δ, and *spt4*Δ, but not *elf1*Δ) confirmed as sensitive to toxaphene (Fig. 3.3A). Considering two of these mutants (*mft1*Δ and *thp2*Δ) lacked components of THO, a complex required for efficient transcription elongation (Chávez *et al.*, 2000) and mRNA export (Strässer *et al.*, 2002), we tested strains harboring deletions of the two additional THO subunits (*hpr1*Δ and *tho2*Δ), finding growth defects (Fig. 3.3A). Many of these confirmed strains are also sensitive to the transcription elongation inhibitors MPA and 6-AU (Desmoucelles *et al.*, 2002; Table 3.3), therefore, we examined whether toxaphene affected a set of MPA- or 6-AU-sensitive mutants known to exhibit transcription elongation defects. Indeed, strains lacking subunits of the SAGA histone acetyltransferase (*spt20*Δ), the Paf1p complex (*rtf1*Δ), and the TREX-2 transcriptional export machinery (*sac3*Δ and *thp1*Δ) were sensitive to toxaphene (Fig. 3.3A). Additionally, a gene encoding an RNA polymerase II subunit (*RPB9*), along with genes implicated in RNA polymerase II activation (*CTK3*, *RAD6*, and *SNF6*) or reactivation through deubiquitylation (*BRE5* and *UBP3*) were required for toxaphene tolerance (Fig. 3.3B).

Nitrogen utilization and aromatic amino acid biosynthesis mutants are sensitive to toxaphene
The *dal81*Δ, *stp1*Δ, and *ure2*Δ nitrogen utilization mutants identified in the functional screen (Table 3.1; Appendix 2) were confirmed by growth curve analyses to exhibit severe growth defects in presence of toxaphene (Fig. 3.4A). For unknown reasons, the growth of these mutants is also hindered by the transcription elongation inhibitors MPA and 6-AU (Desmoucelles *et al.*, 2002; Gaillard *et al.*, 2009). Additionally, in agreement with enrichment analyses (Fig. 3.2 and Table 3.2), mutants deficient in aromatic amino acid biosynthesis were toxaphene-sensitive, with the *TRP4* tryptophan biosynthesis gene implicated as the pathway component furthest downstream (Fig. 3.4B). However, neither tryptophan supplementation of YPD media nor titration into defined media altered growth of the BY4743 wild-type strain in toxaphene (data not shown).

Toxaphene exhibits synergy with MPA, but its mechanism of action is not similar
Similarities between the mutant sensitivity profiles for toxaphene and the transcription elongation inhibitors MPA and 6-AU (Table 3.3) prompted us to examine whether the compounds shared a mechanism of action. Both MPA and 6-AU inhibit the guanosine monophosphate (GMP) synthesis enzyme inosine monophosphate dehydrogenase (*IMPDH*), which reduces ribonucleotide levels and increases dependence on transcription elongation factors for transcriptional efficiency (Exinger and Lacroute, 1992; Hedstrom, 2009). As a first step, we assessed synergy between toxaphene and MPA by obtaining growth curves for each condition as well as the mixture. We also considered 4-nitroquinoline-N-oxide (4-NQO), a model carcinogen whose DNA adducts may be repaired by transcription-coupled nucleotide excision repair (Gaillard *et al.*, 2009), and tunicamycin, an endoplasmic reticulum stressor (Elbein, 1981). Both MPA and 4-NQO displayed additive inhibitory growth effects with toxaphene, while the general stressor tunicamycin did not (Fig. 3.5). Second, we examined whether guanine or uracil

supplementation could reverse toxaphene sensitivity, as both can rescue the growth of transcription elongation mutants in the presence of either MPA or 6-AU (Exinger and Lacroute, 1992; Desmoucelles *et al.*, 2002). A flow cytometry assay, in which relative growth of a mutant strain to a wild-type GFP-expressing strain was compared under the indicated conditions, confirmed that neither guanine nor uracil reversed toxaphene sensitivity of transcription elongation mutants (Figs. 6A and B). Third, we tested a strain deleted for *IMD2*, the only yeast *IMPDH* homologue that provides resistance to MPA (Hyle *et al.*, 2003), for toxaphene sensitivity. Although hypersensitive to MPA, the *imd2*Δ strain did not display altered growth in toxaphene (data not shown). Finally, we found toxaphene did not affect strains deleted for *URA2* or *URA4*, enzymes involved in the *de novo* biosynthesis of pyrimidine ribonucleotides (Denis-Duphil, 1989) (data not shown). Collectively, these data suggest that toxaphene's mechanism is not analogous to MPA/6-AU, i.e., it does not alter nucleotide pools or target the *IMPDH* family of enzymes.

Toxaphene does not affect transcription elongation

We next examined toxaphene's potential to obstruct transcription elongation, reasoning that inhibition of this process could still occur via a mechanism distinct from that of MPA/6-AU. The GLAM assay has been developed to indirectly examine defects in transcription elongation (Morillo-Huesca *et al.*, 2006), using the premise that mutants impaired in elongation are less able to transcribe long versus short transcription units. The toxaphene-sensitive transcription elongation mutants identified in this study have previously exhibited low scores when assayed for GLAM (Gaillard *et al.*, 2009; Morillo-Huesca *et al.* 2006). We measured the GLAM-ratios of acid phosphatase activity for a long (*PHO5-lacZ* or *PHO5-LAC4*) versus short transcription unit (*PHO5*) for BY4743 wild-type cells in the presence or absence of toxaphene, but did not find altered ratios upon toxaphene exposure (Fig. 3.7A). Since GLAM is an indirect measurement of transcription elongation that may not recognize all transcription elongation defects, we directly assessed RNA polymerase II elongation by performing an RNA polymerase II processivity assay (Mason and Struhl, 2005), where levels of RNA polymerase II bound to different regions of a long gene are measured. If transcription elongation were compromised under toxaphene treatment, the profile of RNA polymerase II would change in comparison to a non-treated sample, as seen in the case of 6AU and most transcription elongation mutants detected in this study (Mason and Struhl, 2005). However, the patterns of the toxaphene-treated and DMSO-treated samples were very similar, indicating that toxaphene does not affect RNA polymerase II processivity during transcription elongation (Fig. 3.7B).

DISCUSSION

While the complex mixture of chlorinated terpenes known as toxaphene was once the most widely applied pesticide in the United States, its congeners are now considered persistent, bioaccumulative, and toxic. In 2004, these unfavorable characteristics resulted in toxaphene's addition to the Stockholm Convention on Persistent Organic Pollutants treaty as a member of the original “dirty dozen” compounds designated for international elimination or restriction. Those most at risk for exposure include Arctic populations who eat aquatic mammals and people consuming sport-caught fish from the Great Lakes (NTP, 2011). Although toxaphene has been linked to diseases such as cancer and amyotrophic lateral sclerosis (Kamel *et al.*, 2012; Mills *et*

al., 2005; Purdue *et al.*, 2007; Schroeder *et al.*, 2001), cellular and molecular toxicity data associated with exposure are severely lacking.

To discover potential mechanisms of toxicity, we screened the *S. cerevisiae* homozygous diploid non-essential deletion mutant collection to identify strains with altered growth in the presence of toxaphene. The majority of yeast genes confirmed as required for toxaphene tolerance are implicated in transcription elongation and associated processes (Figure 3.3), with additional resistance genes involved in nutrient utilization, drug transport, and various other cellular functions (Fig. 3.4 and 3.8). Our results regarding nutrient utilization mutants are consistent with a report in which the toxicity of toxaphene was approximately 3-fold greater in rats fed a protein deficient diet (Boyd and Taylor, 1971). Both results point to a need of a fully functional catabolic environment to resist toxaphene. Enrichment analyses indicated aerobic respiration mutants were sensitive to toxaphene (Table 3.2), which is consistent with toxaphene's ability to inhibit ATPases (Mourelle *et al.*, 1985; Trottman and Desaiah, 1979; Trottman *et al.*, 1985). However, this group of strains was not studied to a large extent herein, as (1) the *qcr8*Δ strain (which has an electron transport chain defect) was a false positive (data not shown) and (2) most are petite and/or slow growing, which causes inherent competitive fitness defects during pool screens and may thus misinform further analyses. Future studies may elucidate the effects, if any, of toxaphene on aerobic respiration in yeast. The most sensitive strain identified by DSSA (and confirmed by growth curve assays) was *pdr5*Δ, which, not unexpectedly, lacks a drug resistance transporter involved in detoxification (Fig. 3.8). Many yeast genes described in this study are conserved (Table 3.4) and may thus play a role in human toxicity. As the technical toxaphene mixture utilized in this investigation is comprised of hundreds of related chlorinated compounds, the congener(s) responsible for the observed toxic effects in yeast remain unknown. Moreover, both human metabolism and environmental weathering of toxaphene (de Geus *et al.*, 1999) may produce derivatives of differing toxicological relevance than those present in the technical mixture.

Although various -omics approaches have been utilized to examine the molecular effects of toxaphene, its mechanism(s) of toxicity remain ambiguous and findings directly related to transcription elongation have not been reported. Perhaps most relevant to this study is a report indicating that toxaphene altered expression of transcription termination genes in largemouth bass (Mehinto *et al.*, in preparation). Woo and Yum (2011) performed gene expression analyses in marine medaka, showing that toxaphene affected regulation of cytoskeletal, developmental, metabolic, nucleic acid/protein binding, and signal transduction genes. Increased expression of homocysteine methyltransferase, a zinc metalloenzyme involved in the metabolism of various amino acids (Woo and Yum, 2011), may indicate a link to the nutrient utilization genes described in this study (Fig. 3.4). Toxaphene perturbed hepatic expression of one carbon metabolism and ribosomal biogenesis genes in adult male largemouth bass (Sanchez *et al.*, 2011), while another study in the same organism could not establish changes in neuroendocrine signaling or neurotransmitter synthesis transcripts (Martyniuk *et al.*, 2009). Proteomic analyses in the livers of largemouth bass identified differentially expressed proteins following toxaphene exposure, including an ion channel, a component of the pentose phosphate pathway, and a glutathione S-transferase (Sanchez *et al.*, 2009). Functional profiling in yeast has been performed with the

related organochlorine pesticide dieldrin, but its toxic mechanism (altered leucine availability) is different from that of toxaphene (Gaytán *et al.*, 2013).

Toxaphene-sensitive mutants also experience growth defects in MPA and 6-AU (for a comparison, see Table 3.3), two compounds that diminish transcription elongation by inhibiting GMP synthesis (Exinger and Lacroute, 1992; Hedstrom, 2009). By decreasing nucleotide availability, MPA and 6-AU reduce RNA polymerase II elongation rate and processivity (Mason and Struhl, 2005), with transcription elongation mutant sensitivity ascribed to the deleterious combination of transcriptional defects (Kaplan, 2013). Although toxaphene and MPA synergistically inhibit yeast growth (Fig. 3.5), two different elongation assays did not detect any effect of toxaphene on transcription elongation (Fig. 3.7), unlike results seen with MPA and 6-AU (Mason and Struhl, 2005). Intriguingly, several toxaphene tolerance genes, such as *SAC3*, *SPT4*, *THP1*, and those encoding components of the THO complex, are associated with other processes tightly coupled to transcription elongation, such as mRNA processing, mRNA nuclear export, or transcription-coupled nucleotide excision repair (Ding *et al.*, 2010; Fischer *et al.*, 2002; Gaillard *et al.*, 2007; Lei *et al.*, 2003; Saguez *et al.*, 2008; Strässer *et al.*, 2002). The possibility that one of these cellular operations is required for toxaphene resistance led us to examine mRNA export in presence of toxaphene using *in situ* hybridization, however, our findings were inconclusive (data not shown).

By identifying mutants with altered growth in toxaphene, our study advances understanding of the genetic requirements for the toxaphene response in yeast. Despite evidence indicating transcription elongation mutants exhibit sensitivity to toxaphene, our data suggest toxaphene does not affect transcription elongation itself. Instead, we propose toxaphene tolerance requires a yet to be identified cellular process closely associated with transcription elongation, as toxaphene synergism with MPA indicates a likely effect along this pathway. Using data provided in this study, further pathway-specific investigations in yeast or humans may elucidate the distinct mechanism of toxaphene toxicity.

FIGURES

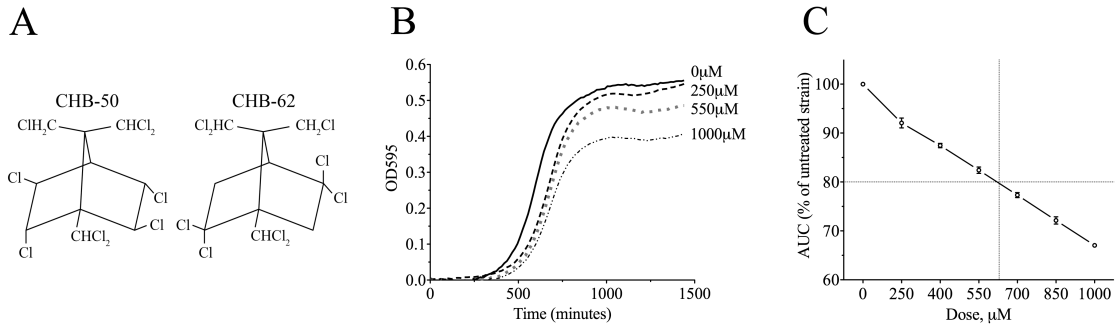

Fig. 3.1. Determining the toxaphene IC20 for functional profiling. (A) The structure of two chlorinated congeners present in the toxaphene technical mixture. (B) Representative growth curves in YPD media for the BY4743 wild-type strain treated with toxaphene. For clarity, only the 250, 550, and 1000μM toxaphene doses are shown, although additional curves were performed at 400, 700, and 850μM. (C) The area under the curve (AUC) was calculated at each dose for three independent experiments, expressed as the mean and SE, and plotted as a percentage of the untreated control. The toxaphene IC20 was determined to be 640μM, as indicated by the dashed lines.

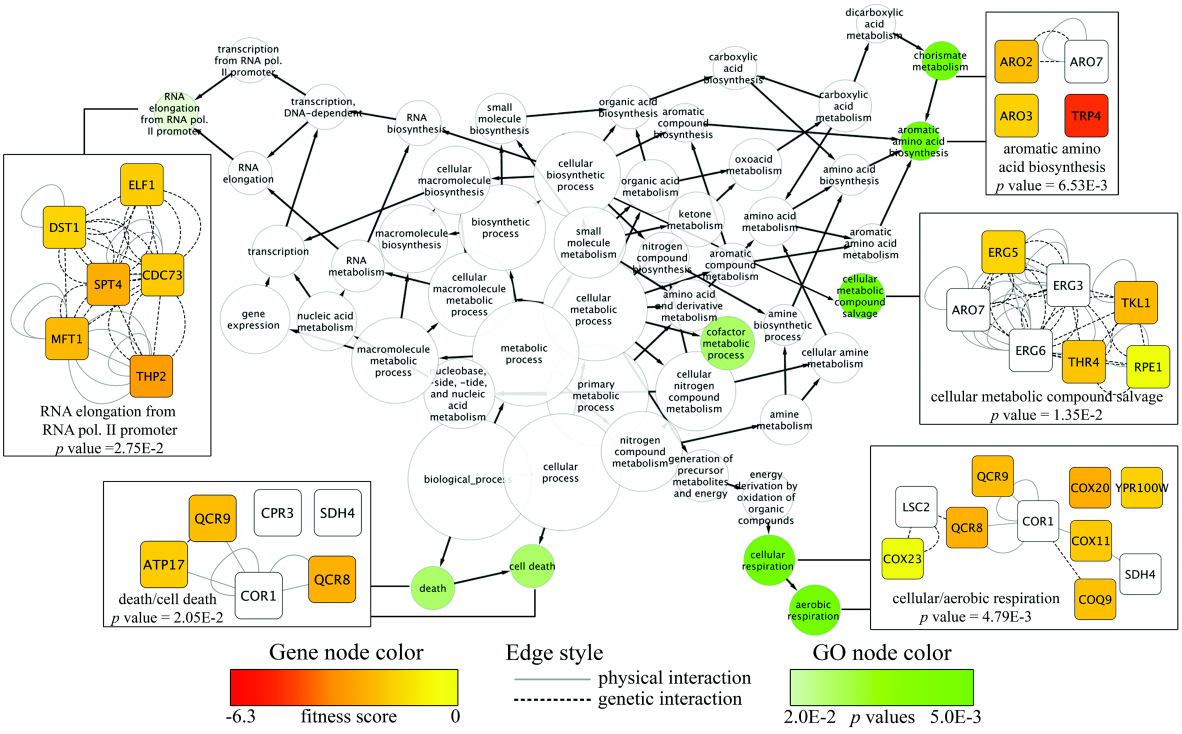

Fig. 3.2. Biological attributes required for toxaphene tolerance are identified by network mapping. Cytoscape was used to map fitness scores (the ratio of the log2 hybridization signals between DMSO and toxaphene exposures) for toxaphene-sensitive strains onto the *Saccharomyces cerevisiae* BioGRID interaction dataset. A subnetwork (n = 104) containing genetic and physical interactions between the sensitive, non-sensitive, and essential genes was created and significantly overrepresented (p value cutoff of 0.03) GO categories were identified. The green node color corresponds to the GO p-value while the node size correlates to the number of genes in the category. Edge arrows indicate hierarchy of GO terms. Networks for various GO categories are shown, where node color corresponds to deletion strain fitness score and edge defines the type of interaction between the genes.

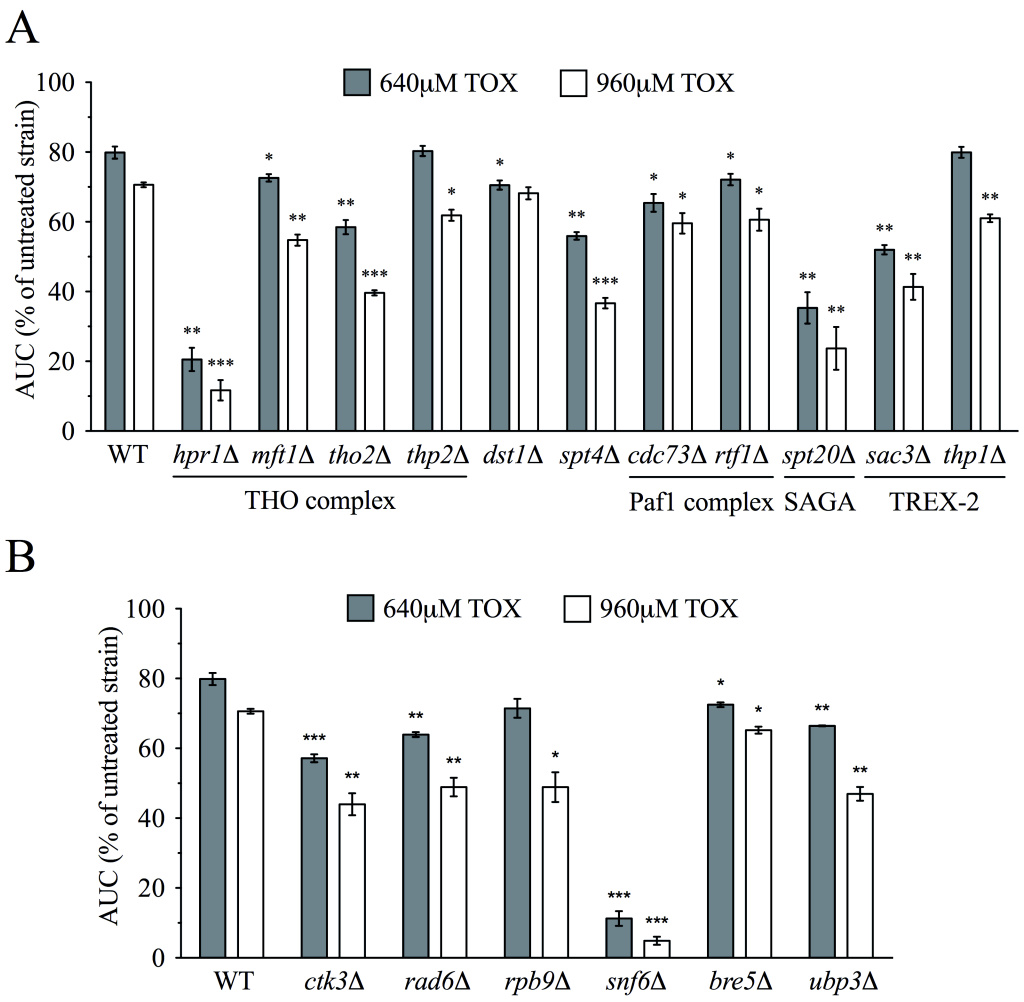

Fig. 3.3. Transcription elongation mutants are sensitive to toxaphene. Growth curves for three independent cultures were obtained for the indicated strains and toxaphene concentrations. The AUC was calculated for each curve and is shown as a percentage of the untreated strain. Statistical significance between the wild-type and mutant strains was calculated with Student's *t*-test, where ***$p<0.001$, **$p<0.01$, and *$p<0.05$. (A) Mutants with known defects in transcription elongation are sensitive to toxaphene, including members of the THO, Paf1p, SAGA, and TREX-2 complexes. (B) Additional mutants lacking genes implicated in transcription elongation are sensitive to toxaphene.

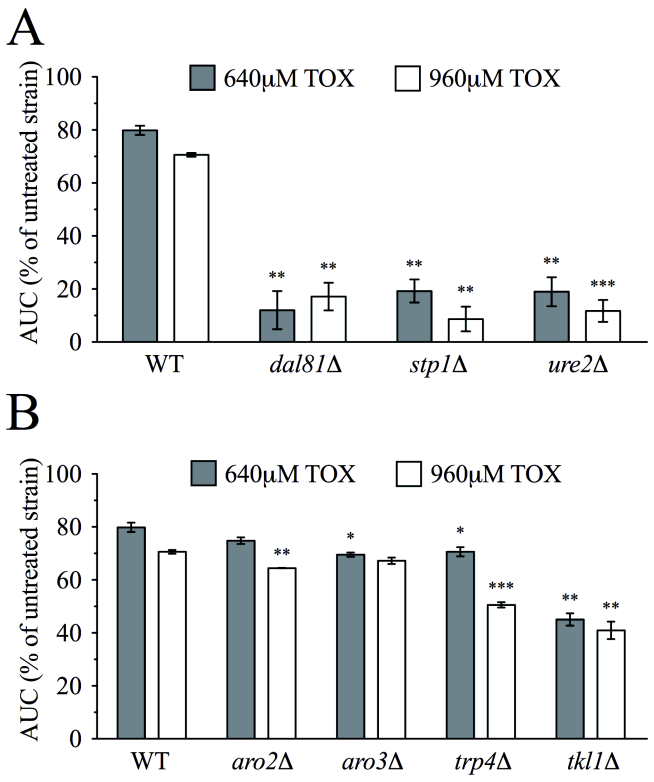

Fig. 3.4. Nitrogen utilization and aromatic amino acid synthesis genes are required for toxaphene tolerance. The AUC was calculated for strains treated with 640μM or 960μM toxaphene and expressed as a percentage of the AUC for the untreated strain. Bars signify the mean and SE for three independent cultures. (A) Mutants lacking components of the nitrogen response display hypersensitivity to toxaphene. (B) Genes involved in aromatic amino acid biosynthesis are required for toxaphene tolerance.

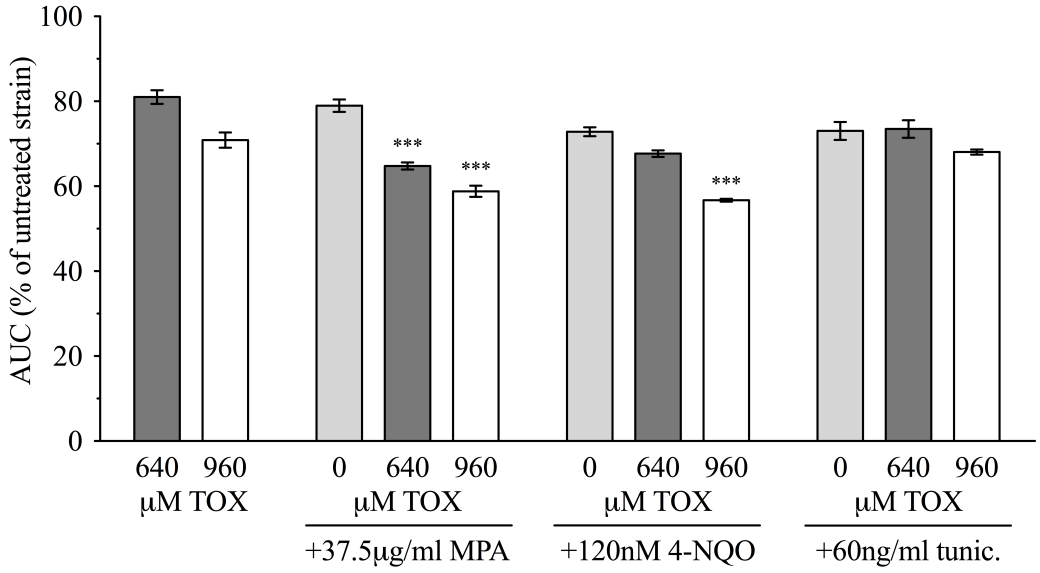

Fig. 3.5. Toxaphene exhibits synergy with MPA and 4-NQO. Growth curve assays were performed for three independent cultures of the BY4743 wild-type strain with the indicated compounds. Both MPA (a transcription elongation inhibitor) and 4-NQO (a genotoxicant) displayed synergy with toxaphene, while tunicamycin (an endoplasmic reticulum stressor) did not. Statistical significance was determined with one-way ANOVA with a Tukey post-test. *** represents significance observed at $p<0.001$ between both toxaphene/toxaphene+synergist and synergist/toxaphene+synergist comparisons.

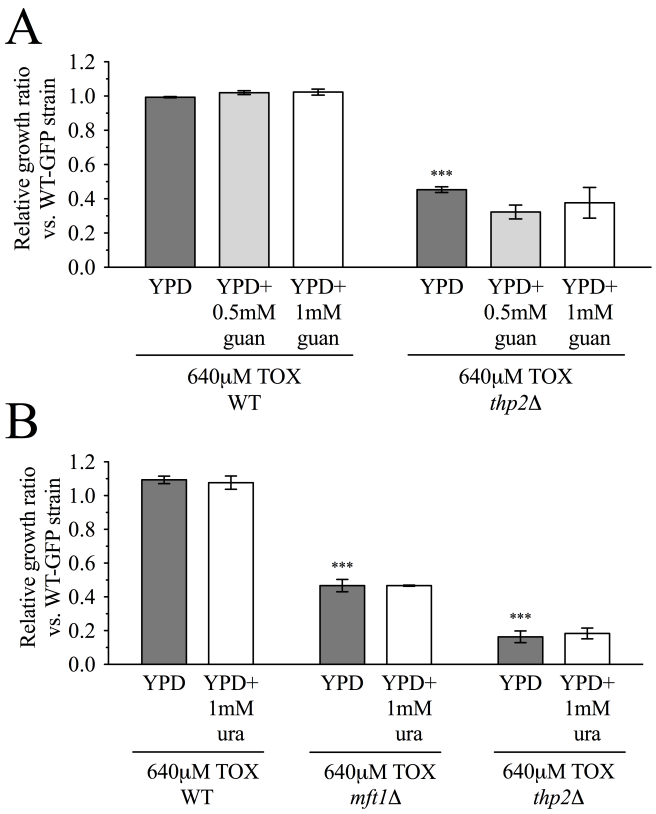

Fig. 3.6. Neither guanine nor uracil rescues toxaphene sensitivity of transcription elongation mutants. Relative growth ratios (treatment vs. control) to a GFP-expressing wild-type strain were obtained for three independent cultures and the means and SEs are shown. One-way ANOVA followed by a Bonferroni post-test determined statistical significance. ***$p<0.001$ for wild-type/mutant comparisons. (A) The toxaphene sensitivity of the *thp2*Δ strain cannot be rescued by guanine. YPD media was supplemented with the indicated concentrations of guanine and toxaphene. (B) Uracil cannot reverse the toxaphene sensitivity of the *mft1*Δ or *thp2*Δ strains. Uracil and toxaphene were added to YPD media at the indicated concentrations.

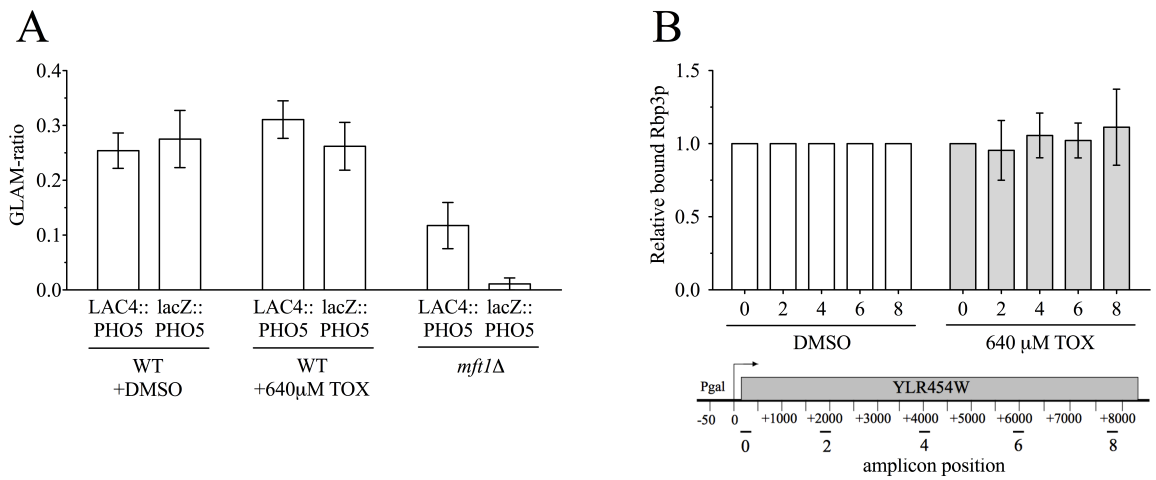

Fig. 3.7. Toxaphene does not inhibit transcription elongation. (A) GLAM-ratios are not altered upon toxaphene treatment. The acid phosphatase activity of long (*PHO5-lacZ* or *PHO5-LAC4*) versus short (*PHO5*) transcriptional units was measured and the means and SE are shown for three independent experiments. The *mft1*Δ strain was used as a positive control. (B) Toxaphene does not affect RNA processivity. Levels of RNA polymerase II bound to different regions of a long gene were measured by chromatin immunoprecipitation.

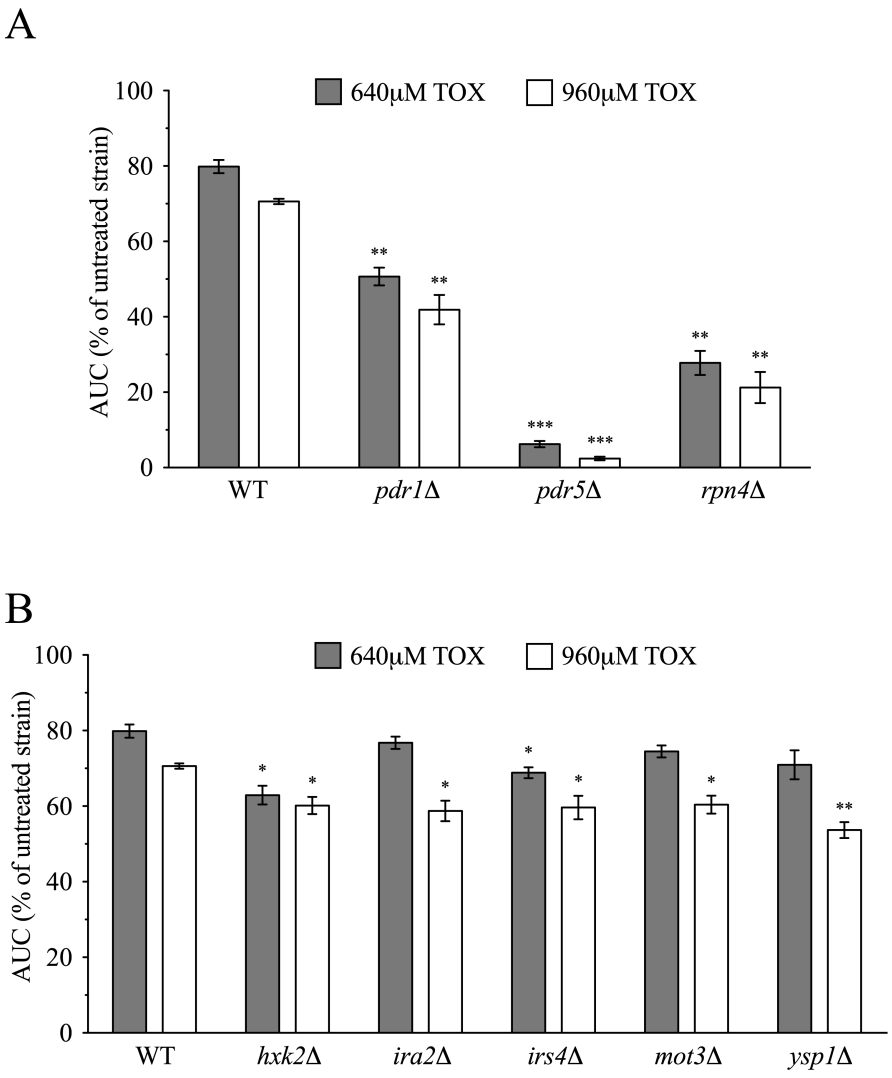

Fig. 3.8. Additional genes required for toxaphene tolerance. The area under the curve (AUC) was calculated for strains treated with 640μM or 960μM toxaphene and expressed as a percentage of the AUC for the untreated strain. All bars represent the mean and SE for three independent cultures. (A) Mutants lacking drug resistance genes are sensitive to toxaphene. (B) Various mutants were confirmed to display sensitivity to toxaphene.

Table 3.1. Fitness scores for the top 30 deletion strains identified as significantly sensitive to toxaphene after 15 generations of growth. The log2 ratios of strain growth in the presence vs. absence of toxaphene quantify the genetic requirements for growth. Appendix 2 lists all mutants displaying altered growth in the screen.

ORF	Deleted Gene	25% IC20 160µM	50% IC20 320µM	100% IC20 640µM	Function of deleted gene
YOR153W	***PDR5***	-6.30	-5.80	-6.05	Plasma membrane multidrug transporter
YDL020C	***RPN4***	-3.15	-3.05	-2.55	Transcription factor; stimulates expression of proteasome genes
YIR023W	***DAL81***	-3.10	-3.50	-3.00	Positive regulator of genes in nitrogen degradation pathways
YDR354W	***TRP4***	-2.90	-4.50	-4.70	Anthranilate phosphoribosyl transferase for tryptophan biosynthesis
YDR126W	***SWF1***	-2.90	-3.20	-3.00	Palmitoyltransferase; acts on various SNAREs
YNL229C	***URE2***	-2.75	-2.45	-2.95	Nitrogen catabolite repression transcriptional regulator
YDR463W	***STP1***	-2.50	-3.10	-3.00	Transcription factor for amino acid permease genes
YGR153W	**-**	-2.50	-2.60	-2.60	Putative protein of unknown function
YDR008C	**-**	-2.30	-2.80	-3.10	Dubious ORF; partially overlaps *TRP1* tryptophan biosynthetic enzyme
YBR171W	***SEC66***	-2.30	-2.60	-2.40	Subunit of Sec63 complex; involved in ER protein translocation
YEL045C	**-**	-2.20	-2.60	-2.40	Dubious ORF
YGL013C	***PDR1***	-2.15	-2.25	-2.70	Transcriptional regulator of multidrug resistance genes
YGR063C	***SPT4***	-2.00	-1.85	-1.95	Regulates Pol I and Pol II transcription
YKR019C	***IRS4***	-1.75	-2.50	-2.00	Regulates phosphatidylinositol 4,5-bisphosphate levels and autophagy
YKL077W	**-**	-1.75	-1.45	-1.20	Putative protein of unknown function
YHR167W	***THP2***	-1.65	-2.00	-2.50	Subunit of the THO complex; involved in transcription elongation
YDR203W	**-**	-1.60	-1.90	-2.20	Dubious ORF; partially overlaps *RAV2*
YIL090W	***ICE2***	-1.50	-1.50	-2.20	Integral ER membrane protein
YPR074C	***TKL1***	-1.50	-1.40	-1.70	Transketolase in the pentose phosphate pathway
YGL005C	***COG7***	-1.50	-1.40	-1.40	Component of the COG golgi transport complex
YDR231C	***COX20***	-1.45	-1.85	-2.05	Mitochondrial inner membrane protein
YCR071C	***IMG2***	-1.40	-1.70	-2.60	Mitochondrial ribosomal protein of the large subunit
YDR455C	**-**	-1.40	-1.50	-1.30	Dubious ORF; partially overlaps *NHX1*
YJL130C	***URA2***	-1.30	-1.40	-1.55	Involved in *de novo* biosynthesis of pyrimidines
YNL032W	***SIW14***	-1.30	-1.30	-1.30	Tyrosine phosphatase
YOR070C	***GYP1***	-1.25	-1.55	-1.50	Cis-golgi GTPase-activating protein (GAP) for the Rab family
YHR155W	***YSP1***	-1.25	-1.50	-1.75	Mitochondrial protein; potential role in programmed cell death
YJL120W	**-**	-1.25	-1.30	-1.35	Dubious ORF; partially overlaps RPE1
YMR264W	***CUE1***	-1.20	-1.00	-1.15	ER membrane protein; regulates ubiquitination
YGR178C	***PBP1***	-1.20	-0.90	-1.10	Component of glucose deprivation induced stress granules

Table 3.2. Genes required for toxaphene tolerance and their associated GO or MIPS categories. Strains exhibiting sensitivity to three doses of toxaphene in the functional screen were entered into FunSpec and analyzed for overrepresented biological attributes (see Materials and Methods section). [a]Number of genes in category identified as sensitive to toxaphene. [b]Number of genes in GO or MIPS category.

GO Biological Process	***p* value**	**Genes identified**	**k[a]**	**f[b]**
mitochondrial respiratory chain complex IV biogenesis (GO:0097034)	3.14E-004	*PET122, PET54, PET494*	3	8
regulation of ER to Golgi vesicle-mediated transport (GO:0060628)	3.33E-004	*UBP3, BRE5*	2	2
transcription elongation from RNA polymerase II promoter (GO:0006368)	4.21E-004	*DST1, SPT4, THP2, ELF1, CDC73, MFT1*	6	54
Group I intron splicing (GO:0000372)	6.56E-004	*PET54, CBP2, MRS1*	3	10
aerobic respiration (GO:0009060)	8.16E-004	*COX20, QCR9, QCR8, COQ9, COX11, MRPL51*	6	61
response to arsenic-containing substance (GO:0046685)	8.90E-004	*RPN4, GET3, TIM18*	3	11
heme a biosynthetic process (GO:0006784)	9.87E-004	*COX15, COX10*	2	3
ribophagy (GO:0034517)	9.87E-004	*UBP3, BRE5*	2	3
aromatic amino acid family biosynthetic process (GO:0009073)	1.17E-003	*ARO3, TRP4, ARO2*	3	12
MIPS Functional Classification	***p* value**	***Genes identified***	**k[a]**	**f[b]**
transcription elongation (11.02.03.01.04)	1.69E-005	*DST1, SPT4, THP2, ELF1, CDC73, MFT1*	6	31
aerobic respiration [02.13.03)	4.85E-004	*COX20, QCR9, COX23, QCR8, COQ9, COX11, MRPL51*	7	77

Table 3.3. Mutants displaying sensitivity to both toxaphene and MPA, 6-AU, or 4-NQO. A literature search identified overlapping mutant sensitivities. Numbers indicate the references cited below.

Transcription elongation mutants			
Toxaphene-sensitive strain	**Sensitivity to**		
	MPA	**6-AU**	**4-NQO**
*hpr1*Δ	2	2	
*mft1*Δ	7		
*tho2*Δ	4		4
*dst1*Δ	2, 4, 6, 7	2, 10	
*spt4*Δ	4	9	4
*cdc73*Δ	4		4
*rtf1*Δ	2, 4	2	
*spt20*Δ	3, 4	2	4
*sac3*Δ	2		
*thp1*Δ	10	10	
*ctk3*Δ	4	2	4
*rad6*Δ	2, 4		4
*rpb9*Δ	1, 4, 5		4
*snf6*Δ	2, 4	2	
*ubp3*Δ	7, 10	8, 10	
*mot3*Δ	2	2, 10	

Nutrient utilization mutants			
Toxaphene-sensitive strain	**Sensitivity to**		
	MPA	**6-AU**	**4-NQO**
*dal81*Δ	2, 7		
*stp1*Δ	2, 10	10	
*ure2*Δ	4		
*ira2*Δ	2		

1. Betz, J. L., Chang, M., Washburn, T. M., Porter, S. E., Mueller, C. L., Jaehning, J. A. (2002). Phenotypic analysis of Paf1/RNA polymerase II complex mutations reveals connections to cell cycle regulation, protein synthesis, and lipid and nucleic acid metabolism. *Mol. Genet. Genomics*. **268**, 272–285.
2. Desmoucelles, C., Pinson, B., Saint-Marc, C., Daignan-Fornier, B. (2002). Screening the yeast "disruptome" for mutants affecting resistance to the immunosuppressive drug, mycophenolic acid. *J. Biol. Chem.* **277**, 27036–27044.
3. Dudley, A. M., Janse, D. M., Tanay, A., Shamir, R., Church, G. M. (2005). A global view of pleiotropy and phenotypically derived gene function in yeast. *Mol. Syst. Biol.* **1**, 2005.0001.
4. Gaillard, H., Wellinger, R. E., Aguilera, A. (2007). A new connection of mRNP biogenesis and export with transcription-coupled repair. *Nucleic Acids Res.* **35**, 3893–3906.
5. Gibney, P. A., Fries, T., Bailer, S. M., Morano, K. A. (2008). Rtr1 is the Saccharomyces cerevisiae homolog of a novel family of RNA polymerase II-binding proteins. *Eukaryotic Cell*. **7**, 938–948.
6. Gómez-Herreros, F., De Miguel-Jiménez, L., Morillo-Huesca, M., Delgado-Ramos, L., Muñoz-Centeno, M. C., Chávez, S. (2012). TFIIS is required for the balanced expression of the genes encoding ribosomal components under transcriptional stress. *Nucleic Acids Res.* **40**, 6508–6519.
7. Kapitzky, L., Beltrao, P., Berens, T. J., Gassner, N., Zhou, C., Wüster, A., *et al*. (2010). Cross-species chemogenomic profiling reveals evolutionarily conserved drug mode of action. *Mol. Syst. Biol.* **6**, 451.
8. McCullock, S., Kinard, T., McCullough, L., Formosa, T. (2006). blm3-1 is an allele of UBP3, a ubiquitin protease that appears to act during transcription of damaged DNA. *J. Mol. Biol.* **363**, 660–672.
9. Morillon, A., O'Sullivan, J., Azad, A., Proudfoot, N., Mellor, J. (2003). Regulation of elongating RNA polymerase II by forkhead transcription factors in yeast. *Science*. **300**, 492–495.
10. Riles, L., Shaw, R. J., Johnston, M., Reines, D. (2004). Large-scale screening of yeast mutants for sensitivity to the IMP dehydrogenase inhibitor 6-azauracil. *Yeast*. **21**, 241–248.

Table 3.4. Human orthologs of yeast genes required for toxaphene tolerance. Deletion of any of these yeast genes caused sensitivity to toxaphene (listed in alphabetical order).

Yeast gene	Human ortholog(s)	Human protein description
CDC73	*CDC73*	Tumor suppressor; involved in transcriptional/post-transcriptional pathways
DST1	*TCEA1*	Transcription elongation factor A (SII)
HXK2	*HK2*	Hexokinase 2
IRA2	*NF1*	Neurofibromin 1, tumor suppressor
PDR5	*ABCG2*	ATP-binding cassette protein
RAD6	*UBE2A/UBE2B*	Ubiquitin-conjugating enzyme E2A
RPB9	*POLR2I*	DNA-directed RNA pol. II subunit *RPB9*
RTF1	*RTF1*	Role in transcription-coupled histone modification
SAC3	*GANP*	Synonym MCM3AP, minichromosome maintenance protein 3
SPT4	*SUPT4H1*	Regulates mRNA processing and transcription elongation by RNA pol. II
STP1	*ZNFN1A4*	Zinc finger protein, subfamily 1A, 4 (Eos)
THO2	*THOC2*	Component of the THO subcomplex of the TREX complex
THP1	*PCID2*	PCI domain containing 2
TKL1	*TKTL1/2, TKT*	Transketolase
UBP3	*USP10*	Ubiquitin specific peptidase 10

REFERENCES

Agency for Toxic Substances and Disease Registry (ATSDR). (2010). *Toxicological profile for toxaphene.* US Dept of Health and Human Services, ATSDR, Atlanta, GA, USA.

Blackman, R. K., Cheung-Ong, K., Gebbia, M., Proia, D. A., He, S., Kepros, J., Jonneaux, A., Marchetti, P., Kluza, J., Rao, P. E., *et al*. (2012). Mitochondrial electron transport is the cellular target of the oncology drug elesclomol. *PLoS ONE.* **7**, e29798.

Boyd E. M., Taylor F. I. (1971). Toxaphene toxicity in protein-deficient rats. *Toxicol. Appl. Pharmacol.* **18,** 158–167.

Chávez, S., Beilharz, T., Rondón, A. G., Erdjument-Bromage, H., Tempst, P., Svejstrup, J. Q., Lithgow, T., Aguilera, A. (2000). A protein complex containing Tho2, Hpr1, Mft1 and a novel protein, Thp2, connects transcription elongation with mitotic recombination in *Saccharomyces cerevisiae*. *EMBO J.* **19**, 5824–5834.

de Geus, H. J., Besselink, H., Brouwer, A., Klungsøyr, J., McHugh, B., Nixon, E., Rimkus, G. G., Wester, P. G., de Boer, J. (1999). Environmental occurrence, analysis, and toxicology of toxaphene compounds. *Environ. Health Perspect*. **107**, 115–144.

Denis-Duphil, M. (1989). Pyrimidine biosynthesis in *Saccharomyces cerevisiae*: the ura2 cluster gene, its multifunctional enzyme product, and other structural or regulatory genes involved in de novo UMP synthesis. *Biochem. Cell Biol.* **67**, 612–631.

Desmoucelles, C., Pinson, B., Saint-Marc, C., Daignan-Fornier, B. (2002). Screening the yeast "disruptome" for mutants affecting resistance to the immunosuppressive drug, mycophenolic acid. *J. Biol. Chem.* **277**, 27036–27044.

Ding, B., LeJeune, D., Li, S. (2010). The C-terminal repeat domain of Spt5 plays an important role in suppression of Rad26-independent transcription coupled repair. *J. Biol. Chem.* **285**, 5317–5326.

dos Santos, S. C., Teixeira, M. C., Cabrito, T. R., Sá-Correia, I. (2012). Yeast toxicogenomics: Genome-wide responses to chemical stresses with impact in environmental health, pharmacology, and biotechnology. *Front. Genet.* **3**, 63.

Elbein, A. D. (1981). The tunicamycins - useful tools for studies on glycoproteins. *Trends Biochem. Sci*. **6**, 219–221.

Exinger, F., Lacroute, F. (1992). 6-Azauracil inhibition of GTP biosynthesis in *Saccharomyces cerevisiae*. *Curr. Genet.* **22**, 9–11.

Fischer, T., Strässer, K., Rácz, A., Rodriguez-Navarro, S., Oppizzi, M., Ihrig, P., Lechner, J., Hurt, E. (2002). The mRNA export machinery requires the novel Sac3p-Thp1p complex to dock at the nucleoplasmic entrance of the nuclear pores. *EMBO J.* **21**, 5843–5852.

Furter, R., Paravicini, G., Aebi, M., Braus, G., Prantl, F., Niederberger, P., Hütter, R. (1986). The TRP4 gene of *Saccharomyces cerevisiae*: isolation and structural analysis. *Nucleic Acids Res.* **14**, 6357–6373.

Gaillard, H., Tous, C., Botet, J., González-Aguilera, C., Quintero, M. J., Viladevall, L., García-Rubio, M. L., Rodríguez-Gil, A., Marín, A., Ariño, J., *et al*. (2009). Genome-wide analysis of factors affecting transcription elongation and DNA repair: a new role for PAF and Ccr4-not in transcription-coupled repair. *PLoS Genet.* **5**, e1000364.

Gaillard, H., Wellinger, R. E., Aguilera, A. (2007). A new connection of mRNP biogenesis and export with transcription-coupled repair. *Nucleic Acids Res.* **35**, 3893–3906.

Gaytán, B. D., Loguinov, A. V., Lantz, S. R., Lerot, J.-M., Denslow, N. D., Vulpe, C. D. (2013). Functional profiling discovers the dieldrin organochlorinated pesticide affects leucine availability in yeast. *Toxicol. Sci.* **132**, 347–358.

Giaever, G., Chu, A. M., Ni, L., Connelly, C., Riles, L., Véronneau, S., Dow, S., Lucau-Danila, A., Anderson, K., André, B., *et al*. (2002). Functional profiling of the *Saccharomyces cerevisiae* genome. *Nature*. **418**, 387–391.

Hedstrom, L. (2009). IMP Dehydrogenase: Structure, Mechanism and Inhibition. *Chem Rev*. **109**, 2903–2928.

Hyle, J. W., Shaw, R. J., Reines, D. (2003). Functional distinctions between IMP dehydrogenase genes in providing mycophenolate resistance and guanine prototrophy to yeast. *J. Biol. Chem.* **278**, 28470–28478.

Jo, W. J., Loguinov, A., Wintz, H., Chang, M., Smith, A. H., Kalman, D., Zhang, L., Smith, M. T., Vulpe, C. D. (2009). Comparative functional genomic analysis identifies distinct and overlapping sets of genes required for resistance to monomethylarsonous acid (MMAIII) and arsenite (AsIII) in yeast. *Toxicol Sci*. **111**, 424–436.

Jo, W. J., Ren, X., Chu, F., Aleshin, M., Wintz, H., Burlingame, A., Smith, M. T., Vulpe, C. D., Zhang, L. (2009). Acetylated H4K16 by MYST1 protects UROtsa cells from arsenic toxicity and is decreased following chronic arsenic exposure. *Toxicol. Appl. Pharmacol.* **241**, 294–302.

Kamel, F., Umbach, D. M., Bedlack, R. S., Richards, M., Watson, M., Alavanja, M. C. R., Blair, A., Hoppin, J. A., Schmidt, S., Sandler, D. P. (2012). Pesticide exposure and amyotrophic lateral sclerosis. *Neurotoxicology*. **33**, 457–462.

Kaplan, C. D. (2013). Basic mechanisms of RNA polymerase II activity and alteration of gene expression in *Saccharomyces cerevisiae*. *BBA-Gene Regul. Mech*. **1829**, 39–54.

Lei, E. P., Stern, C. A., Fahrenkrog, B., Krebber, H., Moy, T. I., Aebi, U., Silver, P. A. (2003). Sac3 is an mRNA export factor that localizes to cytoplasmic fibrils of nuclear pore complex. *Mol. Biol. Cell*. **14**, 836–847.

Martyniuk, C. J., Sanchez, B. C., Szabo, N. J., Denslow, N. D., Sepúlveda, M. S. (2009). Aquatic contaminants alter genes involved in neurotransmitter synthesis and gonadotropin release in largemouth bass. *Aquat. Toxicol.* **95**, 1–9.

Mason, P. B., Struhl, K. (2005). Distinction and relationship between elongation rate and processivity of RNA polymerase II in vivo. *Mol. Cell*. **17**, 831–840.

Mills, P. K., Yang, R., Riordan, D. (2005). Lymphohematopoietic cancers in the United Farm Workers of America (UFW), 1988-2001. *Cancer Cause. Control*. **16**, 823–830.

Morillo-Huesca, M., Vanti, M., Chávez, S. (2006). A simple in vivo assay for measuring the efficiency of gene length-dependent processes in yeast mRNA biogenesis. *FEBS J.* **273**, 756–769.

Mourelle M., Garcia M., Aguilar C. (1985). Adenosine triphosphatase activities in plasma liver membranes of rats treated with DDT and toxaphene. *J. Appl. Toxicol.* **5,** 39–41.

National Toxicology Program (NTP). (2011). *Report on carcinogens, twelfth edition.* US Dept of Health and Human Services, NTP, Research Triangle Park, NC, USA.

Purdue, M. P., Hoppin, J. A., Blair, A., Dosemeci, M., Alavanja, M. C. R. (2007). Occupational exposure to organochlorine insecticides and cancer incidence in the Agricultural Health Study. *Int. J. Cancer*. **120**, 642–649.

Robinson, M., Grigull, J., Mohammad, N., Hughes, T. (2002). FunSpec: a web-based cluster interpreter for yeast. *BMC Bioinformatics*. **3**, 35.

Rodríguez-Gil, A., García-Martínez, J., Pelechano, V., Muñoz-Centeno, M. de la C., Geli, V., Pérez-Ortín, J. E., Chávez, S. (2010). The distribution of active RNA polymerase II along the transcribed region is gene-specific and controlled by elongation factors. *Nucleic Acids Res.* **38**, 4651–4664.

Saguez, C., Schmid, M., Olesen, J. R., Ghazy, M. A. E.-H., Qu, X., Poulsen, M. B., Nasser, T., Moore, C., Jensen, T. H. (2008). Nuclear mRNA surveillance in THO/sub2 mutants is triggered by inefficient polyadenylation. *Mol. Cell*. **31**, 91–103.

Sanchez, B. C., Carter, B., Hammers, H. R., Sepúlveda, M. S. (2011). Transcriptional response of hepatic largemouth bass (*Micropterus salmoides*) mRNA upon exposure to environmental contaminants. *J. Appl. Toxicol*. **31**, 108–116.

Sanchez, B. C., Ralston-Hooper, K. J., Kowalski, K. A., Dorota Inerowicz, H., Adamec, J., Sepúlveda, M. S. (2009). Liver proteome response of largemouth bass (*Micropterus salmoides*) exposed to several environmental contaminants: potential insights into biomarker development. *Aquat. Toxicol*. **95**, 52–59.

Schroeder, J. C., Olshan, A. F., Baric, R., Dent, G. A., Weinberg, C. R., Yount, B., Cerhan, J. R., Lynch, C. F., Schuman, L. M., Tolbert, P. E., *et al*. (2001). Agricultural risk factors for t(14;18) subtypes of non-Hodgkin's lymphoma. *Epidemiology*. **12**, 701–709.

Shannon, P., Markiel, A., Ozier, O., Baliga, N. S., Wang, J. T., Ramage, D., Amin, N., Schwikowski, B., Ideker, T. (2003). Cytoscape: a software environment for integrated models of biomolecular interaction networks. *Genome Res.* **13**, 2498–2504.

Skrtić, M., Sriskanthadevan, S., Jhas, B., Gebbia, M., Wang, X., Wang, Z., Hurren, R., Jitkova, Y., Gronda, M., Maclean, N., *et al.* (2011). Inhibition of mitochondrial translation as a therapeutic strategy for human acute myeloid leukemia. *Cancer Cell*. **20**, 674–688.

Steinmetz, L. M., Scharfe, C., Deutschbauer, A. M., Mokranjac, D., Herman, Z. S., Jones, T., Chu, A. M., Giaever, G., Prokisch, H., Oefner, P. J., Davis, R. W. (2002). Systematic screen for human disease genes in yeast. *Nat. Genet.* **31**, 400–404.

Strässer, K., Masuda, S., Mason, P., Pfannstiel, J., Oppizzi, M., Rodriguez-Navarro, S., Rondón, A. G., Aguilera, A., Struhl, K., Reed, R., *et al*. (2002). TREX is a conserved complex coupling transcription with messenger RNA export. *Nature*. **417**, 304–308.

Trottman C. H., Desaiah D. (1979). Adenosine triphosphatase activities in brain, kidney and liver of mice treated with toxaphene. *J. Environ. Sci. Health B* **14,** 393–404.

Trottman C. H., Prasada Rao K. S., Morrow W., Uzodinma J. E., Desaiah D. (1985). In vitro effects of toxaphene on mitochondrial calcium ATPase and calcium uptake in selected rat tissues. *Life Sci* **36,** 427–433.

Woo, S., Yum, S. (2011). Transcriptional response of marine medaka (*Oryzias javanicus*) on exposure to toxaphene. *Comp. Biochem. Phys. C*. **153**, 355–361.

CHAPTER 4

FUNCTIONAL PROFILING OF THE COMMON SOLVENT DMSO IN YEAST

INTRODUCTION

The dipolarity and low toxicity of dimethyl sulfoxide (DMSO) make it an unrivaled solvent in the field of toxicology. DMSO elicits numerous cellular effects, demonstrating the capacity to serve as a cryoprotectant, hydroxyl radical scavenger, and inducer of cellular differentiation and fusion (reviewed by Yu *et al.*, 1994). The pharmacological properties of DMSO have been documented in the treatment of brain edema, amyloidosis, rheumatoid arthritis, and schizophrenia, with infrequently reported systemic toxicities (Santos *et al.*, 2003). The ubiquity of DMSO as a toxicant and drug solvent demands further identification of the cellular and molecular processes it may perturb, primarily to discern whether its effects influence those mediated by a compound of interest.

The unique genetic tools available in the model eukaryote *Saccharomyces cerevisiae* facilitate investigations into the cellular and molecular mechanisms of chemical resistance. The collection of barcoded yeast deletion mutants (Giaever *et al.*, 2002) can be exploited to conduct functional genomic analyses (otherwise known as functional profiling) for a compound of interest. Pools of mutants are subjected to chemical treatment, and after DNA extraction, the strain-specific barcodes are amplified and hybridized to a microarray. Signal intensities correspond to strain numbers present in the pool after exposure, and indicate how the given insult alters the growth of individual mutants. With a high degree of conservation to more complex organisms (Steinmetz *et al.*, 2002), yeast is an appealing model that can help identify human chemical susceptibility or resistance genes (Blackman *et al.*, 2012; Jo *et al.*, 2009a).

In this study, we utilized a genome-wide functional screen to identify yeast mutants exhibiting sensitivity to the common solvent DMSO. During preparation of this manuscript, a study was published implicating transcriptional control machinery and cell wall integrity as necessary for DMSO tolerance in *S. cerevisiae* (Zhang *et al*., 2013). Similarly, our results demonstrate that mutants lacking components of the SWR1 histone exchange complex exhibit hypersensitivity to DMSO. Here we corroborate and extend Zhang *et al*. (2013) by identifying additional SWR1 and conserved oligomeric Golgi (COG) complex members as required for DMSO resistance. We also provide extensive dose-response data for various deletion strains and present several novel DMSO-sensitive mutants. Finally, we indicate that overexpression of histone H2A.Z can confer DMSO resistance. Many yeast genes identified in this investigation have homologs that may contribute to DMSO response in more complex organisms.

MATERIALS AND METHODS

Yeast strains and culture. Functional profiling and confirmation analyses utilized the collection of BY4743 non-essential diploid yeast deletion strains (*MATa/MATα his3Δ1/his3Δ1 leu2Δ0/leu2Δ0 lys2Δ0/LYS2 MET15/met15Δ0 ura3Δ0/ura3Δ0,* Invitrogen). All assays were performed in liquid rich media (1% yeast extract, 2% peptone, 2% dextrose, YPD) at 30°C with shaking at 200 rpm, except overexpression experiments, which used liquid rich media containing 2% galactose and 2% raffinose (YPGal+Raf). For overexpression analyses, the *HTZ1* and *ARP6* HIP FlexGene expression vectors were transformed into strains of the BY4743 background.

Functional profiling of the yeast genome and overenrichment analyses. Growth of the homozygous diploid deletion pools (4607 mutants in total), DNA extraction, PCR-amplification of strain barcodes, hybridization of Affymetrix TAG4 arrays, and differential strain sensitivity analysis (DSSA) were performed as described (Jo *et al.*, 2009b). For DSSA, twelve 1% DMSO replicates were compared to twelve YPD replicates. Data files are available at the Gene Expression Omnibus (GEO) database. Significantly overrepresented Gene Ontology (GO) and MIPS (Munich Information Center for Protein Sequences) categories within the functional profiling data were identified with FunSpec (Robinson *et al.*, 2002), using a *p*-value cutoff of 0.001 and Bonferroni correction.

Growth curve and flow cytometry confirmation assays. Growth curve assays were performed as in North *et al.* (2011), with DMSO (VWR, #EM-MX1458-6) added to the desired final concentrations at a minimum two technical replicates per dose. Confirmation of growth defects by a flow cytometry based relative growth assay was performed as in Gaytán *et al.* (2013a). Briefly, a culture containing GFP-tagged wild-type and untagged mutant cells was treated with DMSO, and a ratio of growth was calculated for untagged cells in treated versus untreated samples, as compared to the GFP strain. All graphs display the mean and standard error of three independent cultures. Three tests – regular *t*-test, Welch's test (*t*-test modification assuming unequal variances) and Wilcoxon Rank Sum (Mann-Whitney) test – were simultaneously applied to assess how possible violations of the assumptions underlying *t*-test (homoscedasticity and normality) affect statistical inference outcomes for the data. Raw *p* values for each test statistic were corrected for multiplicity of comparisons using Benjamini-Hochberg correction. *P*-values indicated on graphs are derived from regular *t*-tests, with Welch and Wilcoxon Rank Sum test results (which are more robust but more conservative in terms of adjusted *p*-values) usually in agreement with regular *t*-tests.

Nematode survival assays. *Caenorhabditis elegans* strains and their food source, the *Escherichia coli* OP50 strain, were purchased from the Caenorhabditis Genetics Center (CGC). Worms were maintained on nematode growth medium as described by Stiernagle (2006). Survival assays were conducted for 48 hours in 96-well plates in S media (Stiernagle, 2006), where three technical replicates each containing 25-50 worms were treated with various doses of DMSO. At the end of the exposure period, live and dead worms were counted. The mean and standard error for 2-3 independent experiments were calculated and displayed as percent survival.

Human cell culture and viability assays. Control (GM0038) and *COG8* mutant fibroblasts were a gift from Hudson Freeze, while *COG7* (HD) mutant fibroblasts were provided by Richard Steet. Cells were maintained at 37°C, 5% carbon dioxide, in low glucose (1g/L) Dulbecco's modified Eagle's medium (DMEM) containing 10% fetal bovine serum (FBS) and 1% penicillin/streptomycin (PS). For the viability assays, approximately 10,000 cells/well were treated with various concentrations of DMSO and incubated at 37°C for 48 hours. Cell viability was assessed with the XTT Cell Viability Assay Kit (Biotium) and data shown are reflective of 2-3 independent experiments.

RESULTS

Functional profiling in yeast identifies genes required for DMSO tolerance

Following growth of yeast homozygous diploid deletion mutant pools for 15 generations in 1% DMSO, DSSA identified 40 strains as sensitive to DMSO, as compared to YPD controls (Table 4.1). To identify the biological attributes required for DMSO tolerance, enrichment analyses for the 40 sensitive strains was performed with FunSpec at a corrected *p*-value of 0.001. The COG complex, as well as its biological functions (cytoplasm to vacuole targeting pathway and intra-Golgi transport), were overrepresented in both GO and MIPS categories (Table 4.2).

Mutants defective in Golgi/ER transport are sensitive to DMSO

Overrepresentation analyses suggested that subunits of COG, a protein complex that mediates fusion of transport vesicles to Golgi compartments, were required for DMSO tolerance. Therefore, we performed relative growth assays in which the growth of COG deletion strains was compared to a wild-type GFP-expressing strain in various DMSO concentrations. Deletion of genes encoding any of the four non-essential subunits of COG (*COG5*, *COG6*, *COG7*, and *COG8*) resulted in dose-dependent sensitivity to DMSO, with statistically significant growth defects observed at DMSO concentrations as low as 0.25% (Fig. 4.1A). Growth curve assays also confirmed sensitivity of the individual COG deletions under non-competitive conditions (Fig. 4.1B). To identify additional sensitive Golgi/ER transport strains not present in the functional profiling data, we tested the DMSO sensitivity of various mutants displaying synthetic lethality or sickness with at least one COG gene. Analysis of relative growth by flow cytometry found that strains lacking vacuolar SNAREs (*vam7*Δ and *gos1*Δ) were DMSO-sensitive (Fig. 4.1A). Growth curve experiments were performed as an alternative for strains demonstrating severe fitness defects in the relative growth assay, with mutants defective in retrograde Golgi transport (*ric1*Δ, *vps51*Δ, and *vps54*Δ) as well as those deleted for components of the Guided Entry of Tailanchored (GET) Golgi/ER trafficking complex (*get1*Δ and *get2*Δ) exhibiting dose-dependent DMSO sensitivity (Fig. 4.1B).

Chromatin remodeling machinery is required for DMSO tolerance

The *yaf9*Δ strain, which lacks a subunit common to the SWR1 histone exchange and NuA4 histone H4 acetyltransferase complexes, was identified by DSSA as DMSO-sensitive (Table 4.1) and confirmed by both competitive growth and growth curve assays to exhibit severe DMSO-dependent growth defects (Figs. 4.2A and 4.2B). This stark phenotype prompted us to examine all non-essential SWR1 and NuA4 deletions for DMSO sensitivity, as SWR1 and NuA4 complexes cooperate to alter chromatin structure in yeast (reviewed by Lu *et al.*, 2009). Except for *swc7*Δ, every SWR1 mutant (*swr1*Δ, *swc2*Δ, *swc3*Δ, *swc5*Δ, *swc6*Δ, *arp6*Δ, and *bdf1*Δ) was confirmed as sensitive to DMSO, with most displaying similar dose-dependent growth inhibition (Figs. 4.2A and 4.2B). Moreover, *htz1*Δ, a strain lacking the histone variant H2A.Z exchanged for histone H2A in nucleosomes by the SWR1 complex (Mizuguchi *et al.*, 2004), displayed growth defects in DMSO (Fig. 4.2A). Several, but not all, non-essential NuA4 deletion mutants (*eaf1*Δ, *eaf3*Δ, and *eaf7*Δ, but not *eaf5*Δ or *eaf6*Δ) were DMSO-sensitive, however, levels of DMSO-mediated growth inhibition did not approach that of the SWR1 mutants (Fig. 4.2A). We tested additional strains exhibiting both (1) defects in histone modification and (2) synthetic lethality or sickness with SWR1 and/or NuA4 genes (Collins *et al.*, 2007; Costanzo *et al.*, 2010;

Hoppins *et* al., 2011; Mitchell *et al.*, 2008). Absence of components of the Set1C histone H3 methylase (*swd1*Δ, *swd3*Δ, and *spp1*Δ), the Set3C histone deacetylase (*set3*Δ, *sif2*Δ, and *hos2*Δ, but not *snt1*Δ), the SAGA acetyltransferase (*gcn5*Δ) and histone H2B deubiquitylation module (*sgf11*Δ and *ubp8*Δ), and the Paf1 transcription initiation complex (*cdc73*Δ) conferred DMSO sensitivity, although none displayed DMSO-mediated growth defects as drastic as SWR1 mutants (Figs. 4.3A, 4.3B, 4.3C, and 4.3D). DSSA and our relative growth assay identified *HIR3*, a gene encoding a subunit of the histone regulation (HIR) nucleosome assembly complex, as required for DMSO tolerance, with additional HIR members (*HIR1*, *HIR2*, *HPC2*) also confirmed as necessary for resistance (Fig. 4.3E).

Additional mutants, including those involved in DNA repair, are sensitive to DMSO

The *NTG1* gene, which encodes a DNA N-glycosylase and apurinic/apyrimidinic lyase involved in base excision repair (Eide *et al.*, 1996), was identified by DSSA as required for DMSO resistance (Table 4.1). Our relative growth assay confirmed *ntg1*Δ as sensitive to DMSO, but interestingly, deletion of the *NTG1* paralog *NTG2* did not markedly alter growth in DMSO (Fig. 4.4A). A strain deleted for *MRE11*, a component of the meiotic recombination (MRX) complex involved in repair of DNA double-strand breaks (and exhibiting synthetic sickness with *EAF1* of NuA4), was also sensitive to DMSO (Fig. 4.4A). Deletions in prefoldin (*pac10*Δ and *yke2*Δ), a complex involved in the folding of tubulin and actin, were sensitive to DMSO (Fig. 4.4B). Other genes necessary for DMSO tolerance included *ROM2* (a GDP/GTP exchange factor for the Rho family), *EDO1 (*of unknown function), *RRP8* (an rRNA methyltransferase), and *KAP123* (a nuclear importer of histones H3 and H4) (Fig. 4.4C).

Overexpression of H2A.Z confers resistance to DMSO

After demonstrating a role for the SWR1 histone exchange machinery and its accessories in DMSO tolerance (Fig. 4.2), we examined whether overexpression of Htz1p (histone H2A.Z exchanged for H2A by SWR1) or Arp6p (the nucleosome binding component of SWR1) could rescue the DMSO sensitivity of various strains. Increased levels of Htz1p reversed the DMSO sensitivity of BY4743 wild-type and *htz1*Δ, but interestingly, caused growth defects with 1% DMSO in the *yaf9*Δ strain (Fig. 4.5). It did not affect sensitivity of the *ntg1*Δ DNA repair mutant (data not shown). Although Arp6p overexpression provided DMSO resistance to the *ntg1*Δ mutant (Fig. 4.5), it did not alter the growth of wild-type, *htz1*Δ, or *yaf9*Δ strains in DMSO (data not shown).

DISCUSSION

DMSO is a polar and aprotic solvent commonly utilized to solubilize chemicals during toxicological or pharmaceutical inquiries (Santos *et al.*, 2003). Compared to other solvents within its class such as sulfolane, *N,N*-dimethylformamide, *N*-methyl-pyrrolidin-2-one, or *N,N*-dimethyl acetamide, DMSO exhibits relatively limited acute toxicity (Tilstam, 2012), thus affording it preferred status within these fields. Despite its universality, DMSO's molecular mechanism(s) of action remain ambiguous, thus requiring investigations into the cellular processes and pathways it may perturb. Here we conducted a genome-wide functional screen in the model eukaryote *S. cerevisiae* to identify the nonessential yeast deletion mutants experiencing growth defects in 1% DMSO, a concentration typical to yeast toxicant or drug

profiling studies. We demonstrate that components of the COG Golgi/ER transport and SWR1 histone exchange complexes are required for DMSO tolerance in yeast, with various mutants displaying sensitivity at concentrations as low as 0.25% (Figs. 4.1 and 4.2). Although many DMSO resistance genes are conserved in humans (Table 4.3), we were unable to confirm a role in DMSO tolerance for the *COG5*, *NTG1*, and *YAF9* homologs in the nematode *Caenorhabditis elegans* or the *COG7* and *COG8* homologs in human fibroblasts (Fig. 4.6). These results may indicate that DMSO's mechanism of toxicity in yeast is different from that exhibited in nematodes or human cells. However, if the toxic mechanism remains similar, it is feasible that compensatory cellular processes or genes are present in these mutants.

During the preparation of this manuscript, a report was published describing functional profiling of yeast mutants in DMSO (Zhang *et al.*, 2013), with findings congruent to those presented in this study (see Fig. 4.7 for a comparison of strains identified). In this section, we discuss various aspects differentiating our investigation from Zhang *et al.* (2013). First, while these researchers assessed growth of individual yeast mutants via colony size on solid media, we performed functional profiling in pooled liquid cultures under competitive growth conditions. Our analyses, in which DNA sequences unique to each strain are hybridized to a microarray after toxicant exposure, are able to discern small growth defects and can identify sensitive strains overlooked by other methods (Fig. 4.7). However, the stringency of our DSSA may hinder identification of slow growing strains or those close to background levels. Nevertheless, these data are extremely relevant to those conducting pooled growth assays, especially considering the increased popularity of automated screens and high-throughput multiplexed barcode sequencing to examine strain growth in DMSO-soluble toxicants or drugs (Smith *et al.*, 2010; Smith *et al.*, 2012). Second, compared to the use of 4% and 8% DMSO in Zhang *et al.* (2013), the concentrations utilized in our screen (1%) and confirmation assays (0.25% – 2%) do not inhibit growth of the BY4743 wild-type strain and represent levels standard to functional screens (1% or less). The contrasting choice of doses may also account for differences in the DMSO-sensitive strains identified by each screen. Third, we provide extensive DMSO dose-response analyses for novel DMSO-sensitive strains as well as those concomitantly identified by Zhang *et al.* (2013). Finally, our overexpression data demonstrates that increased levels of Htz1p or Arp6p can rescue the growth of various deletion strains in DMSO (Fig. 4.5).

We have identified three cellular processes influencing DMSO resistance in budding yeast: Golgi/ER trafficking, SWR1 complex action, and DNA repair. Microarray analyses assessing the response of *S. cerevisiae* to DMSO (Zhang *et al.*, 2003) did not identify any genes described in this study, however, correlation between transcriptional events and genes required for growth under a selective condition is often low (Giaever *et al.*, 2002). The requirement of COG and SNARE Golgi/ER genes for DMSO tolerance (Fig. 4.1) may reflect findings in human and rat hepatocytes, where DMSO altered expression of genes associated with SNARE interactions in vesicular transport (Sumida *et al.*, 2011). Furthermore, as a “chemical chaperone”, DMSO can mimic the function of molecular chaperones (Papp and Csermely, 2006), a group of proteins closely tied to Golgi/ER operations. The DMSO sensitivity of histone H2A.Z and chromatin remodeling mutants (Figs. 4.2 and 4.3) indicate DMSO may affect chromatin structure. Lapeyre and Bekhor (1974) reported that 1% DMSO decreased chromatin thermostability, while higher

concentrations promoted chromatin relaxation. Consistent with these findings, Pommier *et al.* (1983) suggested DMSO increased domain (loop) size by reducing DNA-protein attachment points after finding it enhanced intercalator-induced DNA breakage. DMSO could conceivably cause DNA damage, as demonstrated by DNA repair mutant sensitivity (Fig. 4.4A). DMSO damaged DNA in bull sperm (Taşdemir *et al.*, 2013) and erythroleukemic cells (Scher and Friend, 1978), and additionally altered expression of DNA repair genes in human and rat hepatocytes (Sumida *et al.*, 2011).

The experimental evidence integrating the seemingly discrete processes of Golgi/ER transport, SWR1 complex action, and DNA repair is limited. Strains lacking SWR1 and NuA4 components exhibit synthetic lethality or sickness with various Golgi/ER transport and DNA repair genes (Collins *et al.*, 2007; Costanzo *et al.*, 2010; Hoppins *et* al., 2011; Mitchell *et al.*, 2008), but mechanistic data explaining these findings are lacking. If Golgi/ER transport is the crucial determinant of DMSO tolerance, it is reasonable that loss of SWR1, which may repress transcription by preventing histone H2A.Z deposition into chromatin (Meneghini *et al.*, 2003; Zhang *et al.*, 2005), could confer DMSO sensitivity by decreasing production of Golgi/ER transport genes. Expression of *COG7*, a COG member involved in Golgi/ER trafficking, is downregulated in *htz1*Δ and the SWR1 mutants *swr1*Δ, *swc2*Δ, and *swc5*Δ (Morillo-Huesca *et al.*, 2010), but others report the nonessential COG genes are neither induced nor repressed in the *swr1*Δ background (Meneghini *et al.*, 2003). Alternatively, if SWR1 or H2A.Z activity is the deciding factor in DMSO resistance, defective Golgi/ER transport could prevent appropriate processing and localization of SWR1 components or H2A.Z. However, the expression of Golgi/ER, chromatin remodeling, or DNA repair genes described herein are not altered in *htz1*Δ, and further, *HTZ1* expression is unchanged in SWR1 or NuA4 mutants (Lenstra *et al.*, 2011; Lindstrom *et al.*, 2006; Meneghini *et al.*, 2003). The relationship of SWR1 to DNA repair is evidenced by its ability to cause genetic instability in the absence of H2A.Z (Morillo-Huesca *et al.*, 2010) and also deposit H2A.Z at double-stranded DNA breaks (Kalocsay *et al.*, 2009).

We provide valuable insight into the genetic requirements for DMSO tolerance by identifying three major cellular processes – Golgi/ER transport, SWR1 complex function, and DNA repair – as important in DMSO resistance in *S. cerevisiae*. To separate effects of DMSO from a compound of interest, it is crucial for future yeast profiling studies to recognize that various deletion strains may fall out of pooled cultures during treatment with DMSO-solubilized drugs or toxicants. Data gathered by our study can direct additional experimentation to decipher the cellular and molecular mechanisms of DMSO action.

FIGURES

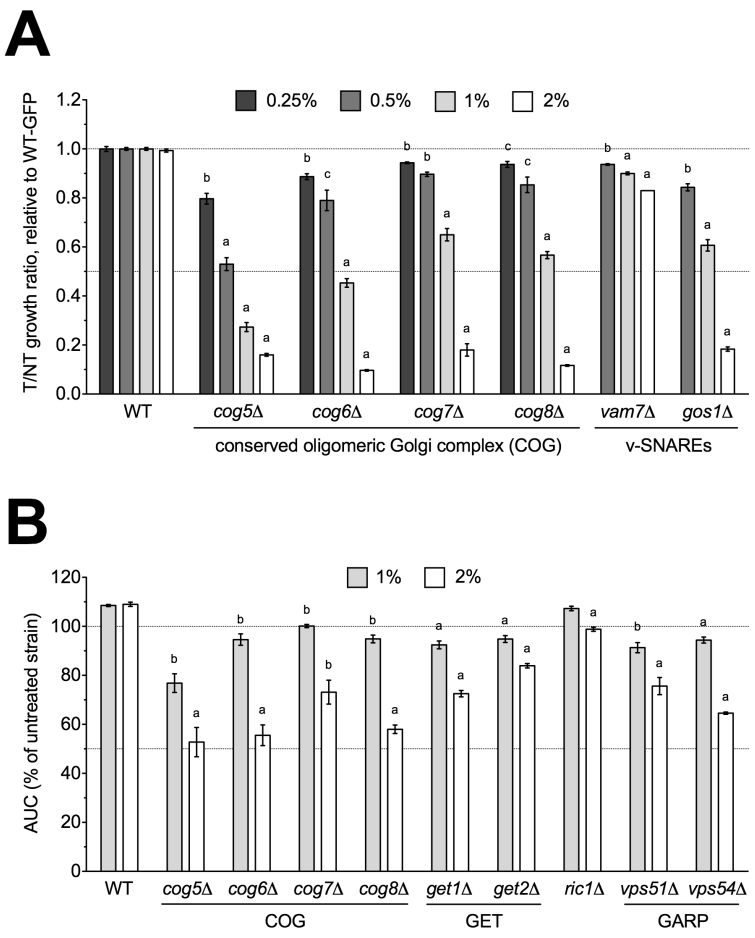

Fig. 4.1. Golgi/ER transport mutants are sensitive to DMSO. Statistical significance between wild-type and mutant strains was calculated by *t*-test, where [a]$p<0.001$, [b]$p<0.01$, and [c]$p<0.05$. (A) DMSO inhibits the growth of COG and vacuolar SNARE mutants. Mutant strains were grown in competition with a GFP-expressing wild-type strain in the indicated DMSO concentrations and relative growth ratios (treatment versus control) were obtained. The ratio means and standard errors are shown for three independent cultures. (B) Deletion of COG, GET, and Golgi-Associated Retrograde Protein (GARP) components confers DMSO sensitivity. Growth curves for three independent cultures were obtained for the indicated strains and doses of DMSO. The area under the curve (AUC) was calculated and is shown as a percentage of the untreated strain's AUC.

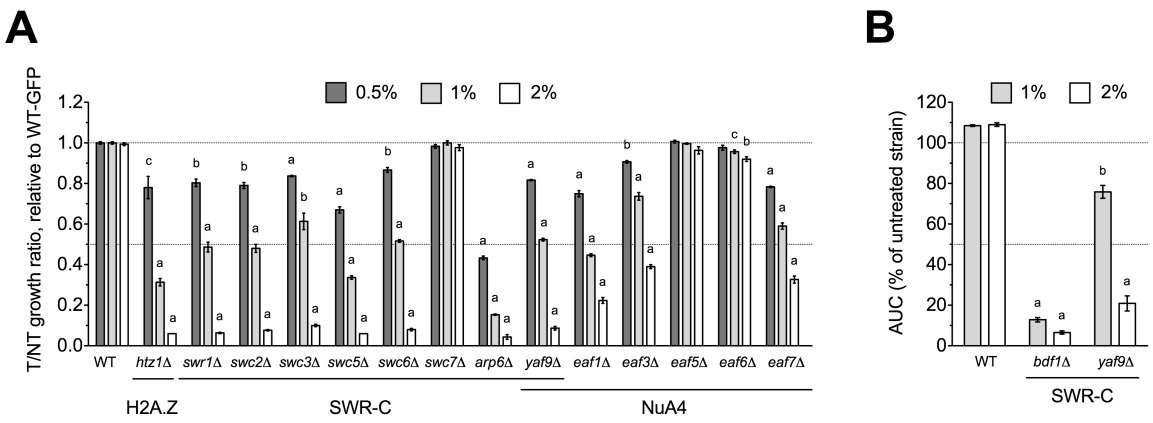

Fig. 4.2. SWR1 histone exchange and NuA4 histone H4 acetyltransferase mutants are sensitive to DMSO. Statistical significance between wild-type and mutant strains was determined by *t*-test, where [a]$p<0.001$, [b]$p<0.01$, and [c]$p<0.05$. (A) Strains lacking components of SWR1 or NuA4 are sensitive to DMSO. Relative growth ratios were obtained for three independent cultures. (B) The *bdf1*Δ and *yaf9*Δ SWR1 mutants are sensitive to DMSO. Growth curves were acquired from three independent cultures at the indicated doses.

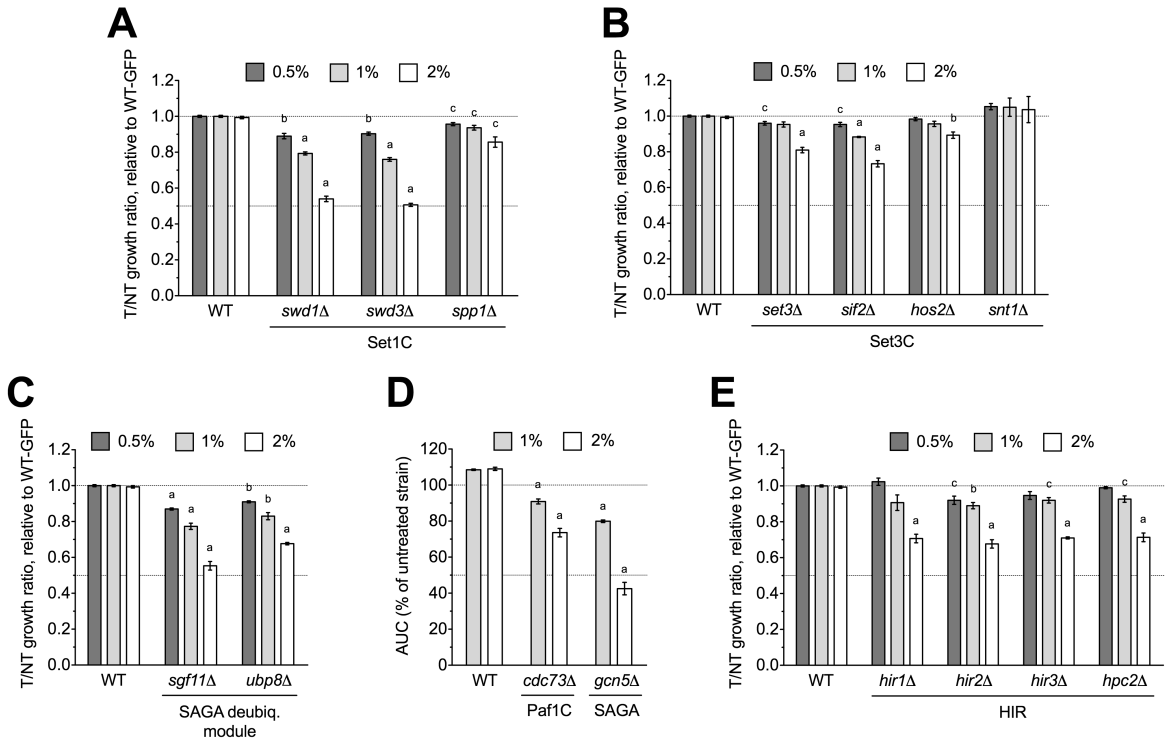

Fig. 4.3. Various chromatin remodeling mutants are sensitive to DMSO. Statistical significance between wild-type and mutant strains was calculated by *t*-test, with $^{a}p<0.001$, $^{b}p<0.01$, and $^{c}p<0.05$. (A) Set1C histone H3 methylase mutants exhibit growth defects in DMSO. (B) Set3C histone deacetylase mutants are DMSO-sensitive. (C) Strains lacking components of the SAGA histone H2B deubiquitylation module are sensitive to DMSO. (D) SAGA and Paf1 mutants experience sensitivity to DMSO. (E) HIR mutants are DMSO-sensitive. For (A), (B), (C), and (E), relative growth ratios were obtained and averaged for three independent cultures, while (D) displays average area under the curve data for growth curves acquired from three cultures.

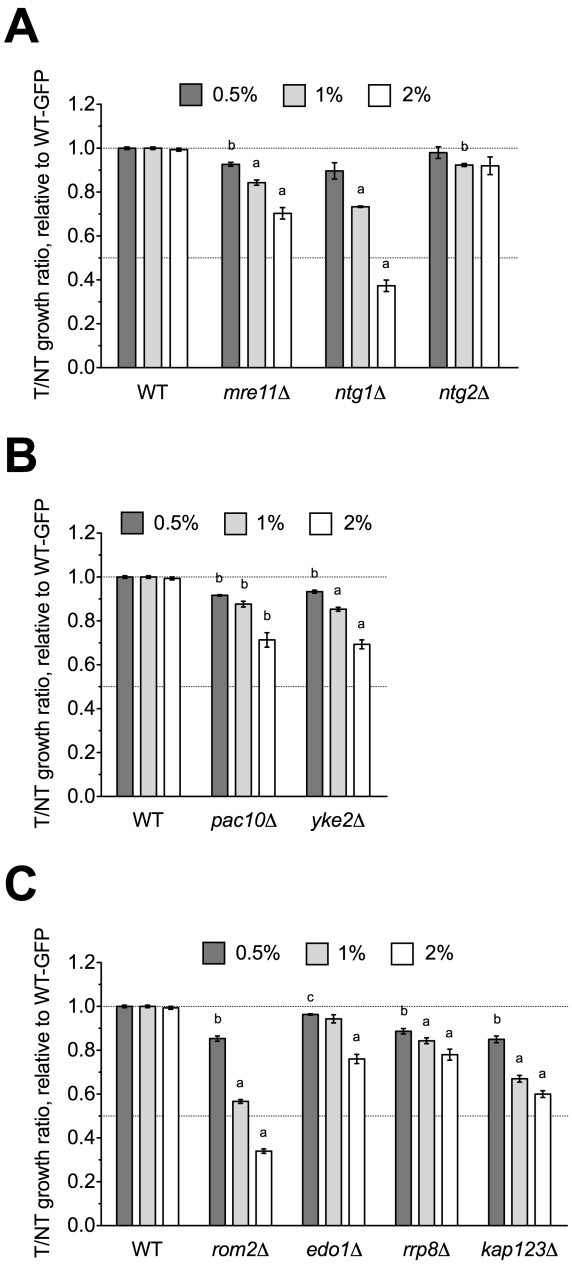

Fig. 4.4. DNA repair and other various mutants are sensitive to DMSO. Relative growth assays were performed for three independent cultures. Ratio means and standard errors are shown, with statistical significance between wild-type and mutant strains calculated by *t*-test, where $^{a}p<0.001$, $^{b}p<0.01$, and $^{c}p<0.05$. (A) DNA repair mutants are DMSO-sensitive. (B) Mutants lacking prefoldin components are sensitive to DMSO. (C) Various mutants experience growth defects in DMSO.

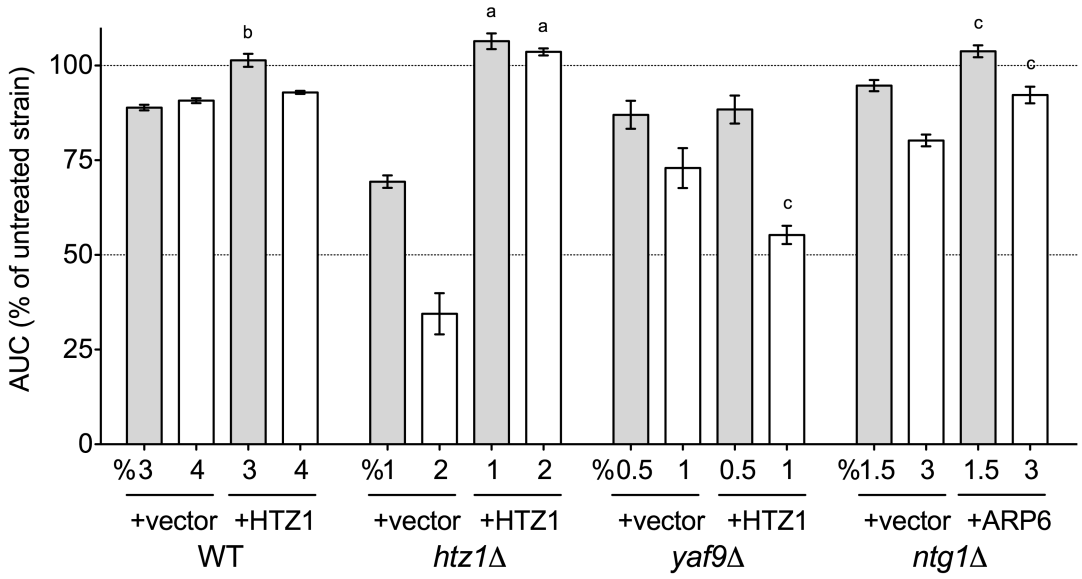

Fig. 4.5. Overexpression of Htz1p or Arp6p rescues DMSO sensitivity in various mutants. Growth curves for three independent cultures were obtained in the indicated doses of DMSO. The area under the curve (AUC) means and standard error are shown. Statistical significance between AUCs for corresponding doses in the empty vector and overexpression strains was calculated by *t*-test, and is indicated by $^{a}p<0.001$, $^{b}p<0.01$, and $^{c}p<0.05$.

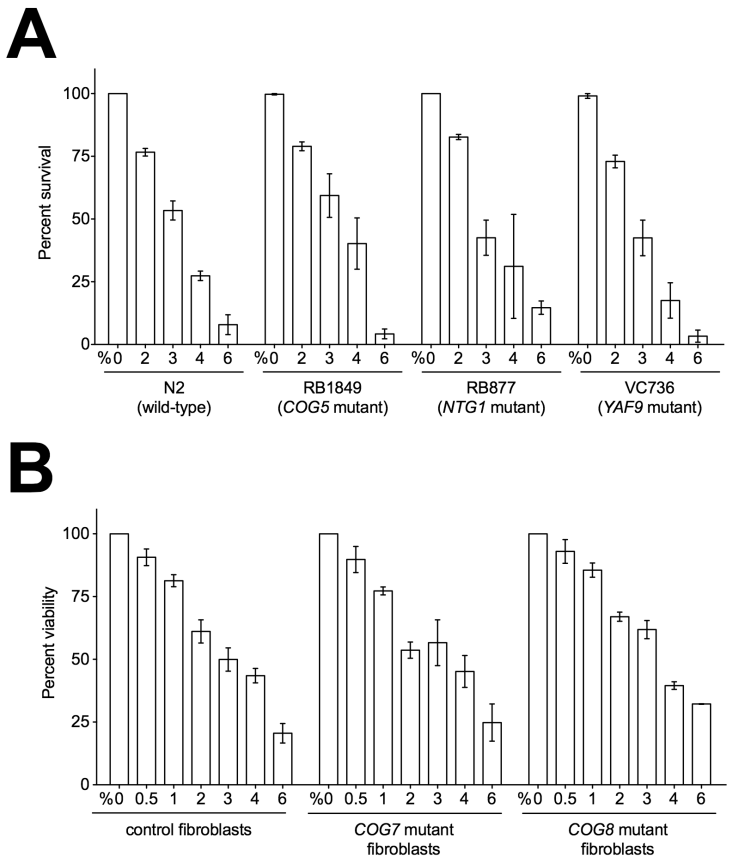

Fig. 4.6. Select nematode and human homologs of yeast DMSO tolerance genes are not involved in the DMSO response. Nematode survival and human cell viability assays were conducted as described in Materials and Methods. *C. elegans* strains were homozygous deletions of the indicated yeast homologs. Mutations in human *COG* genes can cause congenital disorders of glycosylation (Wu *et al.*, 2004). The *COG7* human fibroblasts lack the last 19 nucleotides of exon 1 (Wu *et al.*, 2004), while the *COG8* cells had two *COG8* mutations that severely truncated the protein (Kranz *et al.*, 2007).

DMSO tolerance genes identified by Zhang *et al.* (2013) and this study		DMSO tolerance genes identified by this study		
ARP6	*ROM2*	*COG5*	*KAP123*	*UBC8*
BDF1	*SET3*	*COG8*	*MRE11*	*VPS54*
CDC73	*SWC2 (VPS72)*	*EAF6*	*NTG1*	*YAF9*
COG6	*SWC3*	*EAF7*	*PAC10*	*YKE2*
COG7	*SWC6 (VPS71)*	*EDO1*	*RIC1*	
EAF1	*SWC7*	*GCN5*	*RRP8*	
EAF3	*SWD1*	*GET1*	*SGF11*	
GOS1	*SWR1*	*GET2*	*SIF2*	
HIR2	*VAM7*	*HIR1*	*SPP1*	
HOS2	*VPS51*	*HIR3*	*SWC5*	
HTZ1		*HPC2*	*SWD3*	

Fig. 4.7. A comparison between studies identifying yeast genes responsible for DMSO tolerance. DMSO tolerance genes identified by Zhang *et al.* (2013) were compared to those identified in this study.

Table 4.1. Fitness scores for deletion strains identified as significantly sensitive to 1% DMSO during a 15 generation treatment. Fitness is defined as the normalized log2 ratio of strain growth in the presence versus absence of DMSO. The confirmed column indicates whether the strain was confirmed as sensitive (S) or not sensitive (NS) by relative growth assays. Sensitivity is defined as a relative growth ratio of <0.9 in DMSO versus a wild-type GFP expressing strain. Appendix 3 lists all DSSA-identified strains sensitive and resistant to DMSO.

ORF	Deleted Gene	Log2 value 1% DMSO	Description of deleted gene	Confirmed
YIL162W	***SUC2***	-4.54	Invertase, sucrose hydrolyzing enzyme	NS
YHR010W	***RPL27A***	-2.45	Component of the large (60S) ribosomal subunit	
YDR083W	***RRP8***	-2.41	Nucleolar protein involved in rRNA processing	S
YNL051W	***COG5***	-2.38	Component of COG; functions in protein trafficking	S
YER156C	**-**	-2.31	Putative protein of unknown function	
YOR304C-A	**-**	-2.26	Protein of unknown function	S
YML071C	***COG8***	-2.11	Component of COG; functions in protein trafficking	S
YLR371W	***ROM2***	-2.10	GDP/GTP exchange protein (GEP) for Rho1p and Rho2p	S
YJL132W	**-**	-2.07	Putative protein of unknown function	NS
YKR024C	***DBP7***	-1.93	Putative ATP-dependent RNA helicase; involved in ribosomal biogenesis	NS
YFR034C	***PHO4***	-1.91	Myc-family transcription factor; regulated by phosphate availability	NS
YNL107W	***YAF9***	-1.90	Subunit of NuA4 histone H4 acetyltransferase and SWR1 complex	S
YLR322W	***VPS65***	-1.83	Dubious ORF; overlaps SFH1 gene; deletion causes VPS defects	
YFR036W	***CDC26***	-1.65	Subunit of the Anaphase-Promoting Complex/Cyclosome (APC/C)	NS
YFR045W	**-**	-1.62	Putative mitochondrial transport protein	
YKR019C	***IRS4***	-1.61	Regulates phosphatidylinositol 4,5-bisphosphate levels and autophagy	
YNL041C	***COG6***	-1.57	Component of COG; functions in protein trafficking	S
YLR261C	***VPS63***	-1.54	Dubious ORF; overlaps YPT6 gene ; deletion causes VPS defects	
YBR227C	***MCX1***	-1.50	Mitochondrial matrix protein; putative ATP-binding chaperone	
YGL005C	***COG7***	-1.47	Component of COG; functions in protein trafficking	S
YJL205C	***NCE101***	-1.41	Protein of unknown function; involved in secretion of proteins	
YER032W	***FIR1***	-1.39	Involved in 3' mRNA processing	
YEL039C	***CYC7***	-1.36	Cytochrome c isoform 2	
YER110C	***KAP123***	-1.35	Karyopherin, nuclear importer of ribosomal proteins and histones H3/H4	S
YGL158W	***RCK1***	-1.35	Protein kinase involved in the response to oxidative stress	NS
YBR013C	**-**	-1.28	Putative protein of unknown function	
YGL031C	***RPL24A***	-1.26	Ribosomal protein L30 of the large (60S) ribosomal subunit	
YML116W	***ATR1***	-1.24	Multidrug efflux pump of the major facilitator superfamily	
YJR140C	***HIR3***	-1.22	Subunit of the HIR nucleosome assembly complex	S
YNL198C	**-**	-1.19	Dubious ORF unlikely to encode a protein	
YGL139W	***FLC3***	-1.14	Putative FAD transporter	
YGR089W	***NNF2***	-1.08	Interacts physically and genetically with Rpb8p of RNA pols. I/II/III	
YKL040C	***NFU1***	-1.06	Involved in iron metabolism in mitochondria	
YAL015C	***NTG1***	-1.05	DNA N-glycosylase and AP lyase involved in base excision repair	S
YGR108W	***CLB1***	-1.03	B-type cyclin involved in cell cycle progression	
YCR067C	***SED4***	-0.92	Integral endoplasmic reticulum membrane protein	
YIR001C	***SGN1***	-0.90	Cytoplasmic RNA-binding protein; may have a role in mRNA translation	
YDL211C	**-**	-0.88	Unknown function; GFP-fusion protein localizes to vacuole	
YDR534C	***FIT1***	-0.88	Mannoprotein that is incorporated into the cell wall	
YER098W	***UBP9***	-0.87	Ubiquitin-specific protease that cleaves ubiquitin-protein fusions	

Table 4.2. MIPS or GO categories associated with genes required for DMSO resistance. Strains exhibiting sensitivity to 1% DMSO, as identified by DSSA, were analyzed with FunSpec for overrepresented biological attributes. [a]Number of genes in category identified as sensitive to DMSO. [b]Number of genes in GO or MIPS category.

GO Biological Process category	***p*-value**	**Genes identified**	**k[a]**	**f[b]**
cytoplasm to vacuole targeting (CVT) pathway [GO:0032258]	2.38E-006	*COG7 IRS4 COG8 COG6 COG5*	5	37
intra-Golgi vesicle-mediated transport [GO:0006891]	1.12E-005	*COG7 COG8 COG6 COG5*	4	24
GO Cellular Component category	***p*-value**	**Genes identified**	**k[a]**	**f[b]**
Golgi transport complex [GO:0017119]	7.94E-008	*COG7 COG8 COG6 COG5*	4	8
Golgi membrane [GO:0000139]	6.43E-004	*SED4 COG7 COG8 COG6 COG5*	5	117
MIPS Functional Classification category	***p*-value**	**Genes identified**	**k[a]**	**f[b]**
intra Golgi transport [20.09.07.05]	4.16E-005	*COG7 COG8 COG6 COG5*	4	33

Table 4.3. Human orthologs of yeast genes required for DMSO tolerance. Deletion of the yeast genes listed resulted in sensitivity to DMSO (shown in alphabetical order).

Yeast gene	Human ortholog(s)	Human protein description
ARP6	*ACTR6*	ARP6 actin-related protein 6 homolog
BDF1	*EP300*	histone acetyltransferase
CDC73	*CDC73*	component of the PAF1 complex; tumor suppressor
COG5	*COG5*	component of oligomeric Golgi complex 5
COG6	*COG6*	component of oligomeric Golgi complex 6
COG7	*COG7*	component of oligomeric Golgi complex 7
COG8	*COG8*	component of oligomeric Golgi complex 8
EAF3	*MORF4L1*	component of the NuA4 histone acetyltransferase complex
EAF6	*MEAF6*	component of the NuA4 histone acetyltransferase complex
EAF7	*MRGBP*	component of the NuA4 histone acetyltransferase complex
GCN5	*KAT2A*	histone acetyltransferase
GOS1	*GOSR1*	involved in ER-Golgi transport as well as intra-Golgi transport
HIR1/2	*HIRA*	histone chaperone
HOS2	*HDAC3*	histone deacetylase
HTZ1	*H2AFZ*	variant histone H2A; replaces conventional H2A in a subset of nucleosomes
KAP123	*IPO4*	nuclear transport receptor
MRE11	*MRE11A*	component of MRN complex; involved in DNA double-strand break repair
NTG1	*NTHL1*	apurinic and/or apyrimidinic endonuclease and DNA N-glycosylase
PAC10	*VBP1*	transfers target proteins to cytosolic chaperonin
RRP8	*RRP8*	component of the eNoSC complex; mediates silencing of rDNA
SIF2	*TBL1X*	subunit in corepressor SMRT complex along with HDAC3
SPP1	*CXXC1*	recognizes CpG sequences and regulates gene expression
SWC2	*VPS72*	subunit of acetyltransferase TRRAP/TIP60 and chromatin-remodeling SRCAP
SWC5	*CFDP1*	craniofacial development protein 1; may play role in embryogenesis
SWC6	*ZNHIT1*	zinc finger, HIT-type containing 1
SWD1	*RBBP5*	component of MLL1/MLL histone methyltransferase complex
SWD3	*WDR5*	component of MLL1/MLL histone methyltransferase complex
SWR1	*SRCAP*	catalytic component of the chromatin-remodeling SRCAP complex
UBP8	*USP22*	histone deubiquitinating component of SAGA histone acetylation complex
VAM7	*SNAP25*	t-SNARE involved in the molecular regulation of neurotransmitter release
VPS51	*VPS51*	required for both Golgi structure and vesicular trafficking
VPS54	*VPS54*	required for retrograde transport of proteins from prevacuoles to the late Golgi
YAF9	*YEATS4*	component of the NuA4 histone acetyltransferase complex
YKE2	*PFDN6*	subunit of heteromeric prefoldin; transfers proteins to cytosolic chaperonin

REFERENCES

Blackman, R. K., Cheung-Ong, K., Gebbia, M., Proia, D. A., He, S., Kepros, J. *et al.* (2012). Mitochondrial electron transport is the cellular target of the oncology drug elesclomol. *PLOS ONE*. **7,** e29798. doi:10.1371/journal.pone.0029798

Collins, S. R., Miller, K. M., Maas, N. L., Roguev, A., Fillingham, J., Chu, C. S. *et al.* (2007). Functional dissection of protein complexes involved in yeast chromosome biology using a genetic interaction map. *Nature*. **446,** 806–810.

Costanzo, M., Baryshnikova, A., Bellay, J., Kim, Y., Spear, E. D., Sevier, C. S. *et al.* (2010). The genetic landscape of a cell. *Science*. **327,** 425–431.

Eide, L., Bjørås, M., Pirovano, M., Alseth, I., Berdal, K. G., Seeberg, E. (1996). Base excision of oxidative purine and pyrimidine DNA damage in *Saccharomyces cerevisiae* by a DNA glycosylase with sequence similarity to endonuclease III from *Escherichia coli*. *P. Natl Acad. Sci. USA* **93,** 10735–10740.

Gaytán, B. D., Loguinov, A. V., Lantz, S. R., Lerot, J.-M., Denslow, N. D., Vulpe, C. D. (2013a). Functional profiling discovers the dieldrin organochlorinated pesticide affects leucine availability in yeast. *Toxicol. Sci.* **132,** 347–358.

Gaytán, B. D., Loguinov, A. V., De La Rosa, V. Y., Lerot, J.-M., Vulpe, C. D. (2013b). Functional genomics indicates yeast requires Golgi/ER transport, chromatin remodeling, and DNA repair for low dose DMSO tolerance. *Front. Genet.* **4,** 154.

Giaever, G., Chu, A. M., Ni, L., Connelly, C., Riles, L., Véronneau, S., *et al.* (2002). Functional profiling of the *Saccharomyces cerevisiae* genome. *Nature*. **418,** 387–391.

Hoppins, S., Collins, S. R., Cassidy-Stone, A., Hummel, E., Devay, R. M., Lackner, L. L., *et al*. (2011). A mitochondrial-focused genetic interaction map reveals a scaffold-like complex required for inner membrane organization in mitochondria. *J. Cell Biol.* **195,** 323–340.

Jo, W. J., Ren, X., Chu, F., Aleshin, M., Wintz, H., Burlingame, A., *et al.* (2009a). Acetylated H4K16 by MYST1 protects UROtsa cells from arsenic toxicity and is decreased following chronic arsenic exposure. *Toxicol. Appl. Pharmacol.* **241,** 294–302.

Jo, W. J., Loguinov, A., Wintz, H., Chang, M., Smith, A. H., Kalman, D., *et al.* (2009b). Comparative functional genomic analysis identifies distinct and overlapping sets of genes required for resistance to monomethylarsonous acid (MMAIII) and arsenite (AsIII) in yeast. *Toxicol Sci*. **111,** 424–436.

Kalocsay, M., Hiller, N. J., Jentsch, S. (2009). Chromosome-wide Rad51 spreading and SUMO-H2A.Z-dependent chromosome fixation in response to a persistent DNA double-strand break. *Mol. Cell*. **33,** 335–343.

Kranz, C., Ng, B. G., Sun, L., Sharma, V., Eklund, E. A., Miura, Y., *et al*. (2007). COG8 deficiency causes new congenital disorder of glycosylation type IIh. *Hum. Mol. Genet.* **16,** 731–741.

Lapeyre, J.-N., Bekhor, I. (1974). Effects of 5-bromo-2′-deoxyuridine and dimethyl sulfoxide on properties and structure of chromatin. *J. Mol. Biol*. **89,** 137–162.

Lenstra, T. L., Benschop, J. J., Kim, T., Schulze, J. M., Brabers, N. A. C. H., Margaritis, T. *et al.* (2011). The specificity and topology of chromatin interaction pathways in yeast. *Mol. Cell.* **42,** 536– 549.

Lindstrom, K. C., Vary, J. C., Parthun, M. R., Delrow, J., Tsukiyama, T. (2006). Isw1 functions in parallel with the NuA4 and Swr1 complexes in stress-induced gene repression. *Mol. Cell Biol*. **26,** 6117–6129.

Lu, P. Y. T., Lévesque, N., Kobor, M. S. (2009). NuA4 and SWR1-C: two chromatin-modifying complexes with overlapping functions and components. *Biochem. Cell Biol.* **87,** 799–815.

Meneghini, M. D., Wu, M., Madhani, H. D. (2003). Conserved histone variant H2A.Z protects euchromatin from the ectopic spread of silent heterochromatin. *Cell*. **112,** 725–736.

Mitchell, L., Lambert, J.-P., Gerdes, M., Al-Madhoun, A. S., Skerjanc, I. S., Figeys, D., *et al.* (2008). Functional dissection of the NuA4 histone acetyltransferase reveals its role as a genetic hub and that Eaf1 is essential for complex integrity. *Mol. Cell Biol*. **28,** 2244–2256.

Mizuguchi, G., Shen, X., Landry, J., Wu, W.-H., Sen, S., Wu, C. (2004). ATP-driven exchange of histone H2AZ variant catalyzed by SWR1 chromatin remodeling complex. *Science*. **303,** 343–348.

Morillo-Huesca, M., Clemente-Ruiz, M., Andújar, E., Prado, F. (2010). The SWR1 histone replacement complex causes genetic instability and genome-wide transcription misregulation in the absence of H2A.Z. *PLOS ONE*. **5,** e12143. doi: 10.1371/journal.pone.0012143.

North, M., Tandon, V. J., Thomas, R., Loguinov, A., Gerlovina, I., Hubbard, A. E., *et al.* (2011). Genome-wide functional profiling reveals genes required for tolerance to benzene metabolites in yeast. *PLOS ONE*. **6,** e24205. doi:10.1371/journal.pone.0024205

Papp, E., Csermely, P. (2006). Chemical chaperones: mechanisms of action and potential use. *Handb.Exp. Pharmacol*. 172, 405–416.

Pommier, Y., Zwelling, L. A., Mattern, M. R., Erickson, L. C., Kerrigan, D., Schwartz, R., *et al*. (1983). Effects of dimethyl sulfoxide and thiourea upon intercalator-induced DNA single-strand breaks in mouse leukemia (L1210) cells. *Cancer Res.* **43,** 5718–5724.

Robinson, M., Grigull, J., Mohammad, N., Hughes, T. (2002). FunSpec: a web-based cluster interpreter for yeast. *BMC Bioinformatics*. **3,** 35.

Santos, N. C., Figueira-Coelho, J., Martins-Silva, J., Saldanha, C. (2003). Multidisciplinary utilization of dimethyl sulfoxide: pharmacological, cellular, and molecular aspects. *Biochem. Pharm*. **65,** 1035–1041.

Scher, W., and Friend, C. (1978). Breakage of DNA and alterations in folded genomes by inducers of differentiation in friend erythroleukemic cells. *Cancer Res*. **38,** 841–849.

Smith, A. M., Durbic, T., Kittanakom, S., Giaever, G., Nislow, C. (2012). Barcode sequencing for understanding drug-gene interactions. *Methods Mol. Biol.* **910,** 55–69.

Smith, A. M., Heisler, L. E., St. Onge, R. P., Farias-Hesson, E., Wallace, I. M., Bodeau, J., *et al*. (2010). Highly-multiplexed barcode sequencing: an efficient method for parallel analysis of pooled samples. *Nucleic Acids Res*. **38,** e142.

Steinmetz, L. M., Scharfe, C., Deutschbauer, A. M., Mokranjac, D., Herman, Z. S., Jones, T., *et al.* (2002). Systematic screen for human disease genes in yeast. *Nat. Genet.* **31,** 400–404.

Stiernagle, T. (2006). Maintenance of *C. elegans*. WormBook, ed. The *C. elegans* Research Community, WormBook, doi/10.1895/wormbook.1.101.1, http://www.wormbook.org.

Sumida, K., Igarashi, Y., Toritsuka, N., Matsushita, T., Abe-Tomizawa, K., Aoki, M., *et al.* (2011). Effects of DMSO on gene expression in human and rat hepatocytes. *Hum Exp Toxicol*. **30,** 1701-1709.

Taşdemir, U., Büyükleblebici, S., Tuncer, P. B., Coşkun, E., Özgürtaş, T., Aydın, F. N., *et al.* (2013). Effects of various cryoprotectants on bull sperm quality, DNA integrity and oxidative stress parameters. *Cryobiology*. **66,** 38–42.

Tilstam, U. (2012). Sulfolane: A versatile dipolar aprotic solvent. *Org. Process Res. Dev.* **16,** 1273–1278.

Wu, X., Steet, R. A., Bohorov, O., Bakker, J., Newell, J., Krieger, M., *et al.* (2004). Mutation of the COG complex subunit gene COG7 causes a lethal congenital disorder. *Nat Med*. **10,** 518–523.

Yu, Z. W., Quinn, P. J. (1994). Dimethyl sulphoxide: a review of its applications in cell biology. *Biosci. Rep.* **14,** 259–281.

Zhang, H., Roberts, D. N., Cairns, B. R. (2005). Genome-wide dynamics of Htz1, a histone H2A variant that poises repressed/basal promoters for activation through histone loss. *Cell*. **123,** 219–231.

Zhang, L., Liu, N., Ma, X., Jiang, L. (2013). The transcriptional control machinery as well as the cell wall integrity and its regulation are involved in the detoxification of the organic solvent dimethyl sulfoxide in *Saccharomyces cerevisiae*. *FEMS Yeast Res*. **13,** 200–218.

Zhang, W., Needham, D. L., Coffin, M., Rooker, A., Hurban, P., Tanzer, M. M., *et al*. (2003). Microarray analyses of the metabolic responses of *Saccharomyces cerevisiae* to organic solvent dimethyl sulfoxide. *J. Ind. Microbiol. Biotechnol.* **30,** 57–69.

CHAPTER 5

A SEMI-AUTOMATED FRAMEWORK FOR YEAST FUNCTIONAL PROFILING OF CHEMICAL CONTAMINANTS

INTRODUCTION

Chemical contaminants are ubiquitous in the environment, wildlife, and humans. As examples, the production and use of halogenated flame retardants (HFRs) has grown dramatically on account of strict flammability standards (Babrauskas *et al.*, 2012), whereas the chlorinated antimicrobial compound triclosan (TCS) is widely used in consumer products (Bedoux *et al.*, 2012), with both leaching into the environment throughout their life cycles. Furthermore, large amounts of oil dispersants and organophosphate pesticides have been applied across the globe (Goodbody-Gringley *et al.*, 2013; Saunders *et al.*, 2012). Termed emerging contaminants, the majority of these substances lack adequate toxicological information and are therefore of high concern to public health and ecosystems. Especially ambiguous are the cellular and molecular phenomena underlying the observed adverse effects, which include but are not limited to neurological and developmental toxicity, endocrine disruption, and cancer (reviewed by Dann and Hontela, 2011; Eaton *et al.*, 2008; Flaskos, 2012; DiGangi *et al.*, 2010; Wise and Wise, 2011). On account of the large number of exposures occurring in everyday life, it is important to understand the toxicity of emerging contaminants.

Numerous investigations into drug and toxicant mechanisms of action have utilized the barcoded homozygous and heterozygous deletion collections in the eukaryotic budding yeast *Saccharomyces cerevisiae* (Giaever *et al.*, 2002; reviewed by dos Santos *et al.*, 2012; North and Vulpe, 2010). These libraries, consisting of thousands of mutants, can be examined in parallel for altered growth in a substance of interest, with sensitive and resistant mutants identified by counting the barcodes unique to each strain (North *et al.*, 2011). Previously, these types of analyses were slowed by steps requiring manual operations, such as measurement of deletion pool optical densities for predefined growth periods as well as genomic DNA extractions (Gaytán *et al.*, 2013). Additionally, barcode counting was performed with purpose-built microarrays, a costly methodology that limited throughput. Recently, software has been designed to semi-automate pool growths with a liquid handler and microplate readers (Proctor *et al.*, 2011), and additional robotics can extract DNA in a 96-well format. Furthermore, reports of barcode counting with multiplexed deep sequencing (Han *et al.*, 2010; Smith *et al.*, 2010) promises increased throughput of such assays.

In this study, a liquid handler was utilized in conjunction with microplate readers to robotically expose yeast homozygous deletion pools to a range of contaminants of emerging concern (Table 5.1; see Figure 5.1 for a flow chart). Genomic DNA was extracted by automation, and the barcodes identifying each strain were amplified by PCR, with primers bestowing indexes for 96-plexed Illumina sequencing. The purified PCR products were quantified, pooled, and gel purified in preparation for sequencing. Further studies are needed to separate sequencing data into experimental conditions and replicates, and identification of mutants with altered growth in each of the conditions necessitates a differential strain sensitivity analysis. Future computational and confirmatory analyses are necessary to reveal pathways and cellular processes required for tolerance to the toxicants under study.

MATERIALS AND METHODS

Yeast strains and culture

All experiments utilized the collection of BY4743 non-essential diploid yeast deletion strains (*MATa/MATα his3Δ1/his3Δ1 leu2Δ0/leu2Δ0 lys2Δ0/LYS2 MET15/met15Δ0 ura3Δ0/ura3Δ0,* Invitrogen). Yeast growth assays were performed in liquid rich media (1% yeast extract, 2% peptone, 2% dextrose, YPD) at 30°C in Tecan microplate readers.

Chemicals

Tris(2-chloroethyl) phosphate (TCEP, cat# 119660), tris(1-chloro-2-propyl) phosphate (TCPP, cat# 32952), tris(1,3-dichloro-2-propyl) phosphate (TDCPP, cat# 32951), 3,3′,5,5′-tetrabromobisphenol A (TBBPA, cat# 330396), triclosan (TCS, cat# 72779), 3,5,6-trichloro-2-pyridinol (TCPy, cat# 33972), endosulfan (ENDO, cat# 32015) were purchased from Sigma-Aldrich. Chlorpyrifos oxon (COX, cat# MET-11459B) was purchased from Chem Service, Inc., while Corexit 9500 and Corexit 9527 were gifts from N. Denslow. DE71 was from Wellington Laboratories (cat# TBDE-71X). Ziram, 2-chloro-2'-deoxyadenosine (2-CdA), 4-chloro-*o*-phenylenediamine, tris(2,3-epoxypropyl) isocyanurate, bioallethrin, fludioxonil, captafol, and folpet were provided by Evotec. All compounds were prepared in dimethylsulfoxide (DMSO), except for Corexit 9500 and 9527, which were diluted in water.

IC20 determination and pool exposures

Wild-type yeast diluted to 0.0165 OD600 was treated with toxicant titrated (1% or less by volume) across a 96-well plate. Plates were incubated with intermittent shaking for 24h at 30°C in Tecan microplate readers. IC20s were calculated by either the area under the curve or the average generation time ratio to the control, with the IC20 corresponding to a ratio of approximately 0.8. Deletion pool growth and exposure was conducted in 700µl volumes of YPD in Tecan microplate readers, with OD600 readings taken every 15 min. The ACCESS (YeastGrow) software (Proctor *et al.*, 2011) facilitated Tecan communication with a Multiprobe IIEX liquid handler, allowing for toxicant (7µl) addition at various concentrations, culture growth to 15 generations, and saving of pool samples at 5 and 15 generations onto cold plates (Torrey Pines, cat# RIC20).

DNA extraction and barcode amplification

Methods were similar to Smith *et al.* (2012), with slight modifications. Pelleted yeast pools were resuspended in deep 96-well plates in 125µl sphereoplast buffer (1.2M sorbitol, 0.1M potassium phosphate, 0.5mM magnesium chloride) containing 5µl 1mg/ml zymolase and incubated 2h at 37°C to remove the cell wall. DNA extraction was performed with the Corbett X-tractor Gene robot using QIAGEN DX reagents (cat# 950107) and plasticware (cat# 950037). To amplify the barcode sequences uniquely identifying each deletion strain, 5µl of genomic DNA was added to 22.5µl of Platinum SuperMix (Invitrogen, cat# 11306-016) and 1µl each of 6µM common and indexing primers (200nM final concentration, see Table 5.2 for sequences). PCR was conducted in 96-well format with the following conditions: 95°C/3 min; 25 cycles of 94°C/30 s, 55°C/30 s, 72°C/30 s; followed by 72°C/10 min. PCR products were purified with the ZR-96 DNA Clean & Concentrator-5 (Zymo Research, cat# D4024), quantified with the Quant-iT Broad-Range DNA Assay Kit (Invitrogen, cat# Q-33130), and normalized to a concentration of 2µg/ml. Equal

volumes of normalized, purified PCR product were pooled and further purified by gel purification with the GeneJET gel extraction kit (Thermo Scientific, cat# K0691).

RESULTS

IC20 determinations, robotic exposures, and deletion pool growths

Growth curve assays were performed with various doses of each chemical and IC20s were calculated (Fig. 5.2 and Table 5.3). IC20 determinations for substances not shown in Fig. 5.2 were approximated with the YeastGrow software (Proctor *et al.*, 2011), and a representative analysis is presented in Fig. 5.3. Deletion pool exposures of 5 and 15 generations were semi-automated with the YeastGrow software, microplate readers, and a liquid handler, with a typical screening process shown in Fig. 5.4.

Automated DNA extraction and quantification

DNA extractions were performed as described in Materials and Methods, and quantified using the NanoQuant module on a Tecan microplate reader (Table 5.4). Extractions were typically of good concentration (~20 – 150ng/µl) and quality (260/280 ratios of 1.8 – 2.1), indicating the automated process was similar to manual DNA extractions performed in Chapters 2, 3, and 4.

PCR amplification and purification of barcodes

PCR was performed in 96-well plates utilizing template from the DNA extractions described in Fig. 5.5 and primers listed in Table 5.2. A representative gel is shown for a typical PCR amplification (Fig. 5.5), with almost all wells displaying the correct banding pattern. It is possible that a very limited number of primer combinations do not amplify the barcodes (see Fig. 5.5 legend). After purification, the PCR products were quantified with a fluorescence assay (Table 5.5) using a standard curve (Fig 5.6). Equal volumes of purified quantified PCRs from the corresponding UP and DN reactions were pooled to a concentration of 2µg/ml and gel purified to ~20µg/ml (Fig. 5.7) in preparation for sequencing submission.

DISCUSSION

The presence of chemical contaminants in the environment is of increasing concern, especially considering most lack sufficient toxicological data. Risk assessment analyses would be facilitated by the availability of information pertaining to mechanisms of action as well as potential genes lending susceptibility. In this study, a semi-automated approach was utilized to screen the barcoded yeast homozygous diploid deletion collection for strains exhibiting altered growth in 21 different substances, ranging from flame retardants and oil dispersants to pesticides and antimicrobials (Table 5.1). Although further steps are needed to complete the identification of sensitive and resistant mutants, this framework will provide novel insight into the toxicity of many chemicals and is applicable to additional high-throughput inquires with a range of contaminants.

One class of substances screened against the yeast deletion library are HFRs, pervasive chemical contaminants increasingly detected in the environment, wildlife, and humans (Babrauskas *et al.*, 2012). Although legislation in the European Union and U.S. has restricted the use of certain HFRs, exposures will continue due to environmental ubiquity. Studies demonstrate that exposure

to HFRs may be associated with neurological and developmental effects, endocrine disruption, and cancer (DiGangi *et al.*, 2010). TDCPP, also known as chlorinated Tris, was found to be mutagenic *in vitro* (Gold *et al.*, 1978) and increased the incidence of benign and malignant tumors in Sprague-Dawley rats (Freudenthal and Henrich, 2000), but its use has escalated following the ban of the popular brominated flame retardant pentaBDE. It is expected that yeast DNA repair mutants will experience growth defects in TDCPP and the related compounds TCPP and TCEP. TBBPA is a possible thyroid hormone disruptor and may also be immunotoxic (Covaci *et al.*, 2009). Since yeast lacks an endocrine or immune system, it is difficult to predict which yeast mutants will be affected by TBBPA, however, it clearly causes growth inhibition at relatively low concentrations (Fig. 5.2B and Table 5.3). Additional halogenated compounds examined include the chlorpyrifos pesticide metabolites chlorpyrifos oxon and TCPy, which may disrupt neurodevelopmental processes (Eaton *et al.*, 2008; Flaskos, 2012), as well as endosulfan, an organochlorinated pesticide that causes a range of toxicities (Karami-Mohajeri and Abdollahi, 2011).

Another chemical examined herein is triclosan (TCS), a powerful antimicrobial agent widely found in personal hygiene products, pharmaceuticals, and various household items (NTP, 2008). TCS is a stable lipophilic compound that contains functional groups representative of phenols, diphenyl ethers, and polychlorinated biphenyls (Gee *et al.*, 2008). It is active against both gram-positive and gram-negative bacteria (Bhargava and Leonard, 1996), and also exhibits antifungal and antiviral properties (Jones *et al.*, 2000). At low concentrations, TCS blocks the synthesis of fatty acids essential to microbe survival by inhibiting the enoyl-acyl carrier-protein reductase (ENR) (Heath *et al.*, 1998; Yazdankhah *et al.*, 2006). Since humans use a unrelated enzyme during fatty acid synthesis, TCS cannot disrupt this process in humans (Perozzo *et al.*, 2002). At high concentrations, TCS can intercalate into microbial membranes and disrupt membrane activities (Guillén *et al.*, 2004; Yazdankhah *et al.*, 2006). It is hypothesized that yeast mutants defective in fatty acid processes will be sensitive to TCS, as the mutant phenotype of the yeast 2-enoyl thioester reductase Etr1p, which has a probable role in mitochondrial fatty acid synthesis, is complemented by the ENR from *Escherichia coli* (Torkko *et al.*, 2001). If confirmed, a surprising result would be the sensitivity of DNA repair mutants, which was observed in a preliminary screen (unpublished data).

Following the BP Deepwater Horizon oil spill in 2010, the Corexit 9500 and 9527 chemical dispersant mixtures of surfactants and solvents were used to break down crude oil into smaller particles (Wise and Wise, 2011). The EPA (2013) has posted a list of the substances contained within the Corexits, which include 1,2-propanediol (CAS# 57-55-6), 2-butoxyethanol (CAS# 111-76-2, not included in 9500), butanedioic acid, 2-sulfo-, 1,4-bis(2-ethylhexyl) ester, sodium salt (1:1) (CAS# 577-11-7), sorbitan, mono-(9Z)-9-octadecenoate (CAS# 1338-43-8), sorbitan, mono-(9Z)-9-octadecenoate, poly(oxy-1,2-ethanediyl) derivs. (CAS# 9005-65-6) sorbitan, tri-(9Z)-9-octadecenoate, poly(oxy-1,2-ethanediyl) derivs. (CAS# 9005-70-3), 2-propanol, 1-(2-butoxy-1-methylethoxy)- (CAS# 29911-28-2), and distillates (petroleum), hydrotreated light (CAS# 64742-47-8). The toxic mechanisms of chemical dispersants in humans and marine species remain relatively unknown, as most studies have focused on lethality or other broad-

range endpoints (reviewed by Wise and Wise, 2011). In yeast, surfactants are likely to disrupt membranes or lipid processes.

Finally, deletion pools were exposed to a group of nine EPA ToxCast Phase I compounds deemed potential genotoxicants in ToxCast assays (unpublished data). These included the fungicides ziram, fludioxonil, captafol, and folpet, the anti-leukemic 2-chloro-2'-deoxyadenosine, the dye intermediate 4-chloro-*o*-phenylenediamine, the industrial chemical tris(2,3-epoxypropyl) isocyanurate, and the ectoparasiticide bioallethrin. Reports indicate that some of these substances exhibit mutagenicity and carcinogenicity, such as folpet (US EPA, 1999) and captafol (NTP, 2011). Further analyses are needed to determine distinct repair mechanisms required for tolerance in yeast.

This study provides a foundation for semi-automated screening of the yeast barcoded libraries with any substance of interest. Slight modifications should make it applicable to any barcoded organism, such as those created by the TagModule collection (Oh *et al.*, 2010). Through identification of mutants exhibiting chemical susceptibility or resistance, subsequent follow-up analyses can elucidate pathways, cellular processes, and molecular mechanisms involved in toxicant response. This functional toxicological approach promises to galvanize chemical toxicity testing and will supply novel understanding into the toxic mechanisms of numerous substances.

REFERENCES

Babrauskas, V., Lucas, D., Eisenberg, D., Singla, V., Dedeo, M., Blum, A. (2012). Flame retardants in building insulation: a case for re-evaluating building codes. *Build. Res. Info.* **40**, 738-755.

Bedoux, G., Roig, B., Thomas, O., Dupont, V., Le Bot, B. (2012). Occurrence and toxicity of antimicrobial triclosan and by-products in the environment. *Environ. Sci. Pollut. Res. Int*. **19,** 1044–1065.

Bhargava, H. N., Leonard, P. A. (1996). Triclosan: applications and safety. *Am. J. Infect. Control*. **24**, 209–218.

Covaci, A., Voorspoels, S., Abdallah, M. A.-E., Geens, T., Harrad, S., Law, R. J. (2009). Analytical and environmental aspects of the flame retardant tetrabromobisphenol-A and its derivatives. *J. Chromatogr. A*. **1216**, 346–363.

Dann, A. B., Hontela, A. (2011). Triclosan: environmental exposure, toxicity and mechanisms of action. *J. Appl. Toxicol*. **31**, 285–311.

DiGangi, J., Blum, A., Bergman, Å., Wit, C. A. de, Lucas, D., Mortimer, D., *et al*. (2010). San Antonio statement on brominated and chlorinated flame retardants. *Environ. Health Pers*. **118**, A516–A518.

dos Santos, S. C., Teixeira, M. C., Cabrito, T. R., Sá-Correia, I. (2012). Yeast toxicogenomics: genome-wide responses to chemical stresses with impact in environmental health, pharmacology, and biotechnology. *Front Genet*. **3**, 63.

Eaton, D. L., Daroff, R. B., Autrup, H., Bridges, J., Buffler, P., Costa, L. G., *et al*. (2008). Review of the toxicology of chlorpyrifos with an emphasis on human exposure and neurodevelopment. *Crit. Rev. Toxicol.* **38 Suppl 2**, 1–125.

Flaskos, J. (2012). The developmental neurotoxicity of organophosphorus insecticides: a direct role for the oxon metabolites. *Toxicol. Lett.* **209**, 86–93.

Freudenthal, R. I., Henrich, R. T. (2000). Chronic toxicity and carcinogenic potential of tris-(1,3-dichloro-2-propyl) phosphate in Sprague-Dawley rat. *Int. J. Tox*. **19**, 119–125.

Gaytán, B. D., Loguinov, A. V., Lantz, S. R., Lerot, J.-M., Denslow, N. D., Vulpe, C. D. (2013). Functional profiling discovers the dieldrin organochlorinated pesticide affects leucine availability in yeast. *Toxicol. Sci.* **132**, 347–358.

Gee, R. H., Charles, A., Taylor, N., Darbre, P. D. (2008). Oestrogenic and androgenic activity of triclosan in breast cancer cells. *J Appl Toxicol*. **28**, 78–91.

Giaever, G., Chu, A. M., Ni, L., Connelly, C., Riles, L., Véronneau, S., *et al*. (2002). Functional profiling of the *Saccharomyces cerevisiae* genome. *Nature*. **418**, 387–391.

Gold, M. D., Blum, A., Ames, B. N. (1978). Another flame retardant, tris-(1,3-dichloro-2-propyl)-phosphate, and its expected metabolites are mutagens. *Science*. **200**, 785–787.

Goodbody-Gringley, G., Wetzel, D. L., Gillon, D., Pulster, E., Miller, A., Ritchie, K. B. (2013). Toxicity of Deepwater Horizon source oil and the chemical dispersant, Corexit® 9500, to coral larvae. *PLoS One*. **8**:e45574. doi: 10.1371/journal.pone.0045574

Guillén, J., Bernabeu, A., Shapiro, S., Villalaín, J. (2004). Location and orientation of Triclosan in phospholipid model membranes. *Eur. Biophys. J.* **33**, 448–453.

Han, T. X., Xu, X.-Y., Zhang, M.-J., Peng, X., Du, L.-L. (2010). Global fitness profiling of fission yeast deletion strains by barcode sequencing. *Genome Biology*. **11**, R60.

Heath, R. J., Yu, Y. T., Shapiro, M. A., Olson, E., Rock, C. O. (1998). Broad spectrum antimicrobial biocides target the FabI component of fatty acid synthesis. *J. Biol. Chem.* **273**, 30316–30320.

Jones, R. D., Jampani, H. B., Newman, J. L., Lee, A. S. (2000). Triclosan: a review of effectiveness and safety in health care settings. *Am. J. Infect. Control*. **28**, 184–196.

Karami-Mohajeri, S., Abdollahi, M. (2011). Toxic influence of organophosphate, carbamate, and organochlorine pesticides on cellular metabolism of lipids, proteins, and carbohydrates. *Hum Exp Toxicol*. **30**, 1119–1140.

National Toxicology Program (NTP). (2008). Nomination profile for triclosan: supporting information for toxicological evaluation by the National Toxicology Program. US Dept of Health and Human Services, NTP, Research Triangle Park, NC, USA.

National Toxicology Program (NTP). (2011). *Report on carcinogens, twelfth edition.* US Dept of Health and Human Services, NTP, Research Triangle Park, NC, USA.

North, M., Tandon, V. J., Thomas, R., Loguinov, A., Gerlovina, I., Hubbard, A. E., *et al*. (2011). Genome-wide functional profiling reveals genes required for tolerance to benzene metabolites in yeast. *PLoS ONE*. **6**, e24205.

North, M., Vulpe, C. D. (2010). Functional toxicogenomics: mechanism-centered toxicology. *Int. J. Mol. Sci*. **11**, 4796–4813.

Oh, J., Fung, E., Price, M. N., Dehal, P. S., Davis, R. W., Giaever, G., *et al*. (2010). A universal TagModule collection for parallel genetic analysis of microorganisms. *Nucleic Acids Res.* **38**, e146.

Perozzo, R., Kuo, M., Sidhu, A. bir S., Valiyaveettil, J. T., Bittman, R., *et al*. (2002). Structural elucidation of the specificity of the antibacterial agent triclosan for malarial enoyl acyl carrier protein reductase. *J. Biol. Chem.* **277**, 13106–13114.

Proctor, M., Urbanus, M. L., Fung, E. L., Jaramillo, D. F., Davis, R. W., Nislow, C., *et al* (2011). The automated cell: compound and environment screening system (ACCESS) for chemogenomic screening. *Methods Mol. Biol.* **759**, 239–269.

Saunders, M., Magnanti, B. L., Correia Carreira, S., Yang, A., Alamo-Hernández, U., Riojas-Rodriguez, H., *et al.* (2012). Chlorpyrifos and neurodevelopmental effects: a literature review and expert elicitation on research and policy. *Environ Health*. **11 Suppl 1**, S5.

Smith, A. M., Durbic, T., Kittanakom, S., Giaever, G., Nislow, C. (2012). Barcode sequencing f or understanding drug-gene interactions. *Methods Mol. Biol.* **910**, 55–69.

Smith, A. M., Heisler, L. E., St.Onge, R. P., Farias-Hesson, E., Wallace, I. M., Bodeau, J., *et al*. (2010). Highly-multiplexed barcode sequencing: an efficient method for parallel analysis of pooled samples. *Nucleic Acids Res*. **38**, e142.

Torkko, J. M., Koivuranta, K. T., Miinalainen, I. J., Yagi, A. I., Schmitz, W., Kastaniotis, A. J., *et al*. (2001). *Candida tropicalis* Etr1p and *Saccharomyces cerevisiae* Ybr026p (Mrf1'p), 2-enoyl thioester reductases essential for mitochondrial respiratory competence. *Mol. Cell. Biol.* **21**, 6243–6253.

U.S. EPA. 1997. Reregistration Eligibility Decision: Folpet. Washington, DC: U.S. Environmental Protection Agency. [accessed 10 July 2013]. http://www.epa.gov/oppsrrd1/REDs/0630red.pdf.

U.S. EPA. 2013. EPA response to BP spill in the Gulf of Mexico. Dispersants. Questions and answers [website]. Washington, DC: US Environmental Protection Agency. [accessed 11 July 2013]. http://www.epa.gov/bpspill/dispersants-qanda.html#list.

Wise, J., Wise, J. P., Sr. (2011). A review of the toxicity of chemical dispersants. *Rev. Environ. Health*. **26**, 281–300.

Yazdankhah, S. P., Scheie, A. A., Høiby, E. A., Lunestad, B.-T., Heir, E., Fotland, T. Ø., *et al*. (2006). Triclosan and antimicrobial resistance in bacteria: an overview. *Microb. Drug Resist.* **12**, 83–90.

FIGURES

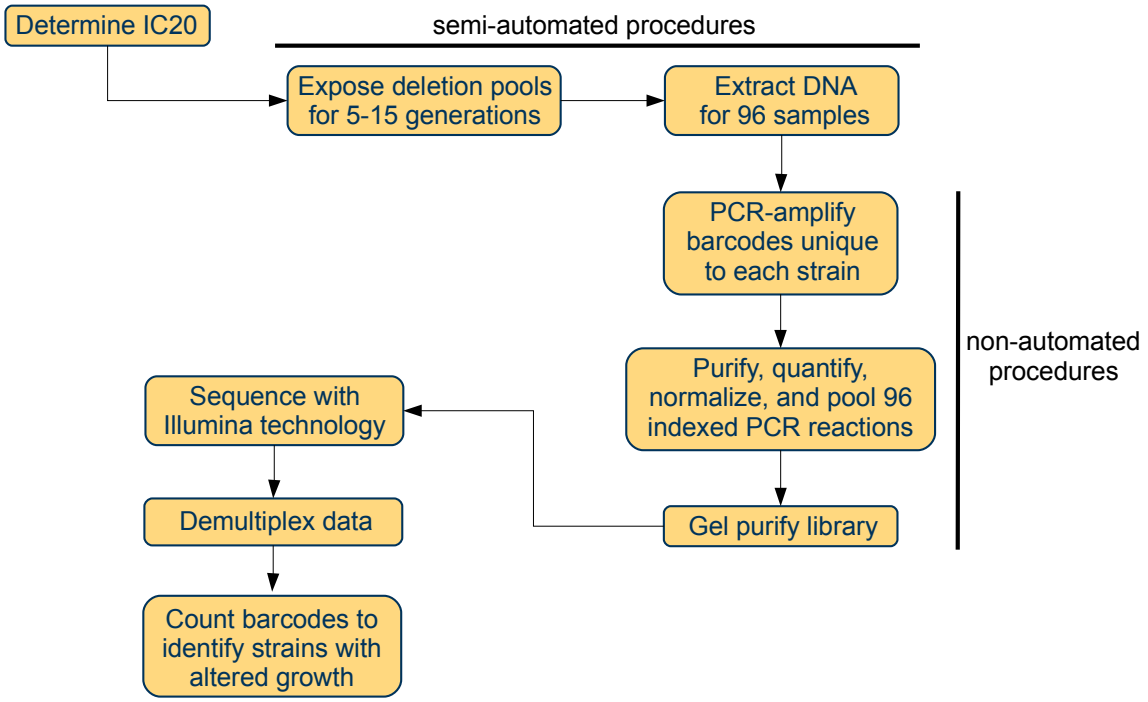

Fig. 5.1. Flow chart for semi-automated functional profiling. Outlined is the process implemented for increased throughput of yeast functional profiling studies, with semi-automated and non-automated steps shown.

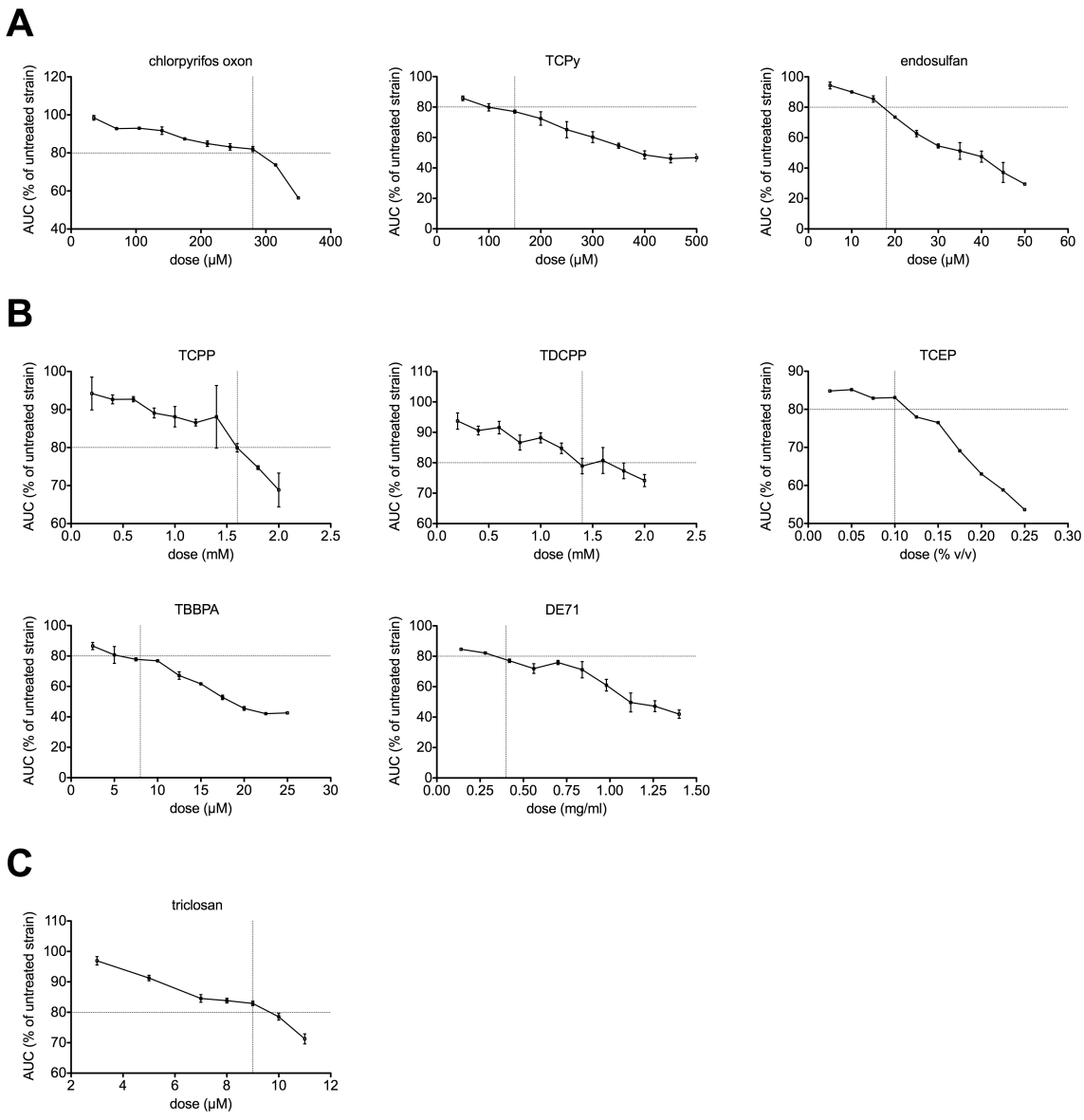

Fig. 5.2. Determining IC20s for robotic functional screening. Growth curves were conducted with wild-type yeast and various doses of chemicals. The area under the curve (AUC) at each dose was expressed as the mean and SEs of two to three independent experiments and plotted as a percentage of the untreated control. Dashed lines indicate the dose at which growth was inhibited by 20% (IC20). (A) Pesticides and metabolites. (B) Chlorinated and brominated flame retardants. (C) The triclosan antimicrobial agent. Table 5.3 lists all calculated IC20s.

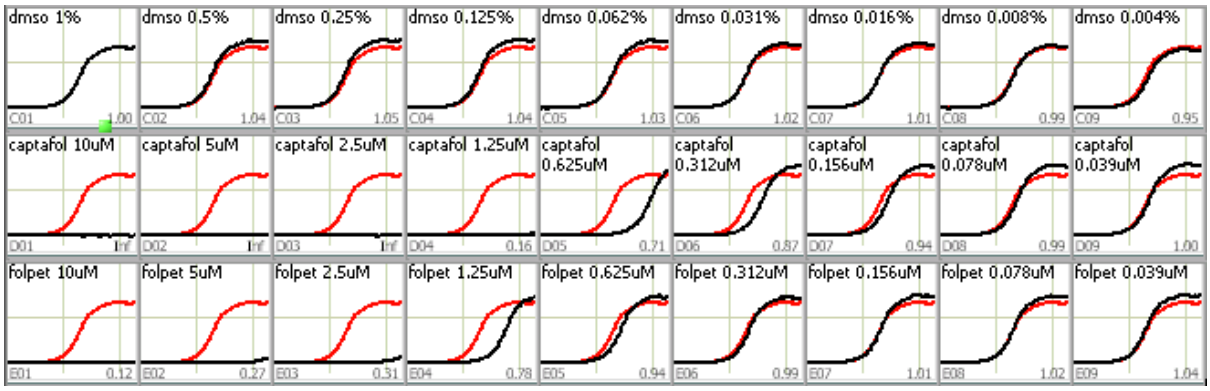

Fig. 5.3. Approximating IC20s with the YeastGrow software. Wild-type yeast was exposed to chemicals titrated across 96-well plates. DMSO controls are show in the top row, while the top left well was used as the reference for all other wells (and shown as a red curve in every well). The IC20 was approximated as a 0.8 value for the average generation time ratio (as compared to the DMSO controls), a number which is indicated in the bottom right corner of each well. The captafol IC20 was calculated as 0.46µM, while the folpet IC20 was determined as about 1.25µM. This analysis is representative of the IC20 determinations conducted by this method. Table 5.3 lists all IC20s.

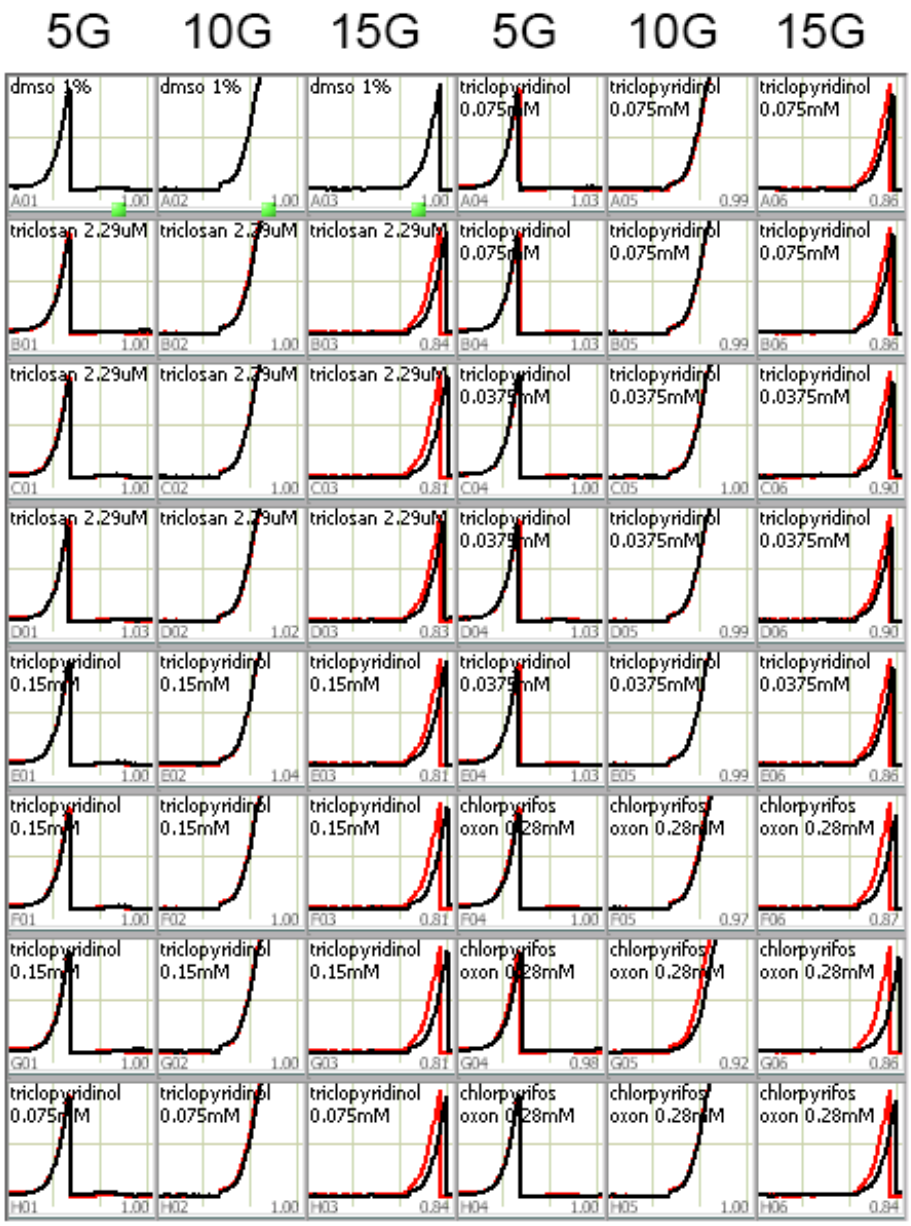

Fig. 5.4. Representative multiple generation deletion pool chemical exposures conducted with robotics. The plate is divided into two halves that show 5, 10, and 15 generation time points for yeast deletion pools exposed to various chemicals. The three top left wells are the DMSO controls used as references (and shown as red curves) for corresponding generation time points in chemically-exposed wells. Numbers in the bottom right well corners indicate the average generation time ratio to the corresponding DMSO wells. When cultures reached 5 generations, an aliquot was transferred to the 10 generation well along with appropriate chemical, and continued until 15 generations. The presence of steep drops in the 5 and 15 generation curves are due to the removal and saving of samples by the liquid handler.

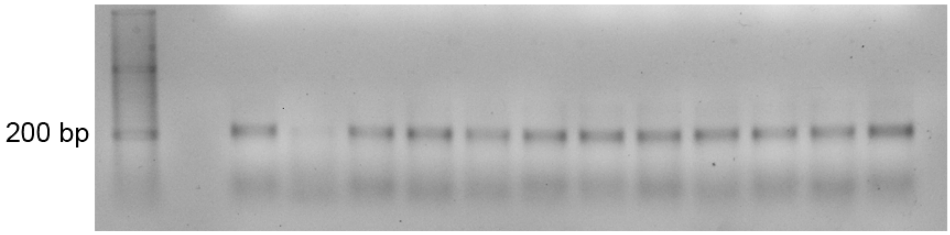

Fig. 5.5. Representative PCR amplification with indexing primers. Banding patterns display the expected approximately 200 base pair product from the down tag amplifications of DNA extraction B (see Table 5.4). At far left is ladder, followed by an empty lane, and then samples A1, B2, C3, D4, E5, F6, G7, H8, G9, F10, E11, and D12 from the 96-well PCR plate. The B2 primer pair generated little product, and this pattern was also seen using DNA from extraction A. A random sampling of primer pairs produced visible bands in a gel containing UP tag amplifications.

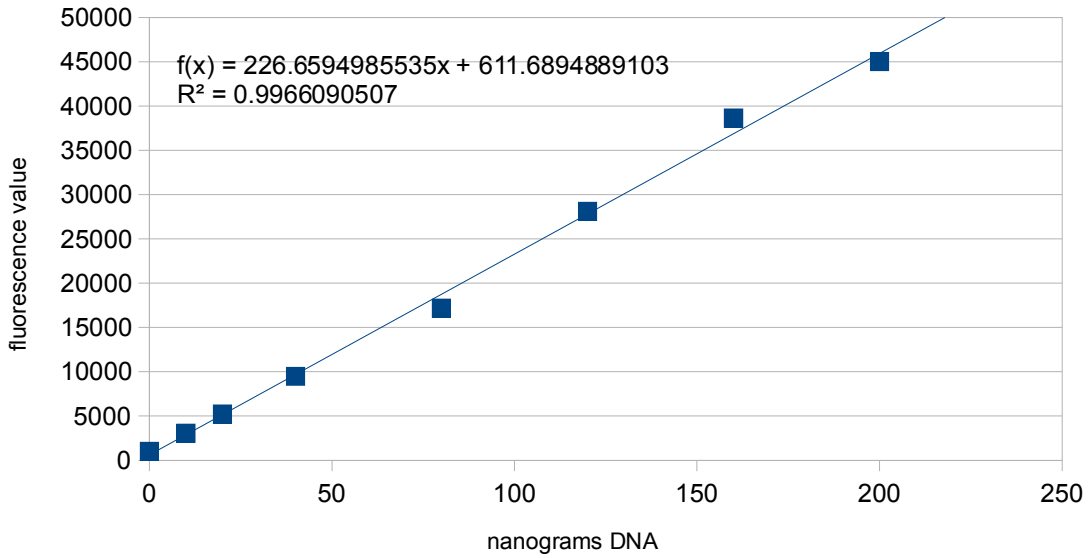

Fig. 5.6. Standard curve generated for PCR quantifications. The Quant-It fluorescence assay was utilized to quantify known amounts of DNA. The PCR product concentrations listed in Table 5.4 were calculated using the equation indicated in the figure above.

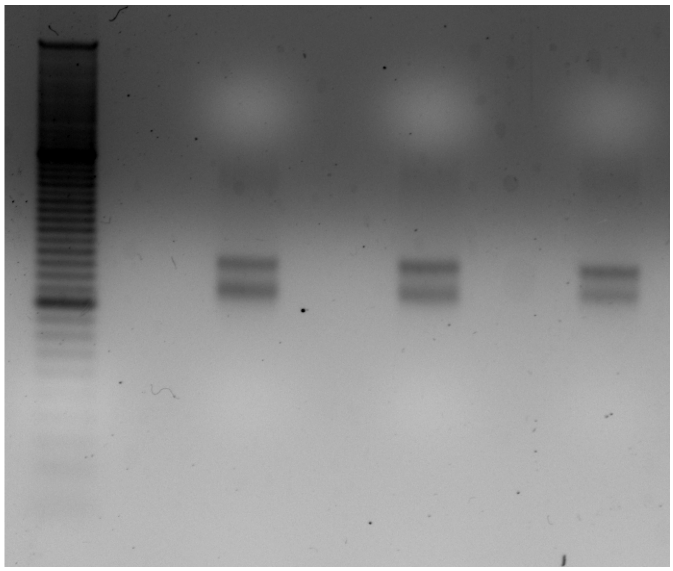

Fig. 5.7. Gel purified multiplexed libraries. The A, B, and C libraries were gel purified and confirmed in preparation for Illumina sequencing. From left to right, the first lane is a 20bp ladder, while the second, third, and fourth lanes are the purified A, B, and C libraries, respectively.

TABLES

Table 5.1. Chemicals functionally profiled in budding yeast using a semi-automated methodology.

Chemical	CAS No.	Description of use
tris(2-chloroethyl) phosphate (TCEP)	115-96-8	chlorinated flame retardant, plasticizer
tris(1-chloro-2-propyl) phosphate (TCPP)	13674-84-5	chlorinated flame retardant
tris(1,3-dichloro-2-propyl) phosphate (TDCPP)	13674-87-8	chlorinated flame retardant
3,3′,5,5′-tetrabromobisphenol A (TBBPA)	79-94-7	brominated flame retardant
BDE-47	5436-43-1	brominated flame retardant
BDE-99	60348-60-9	brominated flame retardant
DE71	117148-05-7	brominated flame retardant mixture
triclosan (TCS)	3380-34-5	chlorinated antibacterial agent
3,5,6-trichloro-2-pyridinol (TCPy)	6515-38-4	organochlorinated metabolite of chlorpyrifos
chlorpyrifos oxon (COX)	5598-15-2	organochlorinated metabolite of chlorpyrifos
endosulfan (ENDO)	115-29-7	organochlorinated pesticide
Corexit 9500	172306-86-4	oil dispersant
Corexit 9527	60617-06-3	oil dispersant
ziram	137-30-4	carbamate fungicide
2-chloro-2'-deoxyadenosine (2-CdA)	4291-63-8	anti-leukemic and immunosuppressant
4-chloro-*o*-phenylenediamine	95-83-0	chemical intermediate in dye production
tris(2,3-epoxypropyl) isocyanurate	2451-62-9	many industrial applications
bioallethrin	22431-63-6	ectoparasiticide
fludioxonil	131341-86-1	broad-spectrum fluorinated fungicide
captafol	2425-06-1	chlorinated fungicide
folpet	133-07-3	chlorinated fungicide

Table 5.2. List of primers and index tags.

Primer name	Sequence
FUP_INDEXING	**AATGATACGGCGACCACCGACACTCTTTCCCTACACGACGCTCTTCCGATCT***NNNNNNNN*GATGTCCACGAGGTCTCT
REVUP_COMMON	**CAAGCAGAAGACGGCATACGAGCTCTTCCGATCT**GCACGTCAAGACTGTCAAGG
FDN_COMMON	**CAAGCAGAAGACGGCATACGAGCTCTTCCGATCT**CAATCGTATGTGAATGCTGG
REVDN_INDEXING	**AATGATACGGCGACCACCGACACTCTTTCCCTACACGACGCTCTTCCGATCT***NNNNNNNN*CGGTGTCGGTCTCGTAG

Index			Index			Index	
INDEX01	AACACCTA		INDEX33	CCTACAAC		INDEX65	GGTCTGAC
INDEX02	AACCGTGT		INDEX34	CCTTTACA		INDEX66	GTACTTGC
INDEX03	AAGATTGC		INDEX35	CGAACTGT		INDEX67	GTAGAGCT
INDEX04	AAGCGGTC		INDEX36	CGACTGGG		INDEX68	GTCCATTA
INDEX05	AATCACAC		INDEX37	CGCATTAA		INDEX69	GTCTACAT
INDEX06	AATGCTGA		INDEX38	CGCTTCTG		INDEX70	GTGACTAC
INDEX07	ACAGTGCA		INDEX39	CGGACGTG		INDEX71	GTGGGATA
INDEX08	ACCGTTAT		INDEX40	CGGTTGAT		INDEX72	GTTGTCCC
INDEX09	ACGTAGCT		INDEX41	CGTCGGCT		INDEX73	GTTTCACT
INDEX10	ACTAACTG		INDEX42	CTAGATTC		INDEX74	TACGAATC
INDEX11	ACTCTAAG		INDEX43	CTAGTCAT		INDEX75	TACTGCGC
INDEX12	AGAACACC		INDEX44	CTCTGTCT		INDEX76	TAGCTAGT
INDEX13	AGGCAATG		INDEX45	CTTAAGAT		INDEX77	TAGTCACA
INDEX14	AGGTCAGT		INDEX46	CTTCGCGC		INDEX78	TATACCGT
INDEX15	AGTAGTGG		INDEX47	GAACGCTG		INDEX79	TATCTCCG
INDEX16	AGTTGCTA		INDEX48	GACACTCT		INDEX80	TCATTAGG
INDEX17	ATATAGGA		INDEX49	GACGTCAA		INDEX81	TCCAGCCT
INDEX18	ATCCTATT		INDEX50	GAGAACTC		INDEX82	TCCTACTA
INDEX19	ATCGCCAG		INDEX51	GAGTTAAC		INDEX83	TCGCGTAC
INDEX20	ATGAGGAA		INDEX52	GATCCAGC		INDEX84	TCGGTACC
INDEX21	ATGCATCC		INDEX53	GATGGAAT		INDEX85	TGAATTCG
INDEX22	ATTGCATC		INDEX54	GCAAGTAG		INDEX86	TGACGCAT
INDEX23	CAAGACCA		INDEX55	GCAGCCTC		INDEX87	TGAGAGTG
INDEX24	CAATCATC		INDEX56	GCGGCGAA		INDEX88	TGATCCGA
INDEX25	CACAGTTG		INDEX57	GCGTTTCG		INDEX89	TGCGGTTA
INDEX26	CACGTGTT		INDEX58	GCTCAGTT		INDEX90	TGGTCTTC
INDEX27	CAGGAGGC		INDEX59	GCTGGCGA		INDEX91	TGTAGGTC
INDEX28	CATTCCAA		INDEX60	GGACGAGA		INDEX92	TGTGCTAT
INDEX29	CCAGCACG		INDEX61	GGATATGG		INDEX93	TTAAACAG
INDEX30	CCATACAC		INDEX62	GGCAGACG		INDEX94	TTCCTCAC
INDEX31	CCGGATAG		INDEX63	GGCGAGGA		INDEX95	TTCTGATG
INDEX32	CCGTCTGA		INDEX64	GGTCCTTG		INDEX96	TTGAGTGT

The 5' tails (bold) are Illumina-specific adaptor sequences incorporated into the forward and reverse primers. The variable sequence (italics) represents the 8-mer indexing tag used in multiplexing (indexing). The 3' tails (underlined) represent the common primers required to amplify the UP and DN tag yeast barcodes. The bottom table is a list of the indexing barcodes.

Table 5.3. Inhibitory concentrations and doses utilized in functional profiling. In the robotic screens, yeast was exposed to a range of concentrations around the IC20. Some chemicals were not concentrated enough to produce an IC20, and those are indicated in the IC20 column below. See text for additional details.

Substance	IC20	Replicates and functional profiling doses
TCEP	0.1% (v/v)	3 replicates each IC20, 50% IC20, 25% IC20
TCPP	1.6mM	3 replicates each IC20, 50% IC20, 25% IC20
TDCPP	1.4mM	3 replicates each IC20, 50% IC20, 25% IC20
TBBPA	8µM	3 replicates each IC20, 50% IC20, 25% IC20
DE71	0.4mg/ml	3 replicates each IC20, 50% IC20, 25% IC20
triclosan	9µM	3 replicates each IC20, 50% IC20, 25% IC20
TCPy	150µM	3 replicates each IC20, 50% IC20, 25% IC20
chlorpyrifos oxon	280µM	3 replicates each IC20, 50% IC20, 25% IC20
endosulfan	18µM	3 replicates each IC20, 50% IC20, 25% IC20
Corexit 9500	1.5% (v/v)	3 replicates each IC20, 50% IC20
Corexit 9527	1% (v/v)	3 replicates each IC20, 50% IC20
ziram	1.5µM	2 replicates IC20
2-chloro-2'-deoxyadenosine	1mM is IC10	2 replicates IC10
4-chloro-*o*-phenylenediamine	1mM	2 replicates IC20
tris(2,3-epoxypropyl) isocyanurate	1mM is IC15	2 replicates IC15
bioallethrin	0.5mM is IC15	2 replicates IC15
fludioxonil	1mM is IC15	2 replicates IC15
captafol	0.46µM	2 replicates IC20
folpet	1.25µM	2 replicates IC20

Table 5.4. Automated DNA extraction and quantifications. DNA was extracted using the Corbett X-tractor Gene robot and quantified with the Tecan NanoQuant plate.

DNA extraction A

	1	2	3	4	5	6	7	8	9	10	11	12
A	DMSO 5.5	DMSO 5.6	DMSO 5.7	DMSO 5.8	DMSO 5.9	DMSO 5.10	DMSO 5.11	DMSO 5.12	DMSO 5.13	DMSO 5.14	DMSO 5.11/5/2013A	DMSO 5.11/5/2013B
B	DMSO 15.5	DMSO 15.6	DMSO 15.7	DMSO 15.8	DMSO 15.9	DMSO 15.10	DMSO 15.11	DMSO 15.12	DMSO 15.13	DMSO 15.14	DMSO 15.11/5/2013B	DMSO 15.11/5/2013B
C	TBBPA 5.100.1	TBBPA 5.100.2	TBBPA 5.100.3	TBBPA 5.50.1	TBBPA 5.50.2	TBBPA 5.50.3	TBBPA 5.25.1	TBBPA 5.25.2	TBBPA 5.25.3	TCPP 5.100.1	TCPP 5.100.2	TCPP 5.100.3
D	TBBPA 15.100.1	TBBPA 15.100.2	TBBPA 15.100.3	TBBPA 15.50.1	TBBPA 15.50.2	TBBPA 15.50.3	TBBPA 15.25.1	TBBPA 15.25.2	TBBPA 15.25.3	TCPP 5.50.1	TCPP 5.50.2	TCPP 5.50.3
E	TCS 5.100.1	TCS 5.100.2	TCS 5.100.3	TCS 5.50.1	TCS 5.50.2	TCS 5.50.3	TCS 5.25.1	TCS 5.25.2	TCS 5.25.3	TCPP 5.25.1	TCPP 5.25.2	TCPP 5.25.3
F	TCS 15.100.1	TCS 15.100.2	TCS 15.100.3	TCS 15.50.1	TCS 15.50.2	TCS 15.50.3	TCS 15.25.1	TCS 15.25.2	TCS 15.25.3	TCPP 15.100.1	TCPP 15.100.2	TCPP 15.100.3
G	TCEP 5.100.1	TCEP 5.100.2	TCEP 5.100.3	TCEP 5.50.1	TCEP 5.50.2	TCEP 5.50.3	TCEP 5.25.1	TCEP 5.25.2	TCEP 5.25.3	TCPP 15.50.1	TCPP 15.50.2	TCPP 15.50.3
H	TCEP 15.100.1	TCEP 15.100.2	TCEP 15.100.3	TCEP 15.50.1	TCEP 15.50.2	TCEP 15.50.3	TCEP 15.25.1	TCEP 15.25.2	TCEP 15.25.3	TCPP 15.25.1	TCPP 15.25.2	TCPP 15.25.3

	1		2		3		4		5		6		7		8		9		10		11		12	
	ng/ul	ratio	ng/ul	ratio	ng/ul	ratio	ng/ul	ratio	ng/ul	ratio	ng/ul	ratio	ng/ul	ratio	ng/ul	ratio	ng/ul	ratio	ng/ul	ratio	ng/ul	ratio	ng/ul	ratio
A	26.4	2.24	63	1.99	60.7	2.26	48.7	1.97	69.1	2.24	66.7	2.04	80.2	2.19	47.8	2.21	48.7	2.14	32	1.9	98.4	2.21	63.8	2.03
B	170.9	2.15	127	2.16	109.3	2.1	198.5	2.14	122.7	2.1	70.3	2.03	111.7	2.12	110.7	2.13	143.6	2.15	88.3	2.06	105	2.09	125.4	2.11
C	114.1	2.17	101	2.14	125.7	2.17	52.2	0.73	118.7	2.15	107.5	2.11	110.9	2.14	97.1	2.1	77.4	2.02	92.6	2.11	105	2.11	77.9	2.09
D	133.4	2.13	123	2.17	98.1	2.14	118.3	2.15	123.7	2.12	103.6	2.13	144.6	2.1	124.3	2.12	98.6	2.12	119.5	2.08	91.6	2.09	77.2	2.06
E	89	2.08	124	2.15	112.2	2.15	101.9	2.12	154.8	2.16	80.9	2.11	98	2.14	57.7	2.09	71.4	2.1	72	2.05	93.7	2.08	87.7	2.08
F	81.2	2.13	90.8	2.17	107.5	2.13	114	2.16	108.5	2.14	91.6	2.06	96.9	2.07	101.4	2.14	137.9	2.13	109.1	2.12	97.3	2.11	116.2	2.14
G	109	2.15	87.4	2.1	114.4	2.17	126.3	2.12	122.4	2.13	89.7	2.06	88.6	2.11	105.4	2.11	99.5	2.03	77.3	2.07	103	2.11	105.1	2.08
H	135	2.13	144	2.17	137.9	2.13	112.8	2.16	137.3	2.14	112.9	2.13	111.7	2.13	103.1	2.12	102.6	2.12	104.5	2.12	99.9	2.11	84	2.12

DNA extraction B

	1	2	3	4	5	6	7	8	9	10	11	12
A	Ziram 5.2	Ziram 5.3	2-chloro-2-deoxyadenosine 5.1	2-chloro-2-deoxyadenosine 5.2	4-chloro-o-phenylenediamine 5.1	4-chloro-o-phenylenediamine 5.2	tris(2,3-epoxypropyl)isocyanurate 5.1	tris(2,3-epoxypropyl)isocyanurate 5.2	bioallethrin 5.1	bioallethrin 5.2	fludioxonil 5.2	fludioxonil 5.3
B	Ziram 15.2	Ziram 15.3	2-chloro-2-deoxyadenosine 15.1	2-chloro-2-deoxyadenosine 15.2	4-chloro-o-phenylenediamine 15.1	4-chloro-o-phenylenediamine 15.2	tris(2,3-epoxypropyl)isocyanurate 15.1	tris(2,3-epoxypropyl)isocyanurate 15.2	bioallethrin 15.1	bioallethrin 15.2	fludioxonil 15.2	fludioxonil 15.3
C	captafol 5.3	captafol 5.4	folpet 5.1	folpet 5.2	water 5.1	water 5.2	water 5.3	water 5.4	water 5.5	water 5.6	water 5.7	water 5.8
D	captafol 15.3	captafol 15.4	folpet 15.1	folpet 15.2	water 15.1	water 15.2	water 15.3	water 15.4	water 15.5	water 15.6	water 15.7	water 15.8
E	TDCPP 5.100.1	TDCPP 5.100.2	TDCPP 5.100.3	TDCPP 5.50.1	TDCPP 5.50.2	TDCPP 5.50.3	TDCPP 5.25.1	TDCPP 5.25.2	TDCPP 5.25.3	water 5.9	water 5.10	water 5.11
F	TDCPP 15.100.1	TDCPP 15.100.2	TDCPP 15.100.3	TDCPP 15.50.1	TDCPP 15.50.2	TDCPP 15.50.3	TDCPP 15.25.1	TDCPP 15.25.2	TDCPP 15.25.3	water 15.9	water 15.10	water 15.11
G	corexit9500 5.100.1	corexit9500 5.100.2	corexit9500 5.100.3	corexit9500 5.50.1	corexit9500 5.50.2	corexit9500 5.50.3	corexit9527 5.100.1	corexit9527 5.100.2	corexit9527 5.100.3	corexit9527 5.50.1	corexit9527 5.50.2	corexit9527 5.50.3
H	corexit9500 15.100.1	corexit9500 15.100.2	corexit9500 15.100.3	corexit9500 15.50.1	corexit9500 15.50.2	corexit9500 15.50.3	corexit9527 15.100.1	corexit9527 15.100.2	corexit9527 15.100.3	corexit9527 15.50.1	corexit9527 15.50.2	corexit9527 15.50.3

	1		2		3		4		5		6		7		8		9		10		11		12	
	ng/ul	ratio	ng/ul	ratio	ng/ul	ratio	ng/ul	ratio	ng/ul	ratio	ng/ul	ratio	ng/ul	ratio	ng/ul	ratio	ng/ul	ratio	ng/ul	ratio	ng/ul	ratio	ng/ul	ratio
A	85.6	2.16	65.7	2.07	115.5	2.12	92.9	2.06	51.6	2.11	89.5	2.08	69.8	2.07	72.5	2	72.2	2.12	76	2.08	38.5	2.08	71.4	2.03
B	135.8	2.18	103.2	2.14	139.2	2.08	125.7	2.15	135.3	2.13	98.3	2.11	118	2.11	90	2.07	103.4	2.1	104.2	2.13	102.1	2.16	121.6	2.13
C	62.8	2.15	154.4	2.19	129.9	1.79	111.7	2.13	93.9	2.13	93	2.1	70.3	2.18	88	2.12	92.5	2.15	41.5	1.95	67.8	2.17	70.3	2.12
D	98.1	2.11	137.8	2.15	51.2	1.8	20.7	1.56	62	2.14	87	2.14	48.8	2.1	101	2.15	53	2.06	54.9	2.1	70.4	2.1	47.9	2.12
E	93	2.16	125.8	2.17	157.5	2.1	78.5	2.02	99.6	2.05	91.1	2.09	63.6	2.11	126.5	2.1	66.5	2.07	65.2	2.07	64	2.13	56.2	2.07
F	152.3	2.16	132.7	2.18	191.5	2.13	133.7	2.14	104.2	2.16	114.2	2.16	75.7	2.07	136.7	2.16	96.1	2.11	87.2	2.16	74.9	2.12	67.3	2.13
G	46.2	2.11	50.1	2.09	49.6	2.13	133.6	2.17	61.6	2.07	39.2	2.06	7.6	1.73	7.5	1.5	7.7	1.64	7.9	1.61	5.8	1.61	9.2	1.77
H	42.6	2.08	22.7	2.01	75.2	2.06	19.8	1.92	45.7	2.08	40.6	2.07	7.7	1.57	9.5	1.64	7.5	1.63	48.4	2.03	61.4	2.07	47.3	2.11

DNA extraction C

	1	2	3	4	5	6
A	BDE47 5.100.1	BDE47 5.100.2	BDE47 5.100.3	BDE99 5.100.1	BDE99 5.100.2	BDE99 5.100.3
B	BDE47 15.100.1	BDE47 15.100.2	BDE47 15.100.3	BDE99 15.100.1	BDE99 15.100.2	BDE99 15.100.3
C	COX 5.100.1	COX 5.100.2	COX 5.100.3	COX 5.50.1	COX 5.50.2	COX 5.50.3
D	COX 15.100.1	COX 15.100.2	COX 15.100.3	COX 15.50.1	COX 15.50.2	COX 15.50.3
E	TCPy 5.100.1	TCPy 5.100.2	TCPy 5.100.3	TCPy 5.50.1	TCPy 5.50.2	TCPy 5.50.3
F	TCPy 15.100.1	TCPy 15.100.2	TCPy 15.100.3	TCPy 15.50.1	TCPy 15.50.2	TCPy 15.50.3
G	ENDO 5.100.1	ENDO 5.100.2	ENDO 5.100.3	ENDO 5.50.1	ENDO 5.50.2	ENDO 5.50.3
H	ENDO 15.100.1	ENDO 15.100.2	ENDO 15.100.3	ENDO 15.50.1	ENDO 15.50.2	ENDO 15.50.3

	1		2		3		4		5		6	
	ng/ul	ratio	ng/ul	ratio	ng/ul	ratio	ng/ul	ratio	ng/ul	ratio	ng/ul	ratio
A	150	1.79	119.8	2.12	91.4	2.14	102.2	2.12	50.3	2.06	91.1	2.08
B	151.1	2.15	108.7	2.16	138.9	2.14	116.7	2.15	125.3	2.12	113.9	2.1
C	56.1	2.14	110.9	2.13	48.5	2.13	88.4	2.1	63	2.11	42.3	2.06
D	77.9	2.14	79.9	2.15	77.4	2.14	87.1	2.13	79.5	2.09	82	2.09
E	36.8	2.03	38	2.12	29.6	2.08	25.8	2.1	40.6	2.04	42.3	2.04
F	70.7	2.18	67.3	2.16	80.9	2.14	48.8	2.1	60.2	2.1	54.3	2.11
G	87	2.14	62.4	2.12	39.1	2.11	45.5	2.09	40.2	2.1	69.3	2.06
H	67.7	2.12	67	2.09	57.2	2.1	72.1	2.1	59	2.07	36.9	2.02

Table 5.5. PCRs quantified with the Quant-It assay. All values are shown in ng/µl and were calculated using the standard curve presented in Fig. 5.5.

PCRs from DNA extraction A

UP TAGS

	1	2	3	4	5	6	7	8	9	10	11	12
A	11.58	20.63	19.34	24.45	24.05	20.77	22.91	23.43	22.76	22.26	16.91	16.86
B	14.48	16.19	18.31	23.24	15.88	17.42	19.96	18.21	20.89	17.23	10.46	14.00
C	10.50	13.79	9.21	15.92	14.07	12.40	9.90	9.13	16.17	10.12	8.38	11.14
D	11.28	11.18	10.89	15.12	20.84	16.91	18.88	18.10	17.23	9.91	10.33	9.08
E	10.01	9.61	9.70	13.99	19.57	22.37	16.91	11.75	15.22	11.63	8.87	9.01
F	12.32	16.15	11.26	18.52	22.61	21.75	21.72	21.82	19.06	11.11	11.01	9.48
G	14.02	10.93	13.18	20.21	19.55	20.73	24.39	22.71	14.04	13.22	11.87	10.27
H	16.93	14.95	21.65	43.56	37.97	25.04	23.11	28.63	30.42	31.41	11.29	8.93

DN TAGS

	1	2	3	4	5	6	7	8	9	10	11	12
A	20.20	19.70	18.83	22.65	26.05	25.13	23.22	24.32	8.98	12.81	21.79	27.39
B	28.47	5.39	23.66	11.46	13.80	9.27	8.30	3.04	9.12	6.56	7.51	2.45
C	20.90	17.45	7.42	13.99	11.49	7.63	11.60	18.79	22.06	15.32	21.66	6.42
D	24.85	25.39	27.21	21.69	21.54	24.59	26.87	17.08	18.63	15.95	23.87	19.40
E	16.17	11.73	8.10	13.55	7.69	11.14	8.48	4.56	8.42	12.50	14.73	17.91
F	20.04	25.69	23.76	25.09	20.33	21.59	27.82	22.50	24.62	21.76	26.31	26.55
G	22.16	22.74	26.27	20.28	21.99	28.40	20.18	21.28	17.00	18.16	18.44	20.52
H	31.89	27.44	37.16	37.92	42.09	32.80	24.32	19.71	23.50	29.31	31.48	23.11

PCRs from DNA extraction B

UP TAGS

	1	2	3	4	5	6	7	8	9	10	11	12
A	20.52	18.71	17.79	19.15	17.99	16.69	20.73	15.19	14.88	11.29	9.61	7.34
B	19.26	13.24	9.12	16.06	12.13	15.25	14.75	15.19	10.80	11.68	6.16	5.58
C	14.72	11.98	2.31	23.48	18.32	21.33	19.33	17.08	21.02	7.60	8.74	10.12
D	12.87	11.00	8.53	18.31	21.39	19.76	21.36	21.31	11.74	12.28	11.93	7.66
E	11.48	8.50	13.06	21.19	14.41	21.49	19.06	9.34	17.85	8.88	9.20	6.20
F	11.63	11.56	8.65	18.71	20.71	13.87	24.91	22.37	10.83	8.77	9.27	11.90
G	12.75	12.20	9.85	17.28	18.58	17.75	25.59	18.11	12.55	10.86	9.04	8.68
H	12.45	13.40	13.78	21.89	24.22	22.93	19.83	18.28	21.53	15.11	18.92	12.72

DN TAGS

	1	2	3	4	5	6	7	8	9	10	11	12
A	16.03	25.76	22.67	25.36	27.92	27.63	20.93	28.05	20.02	34.57	22.20	18.07
B	24.05	4.53	27.78	23.36	21.88	21.59	21.64	24.20	20.43	16.23	25.13	1.96
C	20.65	19.74	19.69	31.40	26.29	24.42	23.14	19.15	19.94	20.83	21.46	21.60
D	30.49	23.10	20.07	10.40	34.31	30.41	25.43	23.80	21.69	25.22	27.53	23.68
E	24.85	20.24	30.01	23.83	28.19	26.47	22.39	14.94	20.68	26.55	25.13	24.42
F	26.82	28.07	23.05	28.69	24.69	24.28	29.10	22.92	25.67	15.95	27.47	26.64
G	6.29	7.97	12.18	10.24	18.83	14.16	10.23	15.65	13.68	15.28	22.38	31.03
H	35.63	30.94	32.47	25.09	25.49	21.14	24.40	20.79	19.36	25.47	30.28	25.22

PCRs from DNA extraction C

UP TAGS

	1	2	3	4	5	6
A	3.21	3.58	13.44	7.14	7.84	7.95
B	2.85	3.52	18.00	20.07	19.90	16.77
C	3.50	4.57	15.09	19.07	18.27	15.14
D	3.06	4.78	16.29	16.40	17.90	13.49
E	3.64	6.89	12.59	18.32	15.65	12.13
F	3.55	5.60	8.74	8.00	6.02	8.86
G	6.58	6.30	7.19	5.70	3.67	3.74
H	9.09	20.94	8.26	18.88	7.03	7.07

DN TAGS

	1	2	3	4	5	6
A	3.09	3.96	18.35	22.89	21.84	22.27
B	3.35	3.43	18.99	17.00	22.43	18.02
C	2.65	3.76	5.61	7.79	9.13	8.34
D	2.82	3.10	4.55	3.56	4.48	6.88
E	3.16	4.97	9.76	11.04	9.60	7.68
F	4.91	14.28	17.19	14.29	14.60	3.40
G	9.95	14.88	13.77	18.25	16.55	14.67
H	19.45	16.29	16.46	22.82	14.42	9.25

CONCLUSIONS

The series of studies presented in this work underscore the value of yeast functional genomics in the field of toxicology. By identifying yeast mutants with altered growth in various toxicants, mechanisms of toxicity have been established or hypothesized for compounds with limited prior cellular and molecular toxicity data. Using these results, further experimentation can expound upon the yeast processes affected by the described toxicants. Considering the favorable conservation between yeast and more complex organisms, candidate toxicant susceptibility genes and/or pathways can be further examined in biological systems such as nematodes or human cell lines. Classified as a method of functional toxicology, a concept described in Chapter 1, this powerful unbiased approach in yeast has a promising future in toxicity testing.

In Chapter 2, functional profiling determined that the organochlorinated pesticide dieldrin altered leucine availability in yeast, and is the first known genome-wide study in any organism identifying the genetic requirements for dieldrin tolerance. First, it was found that mutants defective in amino acid signaling or transport exhibited growth defects in dieldrin, a phenotype that was reversed by the addition of exogenous leucine. Second, by varying leucine concentrations in the media, the dieldrin sensitivity of wild-type or mutant strains was altered. Third, increasing intracellular leucine by overexpressing proteins conferred resistance to dieldrin. Fourth, dieldrin inhibited leucine cellular uptake and thus induced the amino acid starvation response. Finally, it was demonstrated that negative regulation of the Ras/protein kinase A (PKA) signaling pathway was required for dieldrin tolerance, along with components of the pyruvate dehydrogenase complex. It was concluded that by decreasing leucine uptake, dieldrin starves the cell and affects mutants in the amino acid starvation-linked Ras/PKA pathway and pyruvate dehydrogenase complex.

Chapter 3 described yeast functional profiling of toxaphene, an environmentally persistent insecticide composed of many related chlorinated congeners. It was demonstrated that yeast mutants defective in processes associated with transcription elongation and nutrient utilization were sensitive to toxaphene. Growth defects in toxaphene were exacerbated with co-exposure to the known transcription elongation inhibitor mycophenolic acid (MPA). However, it was found that toxaphene did not exhibit the same mechanism as MPA – it did not deplete nucleotides and had no detectable effect on transcription elongation. It was speculated that toxaphene likely perturbs a process closely linked to transcription elongation, such as mRNA processing, mRNA nuclear export, or transcription-coupled nucleotide excision repair. Further studies could elucidate the precise mechanism, and akin to the study with dieldrin (Chapter 2), this is the only known genome-wide inquiry into the genetic requirements for toxaphene tolerance in any organism.

Chapter 4 discussed a screen devised to identify yeast cellular processes and pathways affected by DMSO, a solvent frequently utilized in toxicological and pharmaceutical investigations. It is essential to understand the cellular and molecular targets of DMSO in order to differentiate its intrinsic effects from those elicited by a compound of interest, as many yeast chemical profiling studies (including those described in Chapters 2 and 3) utilize DMSO. Golgi/ER transport

mutants were sensitive to DMSO, including those deleted for components of the conserved oligomeric Golgi (COG) complex. Moreover, strains lacking components of the SWR1 histone exchange complex experienced growth defects in DMSO, with additional chromatin remodeling mutants displaying a range of sensitivities. DNA repair mutants also faced growth difficulties in DMSO. Additionally, it was established that overexpression of histone H2A.Z, which replaces histone H2A in a SWR1-catalyzed reaction, conferred resistance to DMSO. The data provided within this section are useful for (1) future investigations into the cellular and molecular mechanisms of DMSO toxicity and (2) those in the yeast community conducting screens which utilize DMSO as a solvent.

Chapter 5 details a transition to a more high-throughput yeast chemical screening system, involving semi-automation of various stages of the functional screening process. Additionally discussed are the preparations for multiplexed deep sequencing to assess relative strain abundances in a pool after toxicant exposure. Establishment of this high-throughput framework will allow for increased functional profiling of toxicants and provide methodologies valuable to toxicity testing. Screens can be conducted more quickly for a fraction of the prior cost.

This work outlines how functional toxicological methods in yeast can be utilized to understand the cellular and molecular mechanisms of chemical toxicity. Specifically, these approaches helped determine that (1) the organochlorinated pesticide dieldrin alters leucine availability; (2) the toxaphene organochlorinated pesticide mixture likely affects a process linked to transcription elongation; and (3) the common solvent DMSO likely perturbs Golgi/ER transport and/or chromatin modification. Although further studies in yeast or more complex organisms are needed to elucidate the specific molecular phenomena behind the toxicity of these compounds, this work provides significant findings relevant to the fields of toxicology and yeast biology.

APPENDIX 1: Mutants with altered growth in dieldrin. - sensitive, + resistant

log2 values			
25% IC20 115µM	50% IC20 230µM	IC20 460µM	Deleted Gene
-3.9	-4.95	-6.8	*IRA2*
-4	-4.4	-6.1	*GYP1*
-5.6		-5.65	*BAP2*
-3.75	-4.85	-5.6	*PDC1*
-3.1	-3.95	-5.25	*YJL120W*
-4.9	-4.5	-5.05	*PDR5*
-4.7	-5.2	-5	*YCR007C*
-3.1	-3.1	-4.9	*IRS4*
-1.3	-1.6	-4.9	*SOK2*
-1.65	-1.45	-4.85	*TCB3*
-3.8	-5.3	-4.8	*SLT2*
-4.9	-4.9	-4.8	*YML079W*
-4.15	-4.45	-4.7	*TIM18*
-2	-2.4	-4.7	*OPI3*
-3.2	-3.4	-4.6	*SIS2*
-2.55	-2.35	-4.6	*SCJ1*
-4.2	-3.5	-4.5	*SIW14*
-2.1	-2.55	-4.45	*CNB1*
-2.3	-2.75	-4.35	*OSH3*
-1.9	-2.85	-4.25	*UFD2*
-3.05	-4.9	-4.1	*IMP2'*
-3.05	-2.75	-4.1	*BRE5*
-4	-4.3	-4	*SAP4*
-2.9	-3.6	-4	*ECM30*
-2.6	-2.4	-4	*BST1*
-1.9		-4	*TRM10*
-3	-3.3	-3.9	*DMA1*
-1.5	-1.4	-3.9	*YLR169W*
-4.1	-4.6	-3.85	*URE2*
-3.2	-3.8	-3.8	*EMC2*
-2.45	-2.6	-3.8	*YDL172C*
-1.7	-2	-3.8	*COG7*
-3.7		-3.8	*OST5*
-3.7	-3.2	-3.7	*ATP17*
-2.4	-2.05	-3.7	*SNX4*
-3.5	-3.6	-3.6	*CKA1*
-2	-2.8	-3.6	*GCV3*
-2.55	-2.15	-3.55	*URA2*
-3.2	-2.9	-3.5	*TCB1*
	-2.7	-3.5	*GFD2*
-2.7	-3.05	-3.45	*PDB1*
-3.25	-3.35	-3.35	*NPR1*
-3.3	-3.3	-3.3	*YOR352W*
-1.4		-3.3	*CUE1*
-1.8		-3.25	*PCL6*
	-3.25	-3.2	*BOP2*
-2.45		-3.2	*UBP13*
-2.3	-2.1	-3.15	*COG8*
-2.9	-3.6	-3.1	*YCR006C*
-2.7	-2.6	-3.1	*COG6*
	-2.2	-3.1	*GPB2*
-1.3	-2	-3.1	*YMR158W-B*
-3	-3.3	-3	*KAR4*
-3.1	-3.1	-3	*INM1*
-2.1	-2.9	-3	*RMD5*
-2.6	-2.6	-3	*RPL23A*
-2.2	-2.2	-3	*LPD1*
	-1.9	-3	*PTM1*
-1.9	-1.5	-3	*YFL013W-A*
-2		-3	*NAB6*
-3.3	-3.9	-2.9	*MAL31*
-3.3	-3.6	-2.9	*GDT1*
-3	-3.4	-2.9	*YOR021C*
-3	-3	-2.8	*MCR1*
-2.8	-2.8	-2.8	*YJR079W*
-2.5	-2.6	-2.8	*PAR32*
-2.2	-2.2	-2.8	*VPS55*
-2.05		-2.75	*TKL1*
-3.1	-3	-2.7	*SAP1*
-2.5	-2.8	-2.7	*YOR292C*
-2.6	-2.5	-2.7	*AST2*
-2.3	-2.5	-2.7	*UBC8*
-1.5	-2.2	-2.7	*PDX1*
	-1.9	-2.7	*PTK2*
	-1.3	-2.7	*RUD3*
-1.8		-2.7	*DPH2*

log2 values			
25% IC20 115µM	50% IC20 230µM	IC20 460µM	Deleted Gene
-3.45	-3.5	-2.65	*MOT3*
-1.2	-1.3	-2.6	*MRS1*
-2.3		-2.6	*BRE2*
-1.4	-2.2	-2.55	*YJL193W*
-2.8	-2.8	-2.5	*PNS1*
-2.4	-2.8	-2.5	*RPH1*
-2.6	-2.7	-2.5	*APT2*
-2.1	-2.5	-2.5	*PET309*
	-1.9	-2.5	*EMC1*
-2.6		-2.5	*YBL081W*
-2.6		-2.5	*YGR064W*
-2.5		-2.5	*JHD1*
-1.4		-2.5	*IES1*
-2.7	-2.8	-2.4	*RCK2*
-2.2	-2.8	-2.4	*ASG1*
-2.5	-2.3	-2.4	*HXT1*
	-1.9	-2.4	*YEN1*
-1.4	-1.6	-2.4	*VHS2*
	-1.6	-2.4	*PBS2*
-2.5		-2.4	*YMR295C*
-1.4		-2.4	*IRE1*
-1.3		-2.4	*YKR073C*
	-2	-2.35	*YCL046W*
-2.7	-3	-2.3	*TMS1*
-2.3	-3	-2.3	*HEH2*
-2	-2.6	-2.3	*MKK1*
-2.7	-2.5	-2.3	*YOL087C*
-2.8	-2.3	-2.3	*OCA2*
-2.4	-2.3	-2.3	*YNL187W*
-2.8	-2.2	-2.3	*NYV1*
-2.3	-2.2	-2.3	*MDM36*
-2.1	-2.2	-2.3	*YPL030W*
-1.3	-2.1	-2.3	*BCK2*
-1.3	-1.8	-2.3	*SSK1*
-2.5		-2.3	*QCR8*
-2.3	-2.7	-2.2	*REV7*
-2.2	-2.6	-2.2	*YCL056C*
-2.4	-2.5	-2.2	*BUD9*
-2.4	-2.5	-2.2	*MET8*
-2.3	-2.4	-2.2	*RAX1*
	-2.3	-2.2	*PDR16*
	-1.4	-2.2	*ATG13*
-1.6	-1.8	-2.15	*YAK1*
-2.1	-2.7	-2.1	*ARR3*
-1.9	-2.6	-2.1	*SOL2*
-2.9	-2.4	-2.1	*REC104*
-2.55	-2.4	-2.1	*OCA1*
-2.2	-2.2	-2.1	*YER066C-A*
-2	-2	-2.1	*BGL2*
	-2	-2.1	*YBL012C*
-2.1		-2.1	*GLO2*
-1.4		-2.1	*QCR7*
-1.4		-2.1	*PTR2*
-1.1		-2.1	*URA5*
	-1.9	-2.05	*FBP26*
	-1.3	-2.05	*BSD2*
-2.4	-2.4	-2	*YLR297W*
-2.3	-2.4	-2	*YPS3*
-1.7	-2.1	-2	*NFU1*
-4.1	-1.8	-2	*ABZ2*
-1.7	-1.7	-2	*RPI1*
	-1.45	-2	*SAT4*
	-1.4	-2	*STB3*
-2.3		-2	*EMP70*
-1.9		-2	*YJL131C*
-1.6		-2	*YKL098W*
-1.4		-1.95	*YIM1*
-2.6	-2.7	-1.9	*HMG2*
-2.6	-2.2	-1.9	*YDR520C*
-2	-2.1	-1.9	*OCA4*
-1.9	-2	-1.9	*AHP1*
	-1.5	-1.9	*SSK2*
-1.9		-1.9	*SNO2*
-1.3		-1.85	*YDR230W*
-2.6	-3.7	-1.8	*STP2*
	-2.45	-1.8	*RBK1*

log2 values			
25% IC20 115µM	50% IC20 230µM	IC20 460µM	Deleted Gene
	-2.4	-1.8	*VID30*
-2.2	-1.9	-1.8	*YGR117C*
-2.1	-1.8	-1.8	*FRM2*
-2.05	-1.7	-1.8	*ATP2*
-1.9	-1.7	-1.8	*DTD1*
-1.6	-1.5	-1.8	*NMA2*
-1.3	-1.3	-1.8	*YKL091C*
-1.4		-1.8	*COX15*
	-2.1	-1.7	*RUP1*
-1.4	-2	-1.7	*ECM32*
-4.6	-1.5	-1.7	*GAT1*
-1.8	-1.5	-1.7	*PBP1*
-2		-1.7	*PPN1*
	-1.8	-1.6	*PFK26*
-1.7	-1.7	-1.6	*TIR4*
-1.4	-1.55	-1.6	*YND1*
-1.4	-1.4	-1.6	*NUP100*
-1.3		-1.6	*FIG2*
-1.1		-1.6	*SHM2*
-1.5	-1.5	-1.5	*YIL055C*
-1.4	-1.4	-1.5	*RTN2*
-1.2	-1.4	-1.5	*CBR1*
	-1.2	-1.5	*GPB1*
-1.3		-1.5	*XBP1*
-1.1		-1.5	*JEM1*
-1.2	-1.5	-1.4	*YKL063C*
-1.2	-1.4	-1.4	*GAT4*
-1.3	-1.3	-1.4	*YDR029W*
-1.4		-1.4	*YKL071W*
-1.4		-1.4	*YIL089W*
-1.4		-1.4	*YRM1*
-1.2		-1.4	*TRX2*
-1.1		-1.4	*YKL097C*
-1.5	-1.4	-1.3	*HBT1*
	-1.4	-1.3	*TPO2*
	-1.3	-1.3	*YOL046C*
-1.5		-1.3	*YBR225W*
-1.3		-1.3	*LCB4*
-1.3		-1.3	*CAF4*
1.6		-1.3	*TAN1*
	-1.6	-1.2	*POR2*
-5.1	-5.4		*ARO2*
-5.2	-5.05		*YDR455C*
-2.55	-4.3		*RPE1*
-2	-3.25		*LEU3*
-2.9	-3.1		*SPT8*
-2.4	-3.1		*RVS161*
-2.9	-3		*SEC66*
-2.5	-2.8		*YBL100C*
-2.1	-2.6		*UBX4*
-2.45	-2.5		*LST7*
-2.5	-2.4		*PDR1*
-2.5	-2.4		*OCA5*
-2.1	-2.4		*YGL138C*
-2	-2.2		*YOR366W*
-2	-2.1		*GCN2*
-2.2	-2		*MUM2*
-2	-2		*CSF1*
-2	-2		*DBF20*
-1.7	-2		*TAT2*
-1.6	-2		*SYF2*
-1.4	-2		*RNQ1*
-1.8	-1.8		*YHR202W*
-1.45	-1.75		*MUD2*
-1.6	-1.7		*PEX6*
-1.3	-1.7		*NSG1*
-1.4	-1.6		*YPL191C*
-1.1	-1.2		*PLB1*
	-3.3		*NHX1*
	-3		*SPF1*
	-2.4		*YDR290W*
	-2.2		*SNF11*
	-2.2		*YPR146C*
	-2.15		*HTD2*
	-2.1		*YCL001W-A*
	-2.1		*ARG1*

APPENDIX 1: Mutants with altered growth in dieldrin (cont.). - sensitive, + resistant

log2 values			
25% IC20 115µM	50% IC20 230µM	IC20 460µM	Deleted Gene
	-2		*HFA1*
	-2		*REG1*
	-1.9		*LRO1*
	-1.85		*YJR129C*
	-1.8		*YOL013W-A*
	-1.7		*SIP1*
	-1.7		*LAP3*
	-1.6		*CSM1*
	-1.6		*PIC2*
	-1.4		*YIL057C*
	-1.4		*YDR215C*
	-1.4		*RPS8A*
	-1.4		*SCT1*
	-1.3		*YIP4*
	-1.3		*EMP46*
	-1.3		*LIP2*
	-1.2		*QDR2*
-3.4			*RPL34B*
-3.3			*DAL81*
-3.2			*RPN4*
-2.7			*YFL019C*
-2.7			*FLC1*
-2.5			*YJR111C*
-2.4			*MET13*
-2.4			*MFT1*
-2.4			*CDC73*
-2.35			*URA4*
-2.3			*YEL045C*
-2.2			*YNL170W*
-2.2			*LST4*
-2.2			*BNA5*
-2.2			*YNL217W*
-2.2			*YLR073C*
-2.2			*YOR199W*
-2			*YBR184W*
-2			*BRP1*
-2			*YMR099C*
-1.9			*MSS2*
-1.85			*GTR1*
-1.8			*SIC1*
-1.8			*MSC7*
-1.8			*ATP12*
-1.8			*YCR022C*
-1.8			*YLR049C*
-1.8			*PYC1*
-1.7			*GPT2*
-1.7			*WWM1*
-1.7			*UBP3*
-1.7			*YDR338C*
-1.7			*SAN1*
-1.7			*OCA6*
-1.6			*YLL007C*
-1.6			*FMO1*
-1.6			*YOL024W*
-1.6			*YIL032C*
-1.5			*YKR078W*
-1.5			*YLR111W*
-1.5			*YGP1*
-1.5			*YEH2*
-1.5			*YCL023C*
-1.4			*CRS5*
-1.4			*RTT102*
-1.4			*ECM37*
-1.3			*MFB1*
-1.3			*EHT1*
-1.3			*HXK2*
-1.3			*YLR168C*
-1.3			*YFR018C*
-1.3			*YBR239C*
-1.3			*MST27*
-1.3			*YGR022C*
-1.2			*SSE2*
-1.2			*YHR022C*
-1			*SPS2*
		-6.25	*VPS30*
		-5.2	*KSP1*

log2 values			
25% IC20 115µM	50% IC20 230µM	IC20 460µM	Deleted Gene
		-4.5	*SHR5*
		-4.4	*ERF2*
		-4.05	*SYS1*
		-4	*SIN3*
		-3.7	*YLR171W*
		-3.6	*SBP1*
		-3.5	*SIN4*
		-3.5	*SAP30*
		-3.4	*CCZ1*
		-3.35	*LEO1*
		-3.3	*CSG2*
		-3.25	*YLR352W*
		-3.2	*CKB2*
		-3.1	*TOM5*
		-3.1	*VAM7*
		-3.1	*VPS41*
		-3	*YAP3*
		-3	*ATG12*
		-3	*HAL9*
		-2.95	*ARL1*
		-2.9	*LAS21*
		-2.9	*YSP1*
		-2.9	*YML122C*
		-2.9	*COG5*
		-2.8	*IDP1*
		-2.8	*CRD1*
		-2.8	*YGL042C*
		-2.8	*SNC2*
		-2.8	*ARL3*
		-2.8	*COQ9*
		-2.75	*SBE22*
		-2.7	*VAN1*
		-2.7	*LSM1*
		-2.7	*NPR2*
		-2.7	*YER084W*
		-2.7	*ICE2*
		-2.65	*YKL077W*
		-2.6	*CKB1*
		-2.6	*YPT7*
		-2.6	*ATG8*
		-2.6	*ARP1*
		-2.6	*NPR3*
		-2.55	*ISA2*
		-2.55	*ATG3*
		-2.5	*PKH3*
		-2.5	*GSF2*
		-2.5	*YDR467C*
		-2.5	*FUI1*
		-2.4	*DBF2*
		-2.4	*YHR048W*
		-2.4	*PHO84*
		-2.35	*ATG5*
		-2.3	*VPS4*
		-2.3	*ATG7*
		-2.3	*INP53*
		-2.3	*COQ6*
		-2.3	*YPT6*
		-2.3	*GET1*
		-2.25	*IES5*
		-2.25	*ATG15*
		-2.2	*PPR1*
		-2.2	*YNR042W*
		-2.2	*UBP6*
		-2.2	*SLM1*
		-2.2	*CAJ1*
		-2.2	*SWD1*
		-2.2	*OYE2*
		-2.2	*GET3*
		-2.2	*YLR374C*
		-2.2	*CAT5*
		-2.15	*PPT2*
		-2.15	*COX20*
		-2.15	*DSK2*
		-2.1	*FAT1*
		-2.1	*MDM38*
		-2.1	*ATG9*

log2 values			
25% IC20 115µM	50% IC20 230µM	IC20 460µM	Deleted Gene
		-2.05	*ATG2*
		-2	*PET494*
		-2	*APL5*
		-2	*COQ4*
		-2	*QCR9*
		-2	*HOC1*
		-1.9	*ICY2*
		-1.9	*MTF1*
		-1.9	*ATG16*
		-1.9	*YAL066W*
		-1.9	*MON1*
		-1.9	*APM1*
		-1.85	*PTC6*
		-1.8	*RNY1*
		-1.8	*YKL207W*
		-1.8	*PEP4*
		-1.75	*IMP1*
		-1.7	*SER2*
		-1.7	*MGM101*
		-1.7	*PET117*
		-1.7	*MTG2*
		-1.7	*VPS74*
		-1.7	*YOL050C*
		-1.7	*YNL235C*
		-1.7	*ATG18*
		-1.7	*MOH1*
		-1.7	*NHP10*
		-1.7	*SNT1*
		-1.6	*HOS2*
		-1.6	*ERG5*
		-1.6	*YIL170W*
		-1.6	*YMR007W*
		-1.6	*CBP1*
		-1.6	*GSH2*
		-1.6	*CRZ1*
		-1.6	*RCE1*
		-1.55	*CIS1*
		-1.5	*IMP2*
		-1.5	*FLC2*
		-1.5	*IRC24*
		-1.5	*ATG29*
		-1.5	*GRE3*
		-1.5	*ATG10*
		-1.5	*SFL1*
		-1.4	*PHO13*
		-1.2	*YCR001W*
		-1.1	*KTR7*
1.1	1.1	1.2	*RPS14A*
1	1.3	1.4	*BCH2*
1.6	1.6	1.5	*YNR005C*
1.4	1.65	1.5	*YDR357C*
1.8	2.1	1.5	*RTG2*
1.1	1.4	1.6	*NUM1*
2	1.7	1.7	*OPY1*
1.8	1.8	1.7	*RGA1*
2.2	1.65	1.75	*YNL105W*
1.2	1.7	1.8	*CIN8*
1.6	1.8	1.8	*RPS30B*
1.5	1.7	1.85	*YJL016W*
1.7	2	1.9	*VTA1*
1.5	1.5	2	*CAF40*
1.7	2.2	2	*HSV2*
2.6	2.5	2	*PUB1*
1.4	1.65	2.1	*YDR049W*
2.1	1.9	2.1	*BUD20*
1.9	2	2.1	*DUG1*
2.3	2.05	2.1	*NUP170*
1.3	1.3	2.15	*NEW1*
1.2	2	2.15	*VAC7*
1.3	1.9	2.2	*SRN2*
2.7	2.5	2.2	*YML119W*
2.4	2.6	2.2	*HMG1*
1.9	2.2	2.3	*DEM1*
2.1	2.4	2.3	*MTF2*
1.8	1.8	2.35	*BUD31*
1.5	1.9	2.4	*RPS28B*

APPENDIX 1: Mutants with altered growth in dieldrin (cont.). - sensitive, + resistant

log2 values			
25% IC20 115µM	50% IC20 230µM	IC20 460µM	Deleted Gene
1.8	1.9	2.4	*RPL8B*
2	2.4	2.4	*DPB4*
1.55	2.25	2.45	*IRC4*
2	2.2	2.5	*UPS1*
2	2.2	2.5	*RPL9A*
2.3	2.2	2.5	*YER156C*
2	2.5	2.5	*PIF1*
1.4	1.8	2.55	*IST3*
2.6	3	2.55	*SSN2*
1.6	2	2.6	*TMA22*
1.6	2.1	2.6	*RPS16B*
2.4	2.5	2.6	*YEL068C*
2.6	2.5	2.65	*OPI11*
2.2	2.8	2.65	*VPS21*
2.1	2	2.7	*YOR309C*
1.9	2.25	2.7	*RPS11B*
2.1	2.3	2.7	*YDR115W*
2.2	2.4	2.7	*RPS18A*
2.2	2.4	2.7	*RPL24A*
2.3	2.5	2.7	*AFG3*
2.3	2.9	2.7	*MGM1*
2.6	2.6	2.75	*SOH1*
2.5	3	2.75	*SSQ1*
2.4	2.85	2.8	*MRPL11*
1.8	2.4	2.85	*RSM18*
2.3	2.4	2.85	*YMR293C*
1.8	2.3	2.9	*SLX8*
2.5	2.6	2.9	*RPL6B*
3.2	2.7	2.9	*YNL108C*
3.2	3.1	2.9	*IRC2*
1.4	2.05	2.95	*YER139C*
2.3	2.1	2.95	*RPS24A*
2.4	2.3	2.95	*YNL226W*
2.2	2.1	3	*RPL7A*
2.7	2.7	3	*EDE1*
2.3	2.9	3.05	*AEP3*
1.8	2.2	3.1	*RPA49*
2.35	2.7	3.1	*SRO9*
4.5	2.8	3.1	*YGL114W*
2.8	3	3.1	*YOR304C-A*
2.9	3	3.1	*MTQ2*
2	2.9	3.15	*MRPS5*
2.75	3	3.15	*MRP21*
2.8	3	3.2	*MRH4*
2.05	2.5	3.25	*RPS30A*
2.6	2.9	3.25	*MBP1*
2.15	2.8	3.3	*RSM27*
2.9	3.6	3.3	*HAT2*
2.7	3	3.55	*YIL060W*
2.6	3.2	3.6	*RPS0B*
3.1	3.2	3.6	*RSM24*
2.65	3.25	3.7	*MRM1*
3.3	3.25	3.75	*IRC19*
2.5	2.6	3.8	*RRP8*
2.7	3.1	3.8	*YLR091W*
2.75	3.2	3.8	*MRP1*
2.75	3.45	3.8	*FMP38*
2.5	3.2	3.85	*FYV7*
2.95	3.3	3.9	*VAC14*
2.5	3.25	3.95	*RSM7*
3.1	3.3	4	*BUD21*
2.75	3.1	4.05	*RPL2B*
3	3.45	4.1	*MSH1*
2.7	3	4.15	*MNI1*
3	3.8	4.3	*MRPL24*
2.85	3.9	4.35	*MEF2*
2.75	3.3	4.4	*RPS7A*
4.3	4.2	4.6	*SUC2*
3.3	4.2	5.05	*NAM2*
3.5	4.4	5.2	*MEF1*
6.8	6.7	5.6	*YDR431W*
1		1.2	*YBR261C*
1		1.3	*RBS1*
1.4		1.3	*IRC16*
1.7		1.5	*YNL266W*
	1.5	1.55	*RAD16*

log2 values			
25% IC20 115µM	50% IC20 230µM	IC20 460µM	Deleted Gene
	1.6	1.6	*ITC1*
1.4		1.6	*NAP1*
1.7		1.6	*COS1*
1.8		1.6	*YKR047W*
	1.2	1.7	*UBR2*
	1.8	1.7	*YOR051C*
1.3		1.7	*SEC28*
1.6		1.7	*KAP123*
2.2		1.7	*FIR1*
	1.4	1.8	*RPS28A*
	1.6	1.8	*TDH2*
	1.7	1.8	*MMS2*
	2.2	1.8	*YGR102C*
1.6		1.8	*OTU2*
	1.3	1.85	*EAF3*
	1.3	1.9	*TMA20*
	1.5	1.9	*SRP40*
	1.5	1.9	*TMA46*
	1.5	1.9	*RPS29A*
	1.6	1.9	*VPS25*
	2	1.9	*FIG4*
	1.6	2	*RPL19B*
	2	2	*SHE9*
	2.4	2	*UTR1*
1.05		2	*TPO1*
1.3		2	*RPS17B*
1.6		2	*RPL4A*
1.6		2	*UTH1*
	1.4	2.05	*EMI2*
	1.4	2.1	*YDL023C*
	1.5	2.1	*VAC8*
	1.8	2.1	*YLR252W*
	2	2.1	*GGC1*
1.6		2.1	*RPS10B*
2.1		2.1	*RPL2A*
2.5		2.1	*ELM1*
	1.7	2.2	*RPL9B*
	1.8	2.2	*RHR2*
1.5		2.2	*RPS18B*
	1.4	2.3	*NCL1*
	1.4	2.3	*RCO1*
4.8		2.3	*YBR138C*
2.4		2.4	*RRP6*
	2.4	2.45	*YGR219W*
1.4		2.45	*NOP12*
	2	2.5	*FYV1*
	3	2.5	*BNI1*
1.8		2.5	*FYV12*
1.9		2.5	*VPH1*
2.1		2.6	*KAP120*
2.3		2.6	*YDR114C*
	2.2	2.65	*RAD27*
	3	2.65	*CPR7*
1.9		2.65	*ZUO1*
1.7		2.7	*YNL228W*
1.9		2.7	*TOS1*
2.3		2.7	*GIM4*
	2.1	2.75	*SYG1*
	2.1	2.8	*MRPL10*
	2.75	2.8	*GLO3*
2.1		2.8	*REI1*
2.8		2.8	*ISR1*
	2.3	2.85	*YER087W*
	1.8	2.9	*RPS6B*
	2.2	2.9	*RPS6A*
2.2		3.9	*HMO1*
		-2.2	*OYE2*
		-2.2	*GET3*
		-2.2	*YLR374C*
		-2.2	*CAT5*
		-2.15	*PPT2*
		-2.15	*COX20*
		-2.15	*DSK2*
		-2.1	*FAT1*
		-2.1	*MDM38*
		-2.1	*ATG9*

log2 values			
25% IC20 115µM	50% IC20 230µM	IC20 460µM	Deleted Gene
	3.65	4	*DIA4*
	1.1		*YNL010W*
	1.1		*KNS1*
1.4	1.4		*GCN3*
1.1	1.5		*YML100W-A*
1.4	1.5		*YGL214W*
1.5	1.5		*LEU4*
	1.5		*IRC13*
	1.5		*YPL080C*
1.6	1.7		*NCE101*
1.7	1.7		*ARC18*
1.5	1.8		*VPS27*
1.5	1.8		*VAM10*
1.6	1.8		*INP52*
	1.8		*LIA1*
1.95	1.9		*IKI3*
2.1	1.9		*VPS38*
	1.9		*HIT1*
1.9	2		*YLL014W*
	2		*ELP4*
1.8	2.1		*YLR412W*
1.9	2.1		*MRP51*
2	2.1		*YKR074W*
2.3	2.1		*SRB2*
	2.1		*GLN3*
	2.2		*YGL072C*
	2.2		*NUP133*
	2.2		*NST1*
	2.2		*MRPL4*
1.7	2.3		*YLR426W*
2	2.3		*TIF4631*
2.4	2.3		*KTI12*
	2.35		*ASC1*
2.1	2.4		*MRPL38*
2	2.5		*SNT309*
2	2.6		*VPS9*
2.3	2.6		*VPS8*
2.4	2.6		*DBP7*
2.3	2.7		*RPL27A*
2.4	2.7		*YDR065W*
2.4	3.1		*YLR358C*
	3.6		*VPS5*
1			*YJR026W*
1.1			*VPS60*
1.1			*TAH1*
1.2			*LEE1*
1.2			*FIG1*
1.3			*NKP1*
1.3			*YBR139W*
1.3			*BFA1*
1.4			*MSC1*
1.4			*YMR245W*
1.4			*YML116W-A*
1.6			*ATS1*
1.6			*RGA2*
1.6			*CYM1*
1.7			*SOV1*
1.7			*FRE3*
1.7			*YJR038C*
1.9			*URH1*
1.9			*YPL102C*
1.9			*NCS2*
1.9			*SLA1*
1.9			*YGR127W*
2			*EST1*
2			*YML094C-A*
2			*YDR391C*
2.1			*BRO1*
2.2			*SEM1*
2.2			*DIT1*
2.2			*YLR349W*
2.2			*HNT3*
2.3			*ELP6*
2.3			*ETR1*
2.3			*FCY2*
2.4			*EFT2*

APPENDIX 1: Mutants with altered growth in dieldrin (cont.). - sensitive, + resistant

log2 values			
25% IC20 115µM	50% IC20 230µM	IC20 460µM	Deleted Gene
2.4			*SPT10*
2.4			*YKU70*
2.5			*FMP24*
2.5			*FCY22*
2.5			*RPL13A*
2.6			*PDX3*
2.7			*YIL067C*
2.8			*ECM3*
3			*ATO3*
		1.2	*SIP5*
		1.2	*YGR283C*
		1.3	*GIS1*
		1.4	*GIT1*
		1.4	*ENT2*
		1.4	*YDR132C*
		1.4	*YNL115C*
		1.4	*STM1*
		1.6	*RPL34A*
		1.6	*ISY1*
		1.6	*WHI2*
		1.6	*ISW2*
		1.6	*MUB1*
		1.65	*YGL250W*
		1.7	*RPS26B*
		1.7	*CHD1*
		1.7	*RPS21B*
		1.7	*HRK1*
		1.7	*RPS0A*
		1.7	*RPL27B*
		1.75	*VPS28*
		1.8	*GAL1*
		1.8	*YDL062W*
		1.8	*YNL324W*
		1.8	*MRP7*
		1.9	*RPN10*
		1.9	*EPS1*
		1.9	*TIP41*
		1.9	*OPI7*
		1.95	*BRR1*
		2	*RPS7B*
		2	*YMR075C-A*
		2	*YHL044W*
		2.05	*ARX1*
		2.1	*ACE2*
		2.1	*YPR116W*
		2.1	*YLR366W*
		2.1	*RPS4B*
		2.1	*RPS19A*
		2.2	*RPL16B*
		2.2	*RPS23A*
		2.2	*MHR1*
		2.2	*SOD2*
		2.3	*SRB5*
		2.3	*MRPL31*
		2.3	*MRPL16*
		2.3	*RPS1A*
		2.3	*SSZ1*
		2.3	*RPL16A*
		2.35	*RPS21A*
		2.35	*RPA34*
		2.4	*IFM1*
		2.4	*ABF2*
		2.4	*RPS23B*
		2.45	*FYV5*
		2.5	*LRP1*
		2.5	*ECM21*
		2.6	*CYK3*
		2.65	*RPA14*
		2.8	*ADO1*
		2.85	*ATP5*
		2.9	*RPL22A*
		2.9	*YGL088W*
		3.1	*BUD28*
		3.7	*LEA1*

APPENDIX 2: Mutants with altered growth in toxaphene. - sensitive, + resistant

log2 values			
25% IC20 160µM	50% IC20 320µM	IC20 640µM	Deleted Gene
-6.3	-5.8	-6.05	*PDR5*
-3.15	-3.05	-2.55	*RPN4*
-3.1	-3.5	-3	*DAL81*
-2.9	-4.5	-4.7	*TRP4*
-2.9	-3.2	-3	*SWF1*
-2.75	-2.45	-2.95	*URE2*
-2.5	-3.1	-3	*STP1*
-2.5	-2.6	-2.6	*YGR153W*
-2.3	-2.8	-3.1	*YDR008C*
-2.3	-2.6	-2.4	*SEC66*
-2.2	-2.6	-2.4	*YEL045C*
-2.15	-2.25	-2.7	*PDR1*
-2	-1.85	-1.95	*SPT4*
-1.75	-2.5	-2	*IRS4*
-1.75	-1.45	-1.2	*YKL077W*
-1.65	-2	-2.5	*THP2*
-1.6	-1.9	-2.2	*YDR203W*
-1.5	-1.5	-2.2	*ICE2*
-1.5	-1.4	-1.7	*TKL1*
-1.5	-1.4	-1.4	*COG7*
-1.45	-1.85	-2.05	*COX20*
-1.4	-1.7	-2.6	*IMG2*
-1.4	-1.5	-1.3	*YDR455C*
-1.3	-1.4	-1.55	*URA2*
-1.3	-1.3	-1.3	*SIW14*
-1.25	-1.55	-1.5	*GYP1*
-1.25	-1.5	-1.75	*YSP1*
-1.25	-1.3	-1.35	*YJL120W*
-1.2	-1	-1.15	*CUE1*
-1.2	-0.9	-1.1	*PBP1*
-1.1	-1.1	-1.4	*GSF2*
-1.1	-1.05	-1.7	*OSH3*
-1.1	-1	-0.8	*YNL010W*
-1	-1.5	-1.65	*RSM22*
-1	-1.5	-1.4	*COQ4*
-1	-1.3	-1.7	*MFT1*
-1	-1.2	-1.6	*RPE1*
-1	-1	-1.2	*YAK1*
-0.95	-1.35	-1.8	*BRE5*
-0.95	-1.3	-1.35	*PET54*
-0.9	-1.1	-1.5	*CSM1*
-0.8	-0.8	-1	*DST1*
-0.7	-0.9	-1.3	*HXK2*
-2		-1.4	*YGR064W*
-1.9		-2.1	*GET1*
-1.55	-1.4		*SPF1*
-1.5		-1.5	*REG1*
-1.4		-1.7	*ERV14*
-1.35	-1.15		*DCS1*
-1.3	-1.5		*KRE11*
-1.3		-1.6	*PTH1*
-1.3		-1	*ALF1*
-1.2	-1.5		*COQ9*
-1.2	-1		*YLR126C*
-1.2		-0.9	*ARP1*
-1		-1.1	*YER084W*
-0.9	-1.1		*FLC2*
-0.9	-0.8		*BAP2*
-0.8	-0.8		*ALG8*
-0.8		-1.55	*ARO2*
	-1.6	-1.8	*MIP1*
	-1.5	-2.05	*UBP3*
	-1.35	-1.9	*QCR8*
	-1.3	-1.4	*NPR2*
	-1.2	-1.45	*COX15*
	-1.2	-1.4	*SYS1*
	-1.2	-1.4	*YPR099C*
	-1.2	-1.4	*GCN20*
	-1.2	-1.3	*GCN3*
	-1.2	-1.3	*MRS1*
	-1.1	-1.4	*THR4*
	-1.1	-1.4	*PEX6*
	-1.1	-1.4	*YJL022W*
	-1.1	-0.9	*ARO3*
	-1.1	-0.9	*MRPL51*
	-1	-1.3	*MTG2*

log2 values			
25% IC20 160µM	50% IC20 320µM	IC20 640µM	Deleted Gene
	-1	-1	*YDR230W*
	-0.8	-0.9	*PRM9*
-3.3			*YJL175W*
-2.5			*YKL037W*
-1.65			*RVS161*
-1.6			*YGR228W*
-1.5			*PGD1*
-1.4			*PHO4*
-1.4			*RTT106*
-1.3			*GET3*
-1.3			*YPL066W*
-1.25			*DFG5*
-1.2			*ATP17*
-1.2			*IRA2*
-1.2			*TIM18*
-1.2			*YOR052C*
-1.1			*CHS5*
-1			*URA4*
-1			*BRP1*
-1			*YML009C-A*
-0.9			*PTK2*
-0.9			*OPI3*
-0.9			*SIS2*
-0.8			*MOT3*
	-2		*HAC1*
	-1.3		*CDC73*
	-1.2		*YIM2*
	-1.15		*ELF1*
	-1		*ERG5*
	-1		*OCA1*
	-1		*GSH1*
	-1		*PTR2*
	-0.9		*MRPL33*
	-0.9		*TRP1*
	-0.7		*QRI8*
		-1.8	*YGL149W*
		-1.75	*RPL34B*
		-1.7	*VPS52*
		-1.7	*MSM1*
		-1.7	*BST1*
		-1.65	*PET122*
		-1.6	*QCR9*
		-1.5	*PHO88*
		-1.4	*COX23*
		-1.4	*RUD3*
		-1.3	*COG8*
		-1.3	*OXA1*
		-1.3	*COX11*
		-1.3	*MRP20*
		-1.3	*YBL012C*
		-1.2	*COX10*
		-1.2	*NSG1*
		-1.1	*HXT12*
		-1.1	*CBP2*
		-1.1	*MRPL35*
		-1.1	*PET494*
		-1.1	*LRS4*
		-0.9	*MGM101*
		-0.8	*YND1*
4.8	5.6	5.7	*YML119W*
5.7	5.7	5.4	*YEL028W*
5.2	5.5	5.4	*YBR138C*
5.5	5.4	5.3	*YDL010W*
5.4	5.2	5.3	*FMT1*
5.2	5.2	5	*YBL065W*
5	5.2	5	*MRPL39*
3.9	4.4	5	*MSS51*
4.9	4.9	4.9	*ECM3*
4.7	4.7	4.7	*HRQ1*
4.7	4.7	4.7	*YOL118C*
4.4	4.4	4.7	*KIN1*
4	4	4.7	*YLR036C*
4.5	4.5	4.6	*YGL114W*
4.5	4.7	4.5	*SLM2*
4.3	4.6	4.5	*YJL046W*
4.7	4.5	4.3	*YCR007C*

log2 values			
25% IC20 160µM	50% IC20 320µM	IC20 640µM	Deleted Gene
3.7	4.2	4.3	*HNT3*
3.9	4.3	4.2	*YKU70*
4.3	4.2	4.1	*YHI9*
4.1	4.1	4	*YMR119W-A*
4.4	3.9	3.8	*YKL133C*
3.6	3.9	3.8	*ATO3*
3.8	3.8	3.8	*INP1*
3	3.4	3.8	*TPO1*
3.7	3.9	3.7	*YBR074W*
4.1	3.8	3.7	*YMR114C*
3.8	3.8	3.7	*ARA1*
3.8	3.7	3.7	*DYN3*
4.4	4.1	3.6	*YKR041W*
3.9	4.1	3.6	*YNL140C*
3.5	3.6	3.6	*FRE7*
3.8	3.6	3.5	*MET28*
3.2	3.2	3.5	*MSN1*
2.8	2.5	3.5	*CCC1*
3.2	3.5	3.4	*BDF2*
3.7	3.4	3.4	*YJR154W*
2.9	3.1	3.4	*CTS1*
2.6	2.9	3.4	*YLR349W*
2.2	2.5	3.4	*YIL067C*
3.6	3.6	3.3	*YNL108C*
3.7	3.5	3.3	*FET5*
3.1	3.4	3.3	*CAF20*
2.9	3.1	3.3	*YPR014C*
2.8	2.9	3.3	*VPS38*
1.7	2.3	3.2	*MDL1*
3.2	3.6	3.1	*LDB16*
3.4	3.3	3.1	*KTR2*
3.2	3.3	3.1	*YGR242W*
3.4	3.4	3	*YNL105W*
3	3.2	3	*COS6*
2.7	2.8	3	*CHO2*
2.7	2.6	3	*YBR134W*
3.3	3.2	2.9	*FCY22*
2.7	2.8	2.9	*GTB1*
2.8	2.7	2.9	*YDL241W*
2.8	3.1	2.8	*YPR012W*
3	3	2.8	*URH1*
2.8	3	2.8	*YDR124W*
2.9	2.9	2.8	*ETR1*
2.4	2.8	2.8	*YPR096C*
2.4	2.8	2.8	*RPL13A*
2.4	2.7	2.8	*PAP2*
2.15	2.3	2.8	*VAC14*
1.9	2.1	2.8	*SPO77*
2.8	2.9	2.7	*FIR1*
3.1	2.8	2.7	*HXT8*
3	2.8	2.7	*YBL107C*
2.7	2.7	2.7	*VHS3*
1.8	2	2.7	*YLR408C*
3.2	3.5	2.6	*EST3*
2.7	2.8	2.6	*FMP24*
2.7	2.7	2.6	*TAZ1*
1.3	2	2.6	*YLR334C*
2.3	1.9	2.6	*DIT1*
3.1	3.1	2.5	*POT1*
2.3	2.8	2.5	*BUD9*
2.6	2.7	2.5	*YDR336W*
2.3	2.5	2.5	*SCM4*
2.9	2.7	2.45	*SPO16*
2.9	3	2.4	*TFS1*
2.15	3	2.4	*EFT2*
2.8	2.6	2.4	*YKL147C*
1.9	2.6	2.4	*OPI7*
2.4	2.4	2.4	*YGL015C*
2.3	2.4	2.4	*YGR127W*
2.5	2.2	2.4	*YEL023C*
2.9	2.7	2.3	*YFR026C*
2.6	2.6	2.3	*KEL3*
2.6	2.5	2.3	*FCY2*
2.5	2.4	2.3	*YPR196W*
2.5	2.4	2.3	*RPL19A*
2.4	2.4	2.3	*SAS5*

APPENDIX 2: Mutants with altered growth in toxaphene (cont.). - sensitive, + resistant

log2 values			
25% IC20 160μM	50% IC20 320μM	IC20 640μM	Deleted Gene
2.2	2.4	2.3	*PNT1*
1.6	1.6	2.3	*NIT3*
1.3	0.9	2.3	*RPL8B*
2.2	0.5	2.3	*NHX1*
2.5	2.5	2.2	*YKR077W*
2.1	2.5	2.2	*YOL160W*
2.5	2.4	2.2	*HMG1*
2.4	2.4	2.2	*MNT2*
2.4	2.3	2.2	*MRP21*
2.3	2.2	2.2	*YHR032W*
2.1	2	2.2	*YOR251C*
2.4	1.7	2.2	*SRO9*
1.4	1.7	2.2	*YLR177W*
1.1	1.5	2.2	*ADO1*
1.3	1.2	2.2	*YLR413W*
2.5	2.4	2.1	*MDH1*
2.1	2.3	2.1	*AFR1*
2.3	2.2	2.1	*YHR140W*
2.1	2.2	2.1	*ABP140*
1.8	2	2.05	*PUB1*
1.6	1.6	2.05	*FYV7*
2.4	2.5	2	*UGA2*
2.5	2.3	2	*SAE3*
2	2	2	*FRE3*
1.7	2	2	*ESC2*
2	1.9	2	*OPY1*
1.3	1.5	2	*YLR437C*
1.1	1.2	2	*RNP1*
1.35	1.65	1.95	*MEF1*
1.6	1.4	1.95	*REX2*
2.3	2.2	1.9	*UMP1*
2	2.2	1.9	*ARE2*
2.1	2.1	1.9	*YBR259W*
2.3	2	1.9	*TMT1*
2.1	2	1.9	*YBL096C*
2.1	2	1.9	*AXL1*
1.9	2	1.9	*GDE1*
1.8	1.9	1.9	*PNC1*
1.7	1.8	1.9	*SAE2*
0.9	1.2	1.9	*VTA1*
1.7	1.9	1.85	*RPL6B*
1.3	1.9	1.85	*RAD27*
2.2	2.4	1.8	*HSP12*
2.4	2.3	1.8	*MNI1*
2.5	2.1	1.8	*YCR101C*
2	2	1.8	*SLM4*
2	2	1.8	*PEX19*
2.2	1.9	1.8	*MRPL40*
1.7	1.9	1.8	*YOX1*
1.6	1.9	1.8	*YJR079W*
1.7	1.8	1.8	*YDR444W*
1.7	1.8	1.8	*GDH2*
1.6	1.7	1.8	*PPH22*
1.5	1.7	1.8	*BGL2*
0.9	1.2	1.8	*CPR6*
1.3	1.6	1.75	*LEA1*
4.9	4.7	1.7	*TPO5*
1.9	2.1	1.7	*SGE1*
1.9	2.1	1.7	*YDR391C*
1.6	1.9	1.7	*NPL4*
2	1.8	1.7	*RPS27A*
2	1.8	1.7	*TPK1*
2	1.8	1.7	*YMR135W-A*
1.5	1.8	1.7	*GRX3*
1.6	1.7	1.7	*YLR199C*
1.8	1.6	1.7	*IKS1*
1.7	1.6	1.7	*PCL2*
1.5	1.6	1.7	*MUP1*
1.4	1.6	1.7	*RCK2*
1.4	1.5	1.7	*BRR1*
1.35	1.5	1.7	*RPS30A*
2	1.9	1.6	*ATG7*
1.8	1.8	1.6	*TOP1*
1.7	1.8	1.6	*YNL144C*
1.4	1.8	1.6	*CAD1*
1.6	1.7	1.6	*YPR126C*

log2 values			
25% IC20 160μM	50% IC20 320μM	IC20 640μM	Deleted Gene
1.6	1.7	1.6	*AAT1*
1.7	1.65	1.6	*YER156C*
1.6	1.6	1.6	*YBR147W*
1.4	1.6	1.6	*YKL121W*
1.4	1.6	1.6	*AIR2*
1.6	1.5	1.6	*COS1*
1.5	1.5	1.6	*SBE2*
1.4	1.5	1.6	*PST1*
1.4	1.5	1.6	*DOT1*
1.5	1.4	1.6	*YOR186W*
1.4	1.4	1.6	*SLM3*
1.3	1.4	1.6	*YGR068C*
1.6	1.8	1.5	*JLP2*
1.7	1.7	1.5	*YJL185C*
1.6	1.7	1.5	*SIL1*
1.6	1.7	1.5	*YOP1*
1.5	1.7	1.5	*ORM1*
1.4	1.6	1.5	*RGA2*
1.4	1.6	1.5	*TAN1*
1.4	1.6	1.5	*TRM1*
1.5	1.5	1.5	*RIS1*
1.5	1.4	1.5	*MET16*
1.4	1.3	1.5	*ISR1*
1.3	1.3	1.5	*BTS1*
1.3	1.3	1.5	*YMR294W-A*
2.2	1.9	1.4	*DUG1*
1.9	1.9	1.4	*INO4*
1.9	1.8	1.4	*APN2*
1.9	1.7	1.4	*YFL015C*
1.6	1.5	1.4	*YIR024C*
1.6	1.4	1.4	*YER066W*
1.5	1.4	1.4	*MDG1*
1.4	1.4	1.4	*ENT1*
1.4	1.2	1.4	*YNR005C*
2.3	1.9	1.3	*YFR016C*
1.6	1.6	1.3	*YNL266W*
1.3	1.6	1.3	*THI6*
1.4	1.5	1.3	*LOT5*
1.3	1.5	1.3	*SRT1*
1.5	1.4	1.3	*YDR415C*
1.4	1.4	1.3	*YBR013C*
1.3	1.4	1.3	*YHB1*
1.2	1.4	1.3	*YJR038C*
1.2	1.4	1.3	*FIG1*
1.5	1.3	1.3	*YDL199C*
1.3	1.3	1.3	*YOL053W*
1.1	1.3	1.3	*TSA2*
1.1	1.3	1.3	*BRE4*
1.7	1.2	1.3	*YKL131W*
1.2	1.2	1.3	*EFT1*
1.3	1.5	1.2	*LEU4*
1.7	1.3	1.2	*DLD3*
1.3	1.3	1.2	*RPL9A*
1.4	1.2	1.2	*SUT1*
1.3	1.1	1.2	*NFU1*
1	1.2	1	*YDR539W*
	2.2	2.3	*BNI1*
	1.8	2.2	*TOS1*
	1.65	2.2	*NAM2*
	1.3	2.2	*UPS1*
	2.3	2.1	*SKT5*
1.3		1.95	*YLR091W*
	1.9	1.9	*CHS7*
	1.2	1.9	*ACE2*
	1	1.9	*FRE8*
	0.8	1.85	*YLR111W*
	1.75	1.8	*NST1*
	1.7	1.8	*LHS1*
	1.6	1.8	*EST1*
	1.3	1.8	*YLR412W*
2.1		1.8	*MUM2*
	1.5	1.7	*MRPL24*
	1.1	1.7	*YLR364W*
	2.1	1.65	*EAF7*
	1.2	1.6	*VPS9*
	1	1.6	*IRC20*

log2 values			
25% IC20 160μM	50% IC20 320μM	IC20 640μM	Deleted Gene
	1.4	1.55	*RPL38*
	1.3	1.55	*RPL26A*
1.6		1.5	*SSQ1*
	1.2	1.4	*CRR1*
	1.1	1.4	*ENT2*
	0.9	1.4	*SRN2*
	1.3	1.3	*RPL24A*
	1.3	1.3	*YML116W-A*
	1.1	1.2	*MRP1*
	0.9	1.2	*YLR224W*
	0.7	1.2	*YLL032C*
	0.9	1.1	*YLR390W-A*
	1	1	*EDE1*
	0.8	1	*CHS6*
1.9	2.1		*FPR1*
1.4	1.7		*YGR043C*
1.8	1.6		*PHO91*
1.8	1.6		*YFL040W*
1.8	1.6		*YFR018C*
1.4	1.6		*YBR141C*
1.8	1.5		*YEL057C*
1.7	1.5		*TOM70*
1.7	1.5		*MSH4*
1.6	1.5		*PDR17*
1.5	1.5		*SHE9*
1.3	1.5		*MSH6*
1.2	1.5		*YMR052C-A*
1.5	1.4		*HOS4*
1.5	1.4		*IML3*
1.5	1.4		*GLC8*
1.4	1.4		*RNH70*
1.35	1.4		*KAP123*
1.3	1.4		*HIR2*
1.1	1.4		*CTT1*
1.5	1.3		*HIS1*
1.2	1.3		*RNH202*
1.2	1.3		*ITT1*
1.2	1.3		*DOA1*
1	1.3		*YBR027C*
1.6	1.2		*YOL114C*
1.6	1.2		*MRPS8*
1.4	1.2		*RSM18*
1.4	1.2		*GND2*
1.3	1.2		*RRP8*
1.3	1.2		*PFK26*
1.2	1.2		*YMR245W*
1.2	1.2		*THI22*
1.2	1.2		*SFH5*
1.2	1.2		*YFR032C*
1.2	1.2		*YDR274C*
1.1	1.2		*FSH3*
1	1.2		*YDR352W*
1	1.2		*UBP2*
0.9	1.2		*YOL162W*
1.3	1.15		*SSN2*
1.2	1.15		*VAC7*
1.5	1.1		*RAS2*
1.4	1.1		*YNL226W*
1.3	1.1		*SRP40*
1.3	1.1		*OMA1*
1.3	1.1		*YAL064C-A*
1.2	1.1		*YER187W*
1.2	1.1		*DIP5*
1.2	1.1		*PGM2*
1.2	1.1		*YCL049C*
1.1	1.1		*PST2*
1.1	1.1		*YOR062C*
1.1	1.1		*YNL109W*
1.1	1.1		*YDR286C*
1	1.1		*KSS1*
1.3	1		*VPS8*
1.2	1		*YER135C*
1.1	1		*FIG4*
1.1	1		*YPL105C*
1.1	1		*YNL115C*
1.05	1		*RPS24B*

APPENDIX 2: Mutants with altered growth in toxaphene (cont.). - sensitive, + resistant

log2 values			
25% IC20 160µM	50% IC20 320µM	IC20 640µM	Deleted Gene
1	1		*BRO1*
1	1		*UPC2*
0.9	1		*YOR285W*
0.9	1		*ASF2*
1	0.8		*DAL7*
		2.7	*YDL041W*
		2.2	*YLL023C*
		2.2	*ABF1*
		2	*HCR1*
		2	*ELM1*
		2	*YLR358C*
		1.9	*MRPL16*
		1.9	*IZH3*
		1.85	*IKI3*
		1.8	*STE23*
		1.8	*NUP133*
		1.8	*CYK3*
		1.7	*ICT1*
		1.7	*YKE2*
		1.7	*YDR179W-A*
		1.6	*TRX1*
		1.6	*VPS21*
		1.6	*YLR426W*
		1.6	*YOR199W*
		1.6	*NYV1*
		1.6	*HMG2*
		1.6	*NNT1*
		1.6	*FAR10*
		1.55	*AVL9*
		1.55	*APC9*
		1.5	*SUL2*
		1.5	*YLR217W*
		1.5	*TMA7*
		1.5	*POM34*
		1.5	*SLA1*
		1.5	*BNA5*
		1.5	*YKR078W*
		1.5	*SLI15*
		1.4	*IRC19*
		1.4	*MAG2*
		1.4	*MMP1*
		1.4	*DNM1*
		1.4	*ECM22*
		1.4	*SWI4*
		1.4	*DCN1*
		1.4	*YLR063W*
		1.4	*YLR241W*
		1.35	*SMF3*
		1.35	*YLR053C*
		1.3	*SAM1*
		1.3	*ARC18*
		1.3	*SPA2*
		1.3	*KNS1*
		1.3	*YLR049C*
		1.3	*STM1*
		1.3	*YLR124W*
		1.3	*ECM7*
		1.3	*PDR8*
		1.3	*RFX1*
		1.3	*IES3*
		1.3	*YML094C-A*
		1.3	*PEX30*
		1.3	*MRM1*
		1.3	*YLR031W*
		1.3	*CRN1*
		1.3	*YLR057W*
		1.3	*YLR143W*
		1.3	*YEL033W*
		1.3	*ACF2*
		1.3	*PCD1*
		1.3	*ALT1*
		1.3	*MEU1*
		1.3	*CTF3*
		1.3	*YLR065C*
		1.3	*HMX1*
		1.3	*YLR255C*

log2 values			
25% IC20 160µM	50% IC20 320µM	IC20 640µM	Deleted Gene
		1.25	*ZRT2*
		1.25	*AYT1*
		1.2	*YLR225C*
		1.2	*YLL007C*
		1.2	*PSY1*
		1.2	*YEH2*
		1.2	*YLR257W*
		1.2	*ECM38*
		1.2	*YLR218C*
		1.2	*RPS28B*
		1.2	*EMP70*
		1.2	*CCW12*
		1.2	*FMP38*
		1.2	*ECI1*
		1.2	*LDB19*
		1.2	*SRL2*
		1.2	*YDR340W*
		1.2	*YLR312C*
		1.15	*YLR253W*
		1.15	*SPE4*
		1.15	*NEJ1*
		1.15	*MLH2*
		1.15	*YLR072W*
		1.1	*CKI1*
		1.1	*YLR064W*
		1.1	*SNF7*
		1.1	*UBR2*
		1.1	*PAU4*
		1.1	*RSA3*
		1.1	*YLR112W*
		1.1	*YLR434C*
		1.1	*EXG1*
		1.1	*YLR422W*
		1.1	*GAL2*
		1.1	*YLR073C*
		1.1	*YLR108C*
		1.1	*PET309*
		1.1	*SWC5*
		1.1	*HRD3*
		1.1	*YPS3*
		1	*APS1*
		1	*YLR345W*
		1	*YLL044W*
		1	*UBI4*
		1	*XYL2*
		1	*KIN2*
		1	*THI73*
		1	*SKI2*
		1	*AHP1*
		1	*ECM19*
		1	*PPR1*
		1	*VPS36*
		1	*YLR356W*
	1.9		*YML012C-A*
	1.8		*BUD27*
	1.8		*YPL102C*
	1.6		*GYP6*
	1.55		*CBC2*
	1.5		*SGF29*
	1.4		*VPS25*
	1.4		*NUP170*
	1.4		*SSN8*
	1.4		*CYM1*
	1.3		*CPR7*
	1.3		*RPS7A*
	1.3		*DPB4*
	1.3		*VPS28*
	1.3		*SWI5*
	1.2		*ELP6*
	1.2		*ELP4*
	1.2		*RSC2*
	1.2		*SNF8*
	1.2		*PPM1*
	1.2		*PCL8*
	1.2		*MNN2*
	1.2		*YPL071C*

log2 values			
25% IC20 160µM	50% IC20 320µM	IC20 640µM	Deleted Gene
	1.1		*RPS7B*
	1.1		*YBR277C*
	1.1		*YKR074W*
	1.1		*URA7*
	1.1		*ZTA1*
	1.1		*YOR304C-A*
	1.1		*CLB6*
	1.1		*YDR128W*
	1.1		*SRO77*
	1.1		*YBR090C*
	1.1		*RIM9*
	1		*DPB3*
	1		*YPR053C*
	1		*CUP2*
	1		*YJL123C*
	1		*YDR357C*
	1		*YDR249C*
	1		*ISC10*
	1		*ASE1*
2.6			*ROM2*
1.7			*YGR102C*
1.6			*RPS21A*
1.5			*SEM1*
1.5			*NEW1*
1.4			*YIL060W*
1.4			*APE2*
1.4			*YPR170C*
1.4			*CYC7*
1.3			*YCR051W*
1.3			*CDC26*
1.3			*RPL2A*
1.3			*KCC4*
1.3			*YBR184W*
1.3			*YFR017C*
1.3			*LUG1*
1.2			*FYV5*
1.2			*MCT1*
1.2			*MRH4*
1.2			*PIH1*
1.2			*RPL2B*
1.2			*SFT2*
1.2			*NOP13*
1.2			*SCO1*
1.2			*YFR007W*
1.2			*EMP47*
1.2			*YMR320W*
1.2			*HXT5*
1.2			*OSH6*
1.2			*RPS17B*
1.2			*MRPS9*
1.1			*RPS11B*
1.1			*YPR063C*
1.1			*MPC54*
1.1			*YKL070W*
1.1			*YKR104W*
1.1			*VPS24*
1.1			*ALY1*
1.1			*GFD1*
1.1			*YER152C*
1.1			*YFL063W*
1.1			*YNL100W*
1.1			*YER163C*
1			*HEX3*
1			*BUD31*
1			*SSF1*
1			*TMA22*
1			*LYS5*
1			*YIL024C*
1			*DSE1*

APPENDIX 3: Mutants with altered growth in DMSO. - sensitive, + resistant

Deleted Gene	Log2 value 1% DMSO
SUC2	-4.54
RPL27A	-2.45
RRP8	-2.41
COG5	-2.38
YER156C	-2.31
YOR304C-A	-2.26
COG8	-2.11
ROM2	-2.10
YJL132W	-2.07
DBP7	-1.93
PHO4	-1.91
YAF9	-1.90
VPS65	-1.83
CDC26	-1.65
YFR045W	-1.62
IRS4	-1.61
COG6	-1.57
VPS63	-1.54
MCX1	-1.50
COG7	-1.47
NCE101	-1.41
FIR1	-1.39
CYC7	-1.36
KAP123	-1.35
RCK1	-1.35
YBR013C	-1.28
RPL24A	-1.26
ATR1	-1.24
HIR3	-1.22
YNL198C	-1.19
FLC3	-1.14
NNF2	-1.08
NFU1	-1.06
NTG1	-1.05
CLB1	-1.03
SED4	-0.92
SGN1	-0.90
YDL211C	-0.88
FIT1	-0.88
UBP9	-0.87
ABZ2	4.84
YBR113W	4.36
YPR011C	3.65
PAU5	3.55
SSF2	3.54
YFL013W-A	3.33
ANT1	3.27
YNL217W	3.25
BNS1	3.25
YIL032C	3.23
YKR078W	3.12
YER087C-A	3.07
ARG80	3.02
HEH2	2.95
GDT1	2.95
YFR018C	2.82
YLR042C	2.76
HXT10	2.73
AIM24	2.73
PTP1	2.72
UBP15	2.70
FMO1	2.70
TRP4	2.65
YOR021C	2.65
HMG2	2.63
TMA10	2.63
YBR184W	2.59
YJR088C	2.57
SNF8	2.56
YMR291W	2.56
REV7	2.53
SOL2	2.52
GAL10	2.51
PRM10	2.49
YMR244C-A	2.48
YBR042C	2.44

Deleted Gene	Log2 value 1% DMSO
YJL218W	2.44
AGP3	2.43
LPE10	2.40
TAN1	2.38
CKA1	2.37
YGL138C	2.36
YHR177W	2.36
YCR022C	2.33
RAD16	2.32
RIM9	2.31
MET8	2.31
ARE2	2.27
LPD1	2.27
NHX1	2.26
TMS1	2.22
YJL217W	2.22
VPS55	2.19
OTU1	2.18
TVP38	2.18
IOC4	2.17
YKR096W	2.14
YMR074C	2.14
RPH1	2.14
YHL037C	2.14
YOR314W	2.13
ENT1	2.13
YLR297W	2.12
MRPL35	2.12
EMI1	2.11
PNS1	2.11
YNL058C	2.10
YPS3	2.10
YCR006C	2.09
CAF120	2.08
SIA1	2.08
YLR073C	2.06
YJR111C	2.06
YNR024W	2.05
YDL073W	2.04
OAZ1	2.04
IES1	2.03
STP22	2.00
SKS1	2.00
EXO1	1.99
YKR105C	1.98
SIZ1	1.98
NOP13	1.98
MMS2	1.96
SIP18	1.96
TPS3	1.95
WWM1	1.95
FMP29	1.95
DOT6	1.94
YLR202C	1.94
ESC2	1.93
YGR122W	1.93
YFL012W	1.91
GCN2	1.90
HSP12	1.90
YSP2	1.87
YGR107W	1.87
ARR3	1.86
ASP1	1.86
OST5	1.85
SET2	1.85
MSH4	1.85
ATP11	1.84
INM1	1.84
MRPL33	1.84
HNT2	1.82
YCR001W	1.81
VPS36	1.81
SCJ1	1.80
PCH2	1.80
UBX7	1.79
MKK2	1.79

Deleted Gene	Log2 value 1% DMSO
YLR169W	1.78
HST2	1.78
YMR295C	1.77
RIM20	1.76
CYM1	1.76
YLR257W	1.76
SAP4	1.76
DCS1	1.76
CHS5	1.75
SCS7	1.74
BTT1	1.73
MRM2	1.70
YOR352W	1.70
SNU66	1.70
LSP1	1.70
HBT1	1.68
MAL31	1.68
RIM13	1.68
ARR2	1.68
TCM62	1.65
YAL042C-A	1.64
RNH70	1.64
YJR079W	1.64
CUS2	1.64
YBL094C	1.64
ADP1	1.64
MSB2	1.63
BLM10	1.63
QCR9	1.62
PRM9	1.60
ARC18	1.59
PAM1	1.59
YOR366W	1.58
YML047W-A	1.58
ECM7	1.57
TDH3	1.57
DFG16	1.56
RTT102	1.56
FIG1	1.55
NSG1	1.55
YNL187W	1.54
SNO2	1.53
YDR520C	1.53
ERD1	1.52
SWH1	1.50
YOR006C	1.50
YBR056W	1.49
SCO2	1.49
MUM2	1.49
YNL122C	1.49
YNL010W	1.48
ZIP1	1.48
APT2	1.48
VPS74	1.48
SRO77	1.47
CPT1	1.46
ISY1	1.46
HPR5	1.46
RCK2	1.45
YLR356W	1.45
AIP1	1.44
SPO13	1.44
YMR244W	1.44
YCL046W	1.43
YLR111W	1.42
YLR057W	1.42
TRX1	1.40
YLR456W	1.37
YPL033C	1.37
GPH1	1.35
NMA111	1.35
YIR020C	1.35
NYV1	1.34
MKK1	1.34
CCP1	1.34
YPL197C	1.34

Deleted Gene	Log2 value 1% DMSO
ICY1	1.33
YBR225W	1.33
FET4	1.33
LYS14	1.32
HXT5	1.31
YKL098W	1.29
HAL1	1.29
YDR215C	1.29
PAM17	1.28
AYT1	1.28
IRC23	1.28
PEX10	1.26
EHT1	1.25
RDI1	1.25
TIM18	1.24
MFB1	1.23
SLH1	1.19
YOL163W	1.19
YLR053C	1.19
MRPL44	1.16
PDE1	1.14
YMR155W	1.14
YGR117C	1.13
LIN1	1.11
SSE2	1.11
FMP27	1.09
YOR041C	1.04
URA5	1.02
HRB1	1.02
YML131W	1.00
IDP2	1.00
SUM1	0.98
YOR084W	0.95
APE3	0.95
HXT8	0.94
YLR104W	0.92